

AD No.

DDC FILE COPY

ADA058110

RADC-TR-78-69  
Final Technical Report  
March 1978

1 12 8

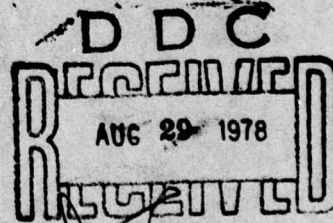


DETERMINATION OF RADAR PERFORMANCE  
DEGRADATION DUE TO TROPOSPHERIC DUCTS

Raytheon Company

LEVEL #

Approved for public release; distribution unlimited



This research was supported by the Air Force In-House  
Laboratory Independent Research Fund

ROME AIR DEVELOPMENT CENTER  
AIR FORCE SYSTEMS COMMAND  
GRIFFISS AIR FORCE BASE, NEW YORK 13441

78 08 28 012

This report has been reviewed by the RADC Information Office (OI) and is releasable to the National Technical Information Service (NTIS). At NTIS it will be releasable to the general public, including foreign nations.

RADC-TR-78-69 has been reviewed and is approved for publication.

APPROVED:

*Koichi Mano*

KOICHI MANO  
Contract Monitor

APPROVED:

*Terence J. Elkins*

TERENCE J. ELKINS, Acting Chief  
Propagation Branch  
Electromagnetic Sciences Division

APPROVED:

*Allan C. Schell*

ALLAN C. SCHELL, Acting Chief  
Electromagnetic Sciences Division

FOR THE COMMANDER:

*John P. Huss*

JOHN P. HUSS  
Acting Chief

This effort was funded totally by the Laboratory Directors' Fund.

If your address has changed or if you wish to be removed from the RADC mailing list, or if the addressee is no longer employed by your organization, please notify RADC (EEP), Hanscom AFB MA 01730.

Do not return this copy. Retain or destroy.

## UNCLASSIFIED

SECURITY CLASSIFICATION OF THIS PAGE (When Data Entered)

REPORT DOCUMENTATION PAGE		READ INSTRUCTIONS BEFORE COMPLETING FORM
1. REPORT NUMBER RADC-TR-78-69	2. GOVT ACCESSION NO.	3. RECIPIENT'S CATALOG NUMBER
6. DETERMINATION OF RADAR PERFORMANCE DEGRADATION DUE TO TROPOSPHERIC DUCTS		4. TYPE OF REPORT & PERIOD COVERED Final Technical Report 29 April - 31 October 1977
7. AUTHOR(s) G. H. Joshi	11. PERFORMING ORGANIZATION NAME AND ADDRESS Raytheon Company, Missile Systems Division Hartwell Road Bedford MA 01730	8. CONTRACT OR GRANT NUMBER(s) F19628-77-C-0145
10. CONTROLLING OFFICE NAME AND ADDRESS Deputy for Electronic Technology (RADC) Hanscom AFB MA 01730 Monitor/Koichi Mano/EEP	12. PROGRAM ELEMENT, PROJECT, TASK AREA & WORK UNIT NUMBERS 51101F 51767702	13. REPORT DATE March 1978
14. MONITORING AGENCY NAME & ADDRESS (if different from Controlling Office) 12 155 P	15. NUMBER OF PAGES 153	16. SECURITY CLASS. (of this report) UNCLASSIFIED
17. DISTRIBUTION STATEMENT (of this Report)  Approved for public release; distribution unlimited.	18a. DECLASSIFICATION/DOWNGRADING SCHEDULE N/A	
18. DISTRIBUTION STATEMENT (of the abstract entered in Block 20, if different from Report)		
19. SUPPLEMENTARY NOTES This research was supported by the Air Force In-House Laboratory Independent Research Fund		
20. KEY WORDS (Continue on reverse side if necessary and identify by block number) Meteorological Ducts Radar Performance Degradation Wave Propagation Geometrical Optics Physical Optics Diffraction Zone		
21. ABSTRACT (Continue on reverse side if necessary and identify by block number) Wave propagation for anomalous meteorological conditions around Canton Island is studied by pursuing the geometrical optics and the physical optics approaches. The relative merits along with the limitations of these two approaches have been established. For ranges beyond line of sight the physical optics approach is applied to the bilinear and the tri-linear refractive index profiles. The numerical analysis to determine the real eigenvalues and the height gain functions has been carried out for the bilinear refractive index profile. This numerical analysis has been carried out for four bilinear		

**UNCLASSIFIED**

SECURITY CLASSIFICATION OF THIS PAGE(When Data Entered)

refractive index profiles and three wavelengths.

**UNCLASSIFIED**

SECURITY CLASSIFICATION OF THIS PAGE(When Data Entered)

EVALUATION

F19628-77-C-0145

1. This is the Final Report on the contract which over the period from 20 April to 31 October 1977 investigated analytically the radar performance degradation due to tropospheric ducts. With the case of low look-angle specially in mind, the physical-optics approach has been employed to study the wave propagation for the cases of bilinear and trilinear profiles of the atmospheric index of refraction.
2. The above work is of value to the Air Force since it will provide basic information which is needed for a proper evaluation of the radar performance related to the detection of low-altitude objects in the presence of the tropospheric ducts.

Koichi Mano  
KOICHI MANO  
Contract Monitor  
Propagation Branch  
Electromagnetic Sciences Division

ACCESSION NR	
ATIS	White Section <input checked="" type="checkbox"/>
DDR	Dark Section <input type="checkbox"/>
UNCLASSIFIED	
NOTIFICATION	
DISTRIBUTION AVAILABILITY CODES	
TYPE	AVAIL. AND SPECIAL
<i>[Signature]</i>	

PREFACE

The author would like to thank the project officers Dr. E. Altshuler, Dr. K. Mano, and Mr. M. Wong of Rome Air Development Center, for their continued interest and support throughout the project. He would also like to thank Mr. R. Roy of Raytheon for assistance in computing the solutions of the transcendental equation.

## TABLE OF CONTENTS

	<u>Page</u>
<b>1. INTRODUCTION</b>	<b>7</b>
1.1 Statement of Problem	7
1.2 Report Outline	11
<b>2. METEOROLOGICAL DATA FROM CANTON ISLAND</b>	<b>13</b>
2.1 Data Format	13
2.2 Data Evaluation & Classification	13
<b>3. GEOMETRICAL VERSUS PHYSICAL OPTICS APPROACH</b>	<b>28</b>
3.1 Geometrical Optics Or Ray Trajectory Approach	28
3.2 Physical Optics Or Guided Mode Approach	34
3.3 Ray Trajectories For Four Refractive Index Profiles	36
<b>4. GUIDED MODE APPROACH - PHYSICAL OPTICS</b>	<b>42</b>
4.1 Propagation Through Stratified Media	42
4.1.1 Propagation Through the Meteorological Duct With Bilinear M-Profile	44
4.1.2 Trilinear Refractive Index Profile	51
4.1.3 Propagation Through Ducts with Trilinear Profiles	54
4.2 Solutions of the Transcendental Equation - The Bilinear Refractive Index Profile	57
4.2.1 Newton-Raphson Technique	58
4.2.2 Secant Method	59
4.2.3 Zero Crossing Technique	59
4.3 Numerical Analysis for Bilinear M-Profile	60
4.3.1 The Zero Crossing Technique For Trapped Modes	61
4.3.2 The Leaky Modes	75
4.4 Height Gain Functions For The Trapped Modes	76

## TABLE OF CONTENTS (CONT.)

	<u>Page</u>
5. CONCLUSION/RECOMMENDATIONS	115
5.1 Summary	115
5.2 Recommendations	116
6. REFERENCES	117 - 118
7. APPENDIXES I and II - COMPUTER PROGRAMS	119 - 151
I-1 thru I-17	119 - 136
II-1 thru II-14	137 - 151

## LIST OF ILLUSTRATIONS

	<u>Page</u>	
<b>Fig. (1-1)</b>	M and N Profiles For Normal Atmosphere	9
<b>Fig. (1-2)</b>	M Profiles For (1) Normal, (2) Subrefractive and (3) Superrefractive Conditions	10
<b>Figure (3-1) thru (3-4)</b>	Typical Ray Trajectories	30 - 33
<b>Fig. (3-5)</b>	Tropospheric Duct Propagation	35
<b>Fig. (3-6) thru (3-9)</b>	Ray Trajectories For Canton Island - 1973	37 - 40
<b>Fig. (4-1)</b>	Canton Island Refractive Index Profiles For Four Days .	43
<b>Fig. (4-2)</b>	Surface Duct - Bilinear Profile	52
<b>Fig. (4-3)</b>	Elevated Surface Duct - Trilinear Profile	52
<b>Figure (4-4)</b>	Elevated Duct - Trilinear Profile	52
<b>Fig. (4-5) thru (4-16)</b>	Plots of $\phi$ ( $z$ ) as a Function of $z$	62 - 73
<b>Fig. (4-17) thru (4-53)</b>	Height Gain Functions For January, April, September and December	77 - 113

## LIST OF TABLES

<b>Table (2-1) thru (2-12)</b>	Refractive Index Profiles For Canton Island For 1973	14 - 25
<b>Table (4-1)</b>	Trapped Wavelengths	60
<b>Table (4-2)</b>	Eigenvalues For Leaky Modes	76

## 1. INTRODUCTION

### 1.1 Statement of the Problem

The frequently occurring meteorological anomalies in certain geographical areas of the world can modify significantly the electromagnetic propagation. The modification in propagation affects the performance of the communication systems in such a fashion as to be able to communicate for distances significantly larger than what is expected during normal meteorological conditions. For ground based tactical missile systems and the long range surveillance radars, the impact is more significant. The radar systems experience range and angular errors for look angles which are greater than a couple of degrees. For elevation angles less than a couple of degrees, the systems can detect targets at significantly large distances. However the signals corresponding to these long ranges of detection are contaminated with the clutter, the primary and multiple time around. Further along with the extended detection ranges, for slightly higher elevation angles the target detection is impaired due to the existence of holes or the shadow zones.

The existence of regions of extended detection ranges, and of regions of shadow zones, are dependent on the meteorological conditions which tend to modify the refractive index profile and hence the propagation behavior. The refractive index  $\eta$  is related to the atmospheric pressure  $P$ , absolute temperature  $T$ , and the partial water vapor pressure  $e$ . The refractive index  $\eta$  is given in terms of different parameters such as  $N$ ,  $M$ , and  $B$  units, etc. In this report we use only the  $N$  and  $M$  units to describe the refractive index and they are defined as follows:

$$N = (\eta - 1) \times 10^6 = \frac{k_1}{T} P + \frac{k_2 e}{T^2}$$

Here the constants  $k_1$  and  $k_2$  have the following empirical values.

$$k_1 = 77.6, \quad k_2 = 3.73 \times 10^5$$

For normal atmosphere  $N$  decreases uniformly with height imparting a downward bending for a ray path. On the other hand, the earth's curvature gives the appearance that the rays tilt upwards. This apparent upward tilt can be nullified by incorporating the curvature of the earth in the refractive index profile which leads to a straight trajectory for a flat earth. The media dependent bending of the ray then is described in terms of modified refractive index profile  $\hat{\eta}$  or in terms of  $M$  - units, and they are defined as follows:

$$\hat{\eta} = \eta + \frac{z}{a}$$

and

$$M = \hat{\eta} = (\eta + \frac{z}{a} - 1) \times 10^6$$

Here  $z$  is the height and  $a$  is the radius of curvature of earth,  
( $a = 6.4 \times 10^6$  m).

Thus M and N units are related to each other in the following fashion:

$$M = \left( N + \left( \frac{z}{a} \times 10^6 \right) \right)$$

For normal meteorological conditions, the plots of M and N units as a function of height reveal that there is a steady increase of M units with height as contrast to steady decrease of N units with height and this is displayed in Fig. (1-1).

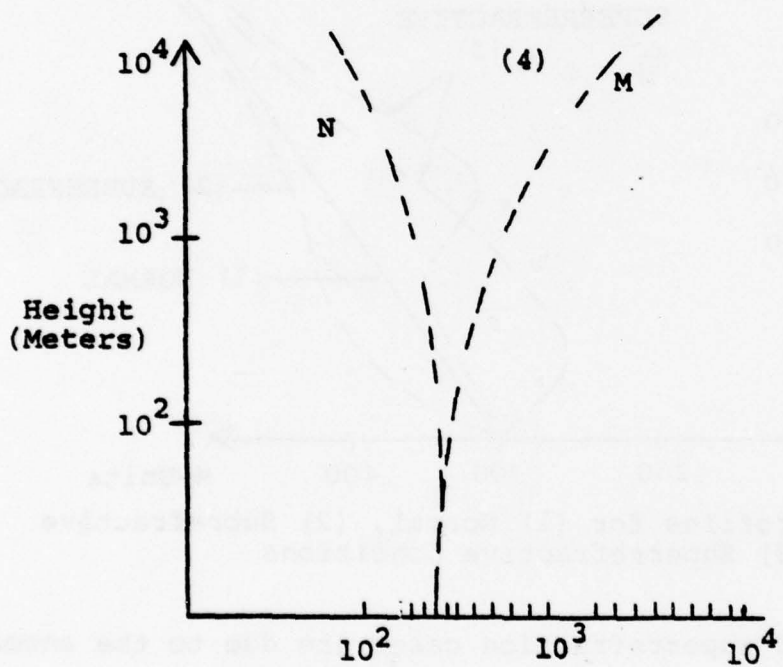


Figure (1-1) - M and N Profiles For Normal Atmosphere

During anomalous meteorological conditions the temperature and the water vapor content change in such a fashion as to cause significant deviations in the refractive index profiles and thus in the profiles of M and N as a function of height.

Some representative plots of M profiles have been reproduced in Fig. (1-2) and they, in general, fall in three major categories:

1. Normal refraction
2. Subrefraction
3. Superrefraction

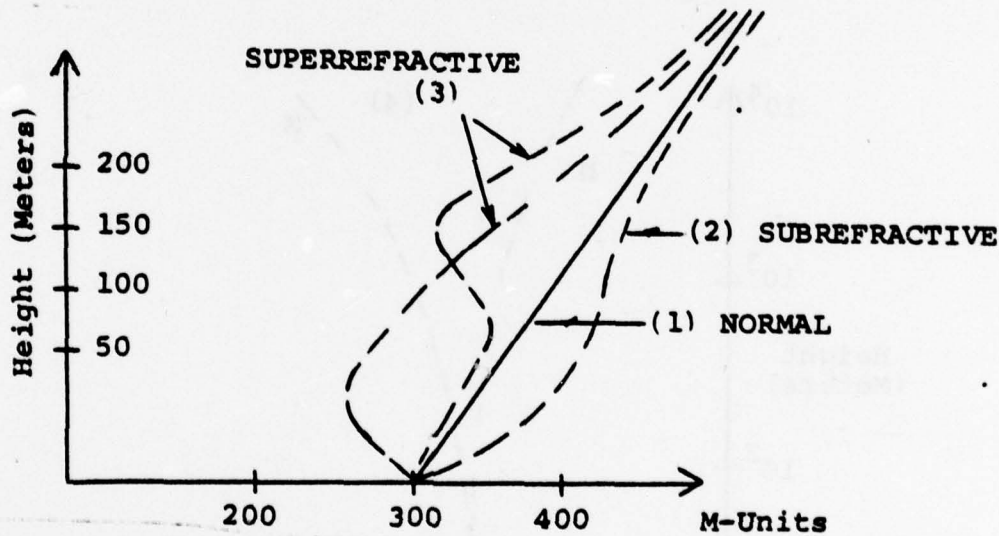


Figure (1-2) - M - Profiles for (1) Normal, (2) Subrefractive and (3) Superrefractive Conditions

The subrefraction and superrefraction cases are due to the anomalous meteorological conditions and this report deals with the electromagnetic propagation through such an anomalous medium.

### 1.2 The Outline of the Report

This section, Section 1, has identified the main topic of this report, namely, the determination of propagation through meteorological ducts.

For the propagation studies, the meteorological data for Canton Island was provided by ESD and Section 2 evaluates the data and classifies it in an appropriate fashion.

The electromagnetic propagation through the medium around Canton Island can be studied by geometrical optics which provides a reasonable characterization of the line of sight propagation. Section 3 discusses this approach and its limitations. The alternate approach, namely the physical optics, is also discussed in this section in order to highlight its application to the diffraction region. Section 3 further provides the ray trajectories for four days of meteorological conditions so chosen as to cover the broad spectrum of variations in the characteristic parameters of the duct such as the duct width and the lapse rate of the M units.

The primary purpose of this investigation is to develop the physical optics approach for propagation through meteorological ducts and hence details of the analytical formulation of the guided mode approach is provided in Section 4 for two refractive index profiles, bilinear and trilinear. The numerical analysis based on several techniques such as Newton-Raphson to determine the characteristic wave numbers has been carried out for the bilinear case and is

discussed in Section 4. Also, the height-gain functions which describe the dependence of electromagnetic field with height for different modes have been included in Section 4 for the bilinear refractive index profile.

Finally, the conclusions and recommendations, the references, and the different appendixes are provided in Sections 5, 6 and 7, respectively.

## 2. METEOROLOGICAL DATA FROM CANTON ISLAND

For the purpose of analysis, it was decided during the early stages of the contract that Raytheon will be provided with sample meteorological data from Canton Island ( $28^{\circ}\text{S}$ ,  $171.6^{\circ}\text{W}$ ).

### 2.1 Data Format

The data was provided by U.S. Air Forces Environmental Technical Applications Centre at Scott Air Force Base, Illinois and was in terms of the meteorological parameters (T, P, e). Here T, P, e, respectively, stand for the temperature, the atmospheric pressure and the partial water vapor pressure. The data provides for the typical refractive index profiles for the year 1973. This data is translated into N units, M units and the rate of change of N with height in tables (2-1) through (2-12). These tables are for twelve months, with two profiles per month. The criterion that is used to determine the presence or absence of a duct is based on the condition that the rate of change of N units with height is less than  $10^6/r$  where r is the radius of the earth ( $r = 6.4 \times 10^6\text{m}$ ).

### 2.2 Data Evaluation and Classification

Based on this criterion, the following observations are made regarding the nature of the refractive index profile:

1. The meteorological duct was present for all the days for which the data has been provided.

2JAN	12	17	M	DN/DH
H	N			
,003	387,400	387,871		
,040	378,900	385,176	-229,730	
1,137	293,800	472,209	-77,5752	
1,473	278,400	509,531	-45,8333	
3,121	228,700	718,422	-30,1578	
4,386	189,000	877,216	-31,3834	
4,972	174,300	954,466	-25,0853	
5,250	161,900	985,688	-44,6043	
5,850	155,500	1073,44	-10,6667	
6,587	141,700	1175,28	-18,7246	
6,742	138,500	1196,40	-20,6452	
7,590	123,700	1314,66	-17,4528	
9,720	95,500	1620,68	-13,2394	
11,010	83,000	1810,60	-9,68992	
12,500	70,100	2031,50	-8,65772	
14,300	56,500	2300,34	-7,55556	
16,610	42,300	2648,61	-6,14719	

3JAN	0	22	M	DN/DH
H	N			
,003	396,100	396,571		
,082	365,400	371,990	-787,179	
,784	301,600	424,619	-85,9838	
1,470	256,200	486,861	-66,1808	
2,550	211,900	612,026	-41,0185	
3,125	207,100	697,450	-8,34783	
4,424	175,300	869,479	-24,4804	
-5,455	155,500	1011,45	-19,2047	
5,860	147,900	1067,40	-18,7654	
7,500	120,600	1311,56	-15,7803	
9,730	94,800	1621,55	-12,0561	
11,020	82,300	1811,47	-9,68992	
11,358	79,400	1861,61	-8,57948	
12,520	69,600	2034,14	-8,43373	
14,330	56,500	2305,05	-7,23757	
16,161	43,300	2579,15	-7,20918	
16,703	40,600	2661,50	-4,98155	
17,495	34,200	2779,37	-8,08081	
18,774	26,600	2972,47	-5,94214	
19,986	21,600	3157,64	-4,12541	
20,660	18,800	3260,60	-4,15430	
22,026	14,700	3470,84	-3,00146	

TABLE (2-1)-Jan. 1973

TABLES (2-1) thru (2-12) - Refractive Index Profiles for Canton Island For 1973

3FEB	O	24	
H	N	M	DN/DH
.003	394,900	395,371	
.076	351,600	363,525	-593,151
1,263	277,400	475,580	-62,5105
1,498	264,900	499,054	-53,1915
3,140	210,600	703,304	-33,0694
4,715	179,400	919,240	-19,0095
5,890	151,800	1076,01	-23,4894
7,620	121,700	1317,37	-17,3988
9,750	95,500	1625,39	-17,3005
11,030	82,800	1813,54	-9,92188
12,530	69,700	2035,81	-8,73333
14,340	56,100	2306,22	-7,51381
16,731	39,800	2665,09	-6,81723
18,240	30,000	2892,07	-6,49437
18,802	26,700	2976,96	-5,87189
20,640	19,100	3260,90	-4,09042
22,825	12,900	3594,42	-2,86374
23,192	11,900	3651,00	-2,72480
23,790	10,800	3783,74	-1,83946

5FEB	O	29	
H	N	M	DN/DH
.003	307,800	398,271	
.081	353,300	366,010	-570,513
1,363	257,300	471,171	-74,8830
1,403	257,100	477,247	-5,00000
1,500	250,600	485,068	-67,0103
1,872	236,900	530,639	-36,8280
2,681	209,400	630,081	-33,9926
3,146	202,300	695,945	-15,2688
5,870	148,200	1069,27	-19,8605
6,662	134,900	1180,25	-16,7929
7,610	121,200	1315,30	-14,4515
9,750	95,600	1625,49	-11,9626
11,030	82,900	1813,64	-9,92188
12,520	69,700	2034,24	-8,85906
14,340	56,200	2306,32	-7,41758
16,710	40,400	2662,40	-6,66667
17,892	32,900	2840,37	-6,34518
18,032	32,200	2861,64	-5,00000
18,325	29,900	2905,31	-7,84983
18,723	27,200	2965,06	-6,78392
20,730	19,000	3271,79	-4,08570
21,775	15,900	3432,66	-2,96651
23,860	10,700	3754,62	-2,49400
24,530	9,700	3858,75	-1,49254
25,023	8,800	3935,21	-1,82556
26,450	7,100	4157,42	-1,19131
26,778	6,700	4208,49	-1,21951
27,311	6,100	4291,52	-1,12570
30,379	3,800	4770,63	-749674

TABLE (2-2) - Feb. 1973

2MAR	O	29	M	DN/DH
H	N			
.003	375.100		375.571	
.062	328.500		338.229	-789.831
1.479	258.100		490.173	-49.6824
2.179	229.600		571.511	-40.7143
3.124	201.600		691.793	-29.6296
5.860	147.800		1067.30	-19.6637
6.601	135.200		1170.98	-17.0040
7.600	120.900		1313.43	-14.3143
8.357	110.700		1422.01	-13.4742
9.740	95.300		1623.62	-11.1352
11.020	82.800		1811.97	-9.74563
12.520	69.600		2034.14	-8.80000
14.330	56.300		2304.85	-7.34807
16.249	43.600		2593.26	-6.61803
16.680	40.600		2657.89	-6.96056
17.590	34.500		2794.58	-6.70330
18.679	28.400		2959.36	-5.60147
19.822	22.300		3132.61	-5.33683
20.600	18.800		3251.19	-4.49871
22.130	14.100		3486.56	-3.07190
23.175	12.000		3648.43	-2.00957
23.770	10.600		3740.40	-2.35294

3MAR	O	15	M	DN/DH
H	N			
.003	391.700		392.171	
.075	373.200		384.968	-256.944
1.494	286.000		520.426	-61.4517
3.142	220.400		713.417	-39.8058
4.613	195.400		909.235	-23.7933
5.870	155.800		1076.87	-23.5481
7.610	122.900		1317.00	-18.9080
9.750	94.900		1624.79	-13.0841
11.050	81.800		1815.68	-10.0769
11.625	75.800		1900.90	-8.69565
12.560	69.000		2039.81	-8.34225
14.390	55.800		2313.76	-7.21311
15.912	46.100		2542.88	-6.37319
16.757	40.100		2669.47	-7.10059
16.929	39.300		2695.66	-4.65116

TABLE (2-3) - March 1973

SAPR	O	27	M	DN/DH
H	N			
.003	394,900	395.371		
.075	349,000	360.768	-637.500	
1.495	267,000	501.583	-57.7465	
3.145	206,100	699.588	-36.9091	
4.307	179,500	855.320	-22.8916	
4.788	167,100	918.395	-25.7796	
5.880	148,500	1071.14	-17.0330	
7.610	121,400	1315.50	-15.6647	
9.154	102,700	1539.07	-12.1114	
9.740	95,500	1623.82	-12.2867	
11.010	83,400	1811.00	-9.52756	
12.500	69,900	2031.30	-9.06040	
14.310	56,100	2301.51	-7.62431	
16.680	40,400	2657.69	-6.62447	
17.663	33,800	2805.34	-6.71414	
17.871	31,700	2835.87	-10.0962	
18.469	29,100	2927.11	-4.34783	
18.700	27,500	2961.75	-6.92641	
19.810	21,900	3130.33	-5.04505	
20.700	18,800	3266.88	-3.48315	
21.081	17,100	3324.96	-4.46194	
23.950	10,400	3768.44	-2.33531	

SAPR	O	20	M	DN/DH
H	N			
.003	383,600	384.071		
.085	331,300	344.638	-637.805	
1.505	251,200	487.353	-56.4085	
3.153	201,900	696.643	-29.9150	
5.262	159,000	984.671	-20.3414	
5.890	147,600	1071.81	-18.1529	
7.630	121,300	1318.54	-15.1149	
9.760	95,700	1627.16	-12.0188	
11.030	83,200	1813.94	-9.84252	
12.530	69,600	2035.71	-9.06667	
14.340	56,100	2306.22	-7.45856	
16.730	39,800	2664.94	-6.82008	
18.760	28,000	2971.67	-5.81281	
18.925	27,200	2996.76	-4.84848	
20.380	20,100	3217.97	-4.87973	
20.730	18,400	3271.19	-4.85714	
23.960	10,500	3770.11	-2.44582	
26.610	6,900	4182.33	-1.35849	
27.898	5,500	4383.03	-1.08696	
29.515	4,400	4635.66	-680272	

TABLE (2-4) - April, 1973

9MAY	O	32	M	DN/DH
H	N			
.003	374,000		374,471	
.084	343,400		356,581	-377,778
.897	312,200		451,381	-38,8543
1,126	274,700		451,383	-156,904
1,504	258,200		494,196	-43,6508
2,186	220,000		563,010	-56,0117
3,158	197,200		692,728	-23,4568
4,348	187,800		870,053	-7,89916
8,789	170,700		922,151	-38,7755
5,890	152,500		1076,71	-16,5304
7,620	120,400		1316,07	-18,5549
9,740	95,300		1623,62	-11,8396
11,020	83,300		1812,47	-9,37500
12,500	70,300		2031,70	-8,78378
14,300	56,600		2300,44	-7,61111
15,563	48,000		2490,02	-6,80918
16,660	34,900		2654,05	-7,38377
17,786	33,000		2823,84	-6,12789
18,700	27,000		2961,25	-6,56455
19,515	23,300		3085,44	-4,53988
19,819	21,600		3131,44	-5,59211
20,730	18,400		3271,19	-3,51262

10MAY	O	23	M	DN/DH
H	N			
.003	372,400		372,871	
.085	348,100		361,438	-296,341
.787	333,300		450,513	-22,3565
.972	300,600		453,118	-145,333
1,500	279,500		514,868	-39,9621
1,839	252,900		541,461	-78,4661
3,150	204,400		698,673	-36,9947
3,527	189,100		742,529	-40,5836
4,586	168,100		887,608	-19,8300
5,900	145,800		1071,58	-16,9711
7,620	120,400		1316,07	-14,7674
9,740	95,700		1624,02	-11,6509
11,010	83,300		1810,90	-9,76378
12,490	70,400		2030,23	-8,71622
15,281	49,500		2447,27	-7,48836
16,654	40,200		2653,41	-6,77349
19,681	22,000		3110,18	-6,01255
20,800	18,700		3282,47	-2,94906
24,026	10,400		3780,37	-2,57285
26,697	6,900		4195,98	-1,31037
30,167	3,900		4737,46	-864553
31,433	3,300		4935,51	-473934
32,904	2,600		5165,63	-475867

TABLE (2-5) - May, 1973

3JUN	O	15	
H	N	M	DN/DH
.003	344.600	365.071	
.083	336.700	349.724	-348.750
1.114	296.100	470.900	-39.3792
1.497	248.800	483.697	-123.499
1.814	237.800	527.438	-34.7003
1.950	246.200	572.178	208.824
3.136	216.400	708.476	-41.9899
3.231	195.500	702.483	-220.000
5.559	151.300	1023.57	-18.9843
5.850	155.200	1073.14	13.4021
6.292	147.600	1133.32	-17.5926
6.600	140.000	1175.62	-23.8994
7.580	120.600	1309.99	-19.7959
9.680	96.000	1614.91	-11.7143
9.799	94.400	1631.98	-13.4454

5JUN	O	23	
H	N	M	DN/DH
.003	371.600	372.071	
.071	344.200	355.341	-402.941
.789	320.000	443.804	-33.7047
1.486	266.300	499.471	-77.0445
1.993	224.200	536.926	-83.0375
2.974	221.200	687.856	-3.05810
3.131	207.700	698.091	-85.9873
3.794	183.500	778.824	-34.5008
4.642	175.100	903.485	-9.90566
5.212	160.800	978.625	-25.0877
5.496	164.700	1027.09	13.7324
5.850	145.900	1063.84	-53.1073
6.105	149.700	1107.65	14.9020
6.368	143.000	1142.22	-25.4753
7.580	122.400	1311.79	-16.9967
8.247	115.400	1409.45	-10.4948
9.690	96.900	1617.38	-12.8205
10.960	83.500	1803.26	-10.5512
12.440	70.300	2022.28	-8.91892
14.230	57.000	2289.86	-7.43017
14.767	53.000	2370.12	-7.44879
15.446	47.600	2471.26	-7.95287
16.590	40.400	2643.57	-6.29371

TABLE (2-6) - June, 1973

3JUL	O	34	M	DN/DH
H	N			
.003	353.300	353.771		
.075	328.600	340.368	-343.056	
1.481	254.400	486.787	-52.7738	
1.682	239.600	503.526	-73.6318	
1.941	225.300	529.866	-55.2124	
3.124	197.300	687.493	-23.6686	
3.954	185.100	805.530	-14.6988	
4.637	166.600	894.201	-27.0864	
5.860	145.900	1065.40	-16.9256	
6.905	131.000	1214.48	-14.2584	
7.570	121.500	1309.32	-14.2857	
8.033	115.100	1375.57	-13.8229	
8.605	108.400	1458.63	-11.7133	
8.883	104.700	1498.55	-13.3094	
9.670	96.000	1613.34	-11.0546	
10.802	84.900	1779.86	-9.80565	
10.940	83.500	1800.12	-10.1449	
12.420	70.700	2019.55	-8.64865	

4JUL	O	31	M	DN/DH
H	N			
.003	370.300	370.771		
.067	345.900	356.413	-381.250	
.888	307.800	447.138	-46.4068	
1.479	237.300	469.373	-119.289	
2.070	222.100	546.908	-25.7191	
2.563	210.200	612.365	-24.1379	
3.122	197.400	687.279	-22.8980	
5.140	157.400	963.928	-19.8216	
5.860	146.300	1065.80	-15.4167	
7.570	121.200	1309.02	-14.6784	
8.799	105.600	1486.27	-12.6932	
9.680	96.400	1615.31	-10.4427	
10.940	84.100	1800.72	-9.76190	
12.410	71.000	2018.28	-8.91156	
14.200	56.900	2265.05	-7.87709	
16.006	44.300	2555.83	-6.97674	
16.540	39.900	2635.22	-8.23970	
17.077	36.400	2715.99	-6.51769	
17.338	33.300	2753.84	-11.8774	
18.640	26.200	2951.04	-5.45315	
20.001	20.800	3159.20	-3.96767	
20.710	18.000	3267.65	-3.94922	
23.147	12.300	3604.34	-2.33898	
23.950	10.500	3768.54	-2.24159	

TABLE (2-7) - July, 1973

2AUG	O	32	M	DN/DH
H.	N			
.003	371.600		372.071	
.093	347.100		361.693	-272.222
.910	303.100		445.890	-53.8556
1.500	267.200		502.568	-60.8475
1.570	235.400		481.752	-454.286
1.826	228.700		515.221	-26.1719
2.635	209.100		622.563	-24.2274
3.133	197.500		689.105	-23.2932
3.337	192.900		716.515	-22.5490
5.538	152.500		1021.46	-18.3553
5.850	147.000		1064.94	-17.6282
7.560	121.200		1307.45	-15.0877
9.660	96.900		1612.67	-11.5714
10.521	88.200		1739.07	-10.1045
10.920	83.700		1797.18	-11.2782
12.300	70.900		2015.04	-8.70748
13.595	61.400		2104.62	-7.88382
14.170	56.800		2280.24	-8.00000
15.531	47.100		2484.10	-7.12711

5AUG	O	32	M	DN/DH	TABLE (2-8) - Aug., 1973
H.	N				
.003	360.700		361.171		
.084	335.300		348.481	-313.580	
.549	371.000		407.145	-30.7527	
1.223	278.700		470.603	-62.7596	
1.483	256.200		488.900	-86.5385	
3.111	196.100		686.253	-35.6880	
3.620	186.800		754.821	-22.2004	
4.627	167.800		893.832	-18.8679	
5.820	146.600		1060.03	-17.6027	
7.530	121.400		1302.95	-14.8538	
8.974	103.300		1511.43	-12.5346	
9.630	96.400		1607.46	-10.5183	
10.600	86.800		1750.07	-9.89691	
10.800	83.700		1792.47	-10.6897	
12.360	71.000		2010.43	-8.63946	
13.417	62.500		2167.79	-8.04163	
14.150	56.700		2277.00	-7.91269	
15.318	48.600		2452.18	-6.93493	
16.235	41.000		2588.47	-8.28790	
16.510	39.100		2629.72	-6.90909	
16.992	36.400		2702.65	-5.60166	
17.814	30.200		2825.43	-7.54258	
18.630	26.200		2949.47	-4.90196	

4SEP H	O N	42 M	DN/DH
.003	391.500	391.971	
.094	370.200	384.950	-234.066
.343	355.800	409.421	-57.8313
.707	321.500	432.437	-94.2308
1.501	293.400	528.925	-35.3904
1.905	262.700	561.617	-75.9901
2.515	223.700	618.334	-63.9344
2.876	210.800	662.079	-35.7341
3.125	219.800	710.150	36.1446
3.473	205.600	750.555	-40.8046
3.986	196.400	821.851	-17.9337
4.116	199.600	845.650	26.1538
4.380	176.500	863.774	-88.2576
5.380	159.600	1003.79	-16.9000
5.650	162.500	1049.05	10.7407
5.830	153.000	1067.80	-52.7778
6.457	146.400	1159.58	-10.5263
7.530	122.300	1303.85	-22.4604
8.330	111.600	1418.68	-13.3750
8.494	112.800	1445.61	7.31707
8.599	109.500	1458.79	-31.4286
8.726	109.300	1478.51	-1.57480
8.920	104.400	1504.05	-25.2577
9.620	96.600	1606.09	-11.1429
10.561	87.300	1744.45	-9.88310

5SEP H	O N	17 M	DN/DH
.003	388.700	389.171	
.102	353.900	369.905	-351.515
.819	301.900	430.411	-72.5244
1.151	286.700	467.306	-45.7831
1.997	246.700	560.053	-47.2813
2.232	242.700	592.928	-17.0213
2.484	223.900	613.660	-74.6032
3.139	197.600	690.147	-40.1527
4.799	164.800	917.821	-19.7590
5.849	146.900	1064.68	-17.0476
6.464	130.600	1150.88	-16.7480
7.565	121.300	1308.34	-13.8945
9.690	96.500	1616.98	-11.6706
10.607	87.200	1751.57	-10.1418
10.950	84.000	1802.19	-9.32945
12.420	70.800	2019.65	-8.97959
14.165	57.300	2279.96	-7.73639

TABLE (2-9) - Sept., 1973

7 OCT	O	37	M	DN/DH
H	N			
.003	385.000		385.471	
.078	357.900		370.139	-361.333
.699	320.500		430.181	-60.2254
1.094	282.200		453.462	-94.9620
1.485	247.200		500.214	-38.3632
2.264	217.300		572.549	-64.0545
3.118	197.600		686.852	-23.0679
3.715	196.500		770.428	-1.84255
4.021	178.800		809.743	-57.8431
5.840	145.900		1062.27	-18.0869
6.290	139.600		1126.58	-14.0000
6.541	134.900		1161.26	-18.7251
7.560	121.500		1307.75	-13.1501
8.103	113.900		1385.36	-13.9963
9.670	96.000		1613.34	-11.4231
10.749	85.400		1772.05	-9.82391
10.940	83.700		1800.32	-8.90052
12.410	70.800		2018.08	-8.77551
14.200	57.000		2285.15	-7.70950
15.132	50.400		2424.79	-7.08155
15.458	47.400		2472.95	-9.20245
16.004	44.200		2555.42	-5.86051

TABLE (2-10) Oct., 1973

8 OCT	O	19	M	DN/DH
H	N			
.003	375.100		375.571	
.084	353.700		366.881	-264.198
.649	317.500		419.336	-64.0708
1.488	283.100		516.585	-41.0012
2.134	259.800		594.650	-36.0681
2.262	238.800		593.735	-164.062
2.480	212.300		601.442	-121.560
3.108	210.500		698.182	-2.86624
5.830	146.300		1061.10	-23.5856
7.550	121.000		1305.69	-14.7093
9.660	96.000		1611.77	-11.8483
10.686	85.900		1762.66	-9.84405
10.920	83.600		1797.08	-9.82906
12.400	70.500		2016.21	-8.85135
14.184	57.100		2282.74	-7.51121
14.806	52.700		2375.94	-7.07395
16.530	40.500		2634.25	-7.07657
16.762	38.000		2668.16	-10.7759
18.274	28.600		2896.01	-6.21693

SNOV	O	20	
H	N	M	DN/DH
.003	371,900	372,371	
.067	347,100	357,613	-387,500
.696	317,000	426,211	-47,8537
1.468	274,700	505,047	-54,7927
1.938	239,700	543,795	-74,4681
3.107	197,400	684,925	-36,1848
5.830	146,300	1061,10	-18,7661
7.550	121,900	1306,59	-14,1860
8.883	104,400	1498,25	-13,1283
9.650	96,400	1610,60	-10,4302
10.727	85,500	1768,69	-10,1207
10.910	83,700	1795,61	-9,83607
12.390	70,600	2014,74	-8,85135
14.180	56,900	2281,91	-7,65363
16.530	40,300	2634,05	-7,06383
17.324	34,300	2752,64	-7,55668
18.592	27,000	2944,31	-5,75710
18.902	24,800	2990,75	-7,09677
20.500	18,800	3249,62	-3,55450
21.516	15,700	3391,82	-3,34773

TABLE (2-11) - Nov., 1973

SNOV	O	17	
H	N	M	DN/DH
.003	363,600	364,071	
.067	342,500	353,013	-329,688
1.468	269,600	499,947	-52,0343
1.698	246,600	513,037	-100,000
2.429	218,700	599,839	-38,1669
3.095	204,900	690,543	-20,7207
5.810	150,200	1061,86	-20,1473
6.163	143,400	1110,45	-19,2635
7.530	121,000	1302,55	-16,3862
9.640	96,600	1609,23	-11,5640
10.715	85,600	1766,91	-10,2326
10.900	84,000	1794,34	-8,64865
12.380	70,500	2013,07	-9,12162
13.298	63,400	2150,02	-7,73420
14.170	56,400	2279,84	-8,02752
14.457	54,400	2322,88	-6,96864
16.540	40,100	2635,42	-6,86510

SDEC	O	27	M	DN/DH
H	N			
.003	374,000		374,471	
.084	355,200		369,381	-232,099
1.429	287,500		521,142	-48,1851
2.092	244,200		572,460	-71,8076
3.114	206,800		695,424	-36,5949
3.935	191,700		809,149	-18,3922
4.418	175,700		868,937	-33,1263
5.379	154,100		998,120	-22,4766
5.810	149,900		1061,56	-9,74478
6.845	134,600		1211,80	-14,5024
7.131	126,700		1245,64	-20,6992
7.520	121,400		1301,38	-13,6247
9.610	97,400		1605,32	-11,0233
10.499	87,900		1735,32	-10,6862
10.870	84,100		1789,73	-10,2426
12.340	71,300		2007,59	-8,70748
13.283	63,800		2148,06	-7,95334
14.110	57,300		2271,33	-7,85973

TABLE (2-12) - Dec., 1973

SDEC	O	33	M	DN/DH
H	N			
.003	366,400		366,871	
.075	351,900		363,668	-201,389
.956	299,200		449,208	-59,8184
1.476	272,100		503,702	-52,1154
1.872	260,800		554,539	-28,5354
2.328	231,000		596,291	-65,3509
3.101	216,800		703,384	-18,3700
4.295	182,800		856,737	-28,4757
4.456	183,000		882,200	1,24224
4.980	161,800		943,222	-40,4580
5.740	152,500		1059,45	-11,6250
6.223	145,500		1121,96	-15,8014
6.338	138,200		1132,71	-63,4783
7.490	123,700		1298,97	-12,5868
8.500	108,600		1442,35	-14,9505
9.540	96,700		1599,92	-11,0185
10.642	88,300		1726,77	-9,74478
10.840	84,600		1785,53	-9,29648
12.300	71,200		2001,22	-9,17808
12.943	66,100		2100,15	-7,69231
14.080	57,200		2266,52	-7,96777
15.819	45,200		2527,39	-6,90052
16.400	40,100		2613,46	-8,77797

2. Eighty percent of the time there existed surface ducts.
3. Twenty percent of the time the duct profiles were more complex with possible existence of elevated ducts.
4. The limited number of data points (M-units versus altitude) force to characterize the surface ducts as bilinear.
5. The duct width, under the circumstances, is inaccurately determined. For the available data, the duct width is most likely the maximum value rather than the likely value.
6. The duct intensity, as determined by the rate of change of N with height, varies from -201/km to -789/km. The minimum intensity occurring in December and the maximum in March. The refractive index profiles based on the radiosonde data are not corrected for different measurement errors. The errors could either be sensor-related or could be the timelag in temperature and humidity measurements. Finally, the most conspicuous error is the lack of correlation between the first radiosonde data point at some altitude which is different than mean sea level and the sea level measurement.

7. The duct widths for the surface ducts, defined as the height at which the minimum for M occurs, varies from 40 meters for January 2nd to 102 meters for September 5th.
8. For the largest duct width of 102 meters, the minimum frequency that is trapped is approximately 350 MHz, and the minimum for the smallest duct of 40 meters, it is 1.43 GHz. This is based on a crude relationship between the maximum wave length trapped and the duct width.

$$\lambda_{\max} \approx 0.014d^{3/2}$$

↓                    ↓  
cm                    feet

### 3. GEOMETRICAL VERSUS PHYSICAL OPTICS APPROACH

The electromagnetic propagation through a medium is governed by the refractive index profile of the medium; and it can be characterized either by the geometrical optics that is the ray treatment, or the physical optics that is the wave treatment. The distinction in the two approaches which was highlighted for optics originally, is equally valid for electromagnetic propagation.

#### 3.1 Geometrical Optics or Ray Trajectory Approach

The geometrical optics approach is primarily based on the Fermat's principle which states that the line integral of the refractive index between two points is stationary. This leads to the well know Snell's law which states that  $n_1 r_1 \cos \theta_1 = n_2 r_2 \cos \theta_2$ . Here,  $n_1$  is the refractive index at  $r_1$  and  $\theta_1$  is the angle of inclination of the ray with the horizontal, and  $n_2$  is the refractive index at  $r_2$  and  $\theta_2$  is the angle of inclination at  $r_2$ .

Based on this, a set of ray trajectories for actual refractive index profiles has been plotted to highlight the salient features of the geometrical optics approach. The ray trajectories are for a specific location for four different days in the month of August at local noon. The antenna height is 50 meters, and the elevation angle is between 0 and 1 degree. All the four ray trajectories reveal most of the features of the ground duct, namely, the trapping of the rays at angles less than  $1^\circ$ , the shadow regions beyond 40 km range, and the modest refraction at or above  $1^\circ$  elevation.

These ray trajectories reveal the cases when the geometrical optics approach is not valid. It is well established that the geometrical optics or ray treatment is valid when two conditions are satisfied and those are:

$$\frac{1}{kn} \frac{\Delta n}{n} \ll 1, \quad \frac{1}{kn} \frac{|\Delta Jl/2|}{Jl/2} \ll 1$$

Here  $J$  is the Jacobian and for detail explanation see Ref. (2), (Paes 52 - 58).

The first condition states that the relative variation of the refractive index per wavelength is smaller than unity. The second condition states that the relative density of the rays in a bundle, or the relative spacing between the rays, is less than a constant. This second condition is quite often not adequately emphasized when the geometrical optics approach is pursued. This second condition is often violated when the duct is present as is evident in the ray trajectories shown in Figures (3-1) thru (3-4). Further, the ray trajectories indicate that there exists a complete blank region with no electromagnetic energy at all, which in practice is not the case. Lastly, the geometrical optics approach is independent of frequency and polarization. This aspect prevents the geometrical optics approach from treating any scattering problems and thus the clutter which is dependent on frequency, polarization and roughness of ground or sea surface. For both communication and radar systems these considerations are of great importance, and the preferred approach is that based on physical

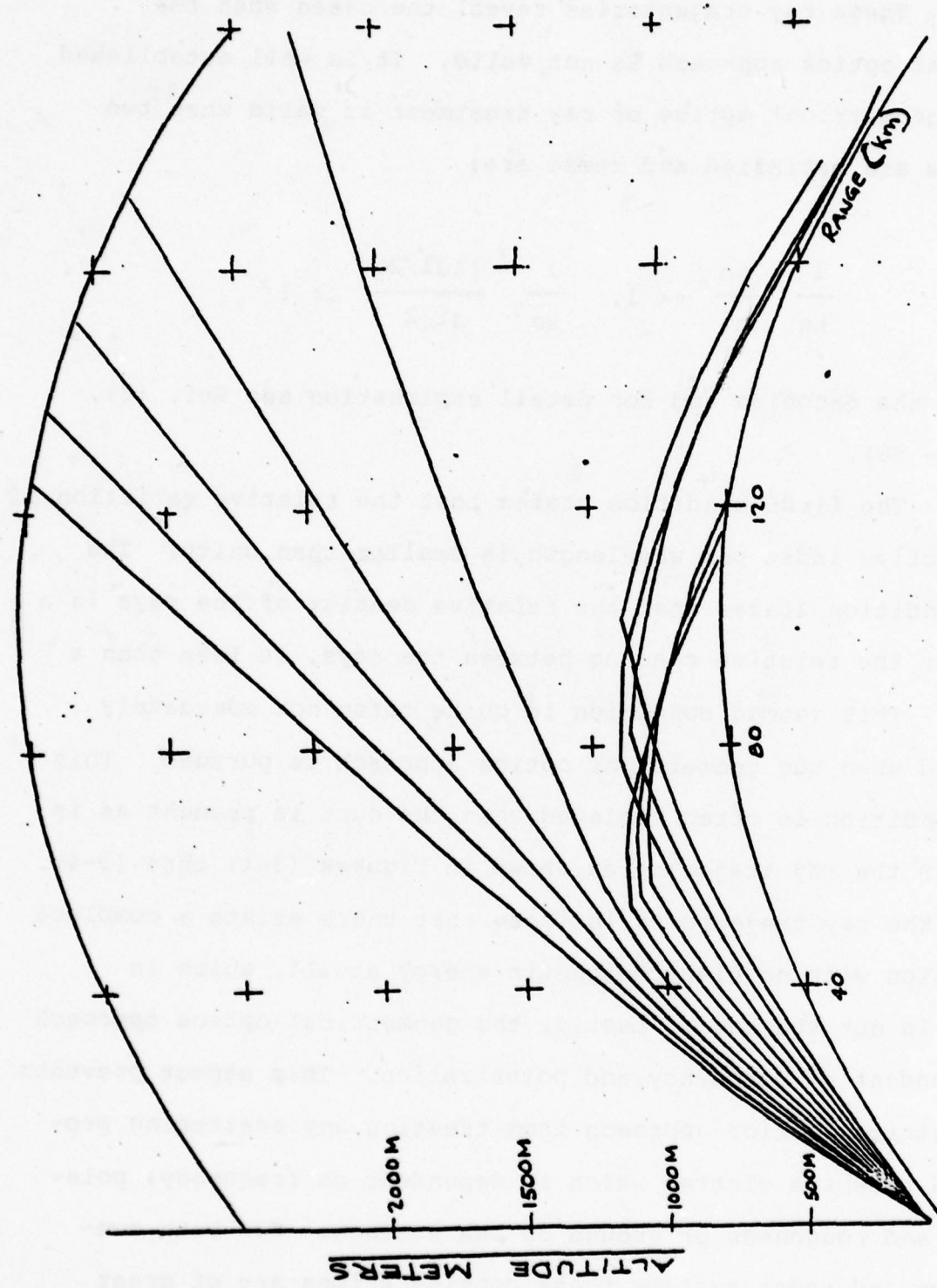


Figure (3-1) Typical Ray Trajectories for August 26

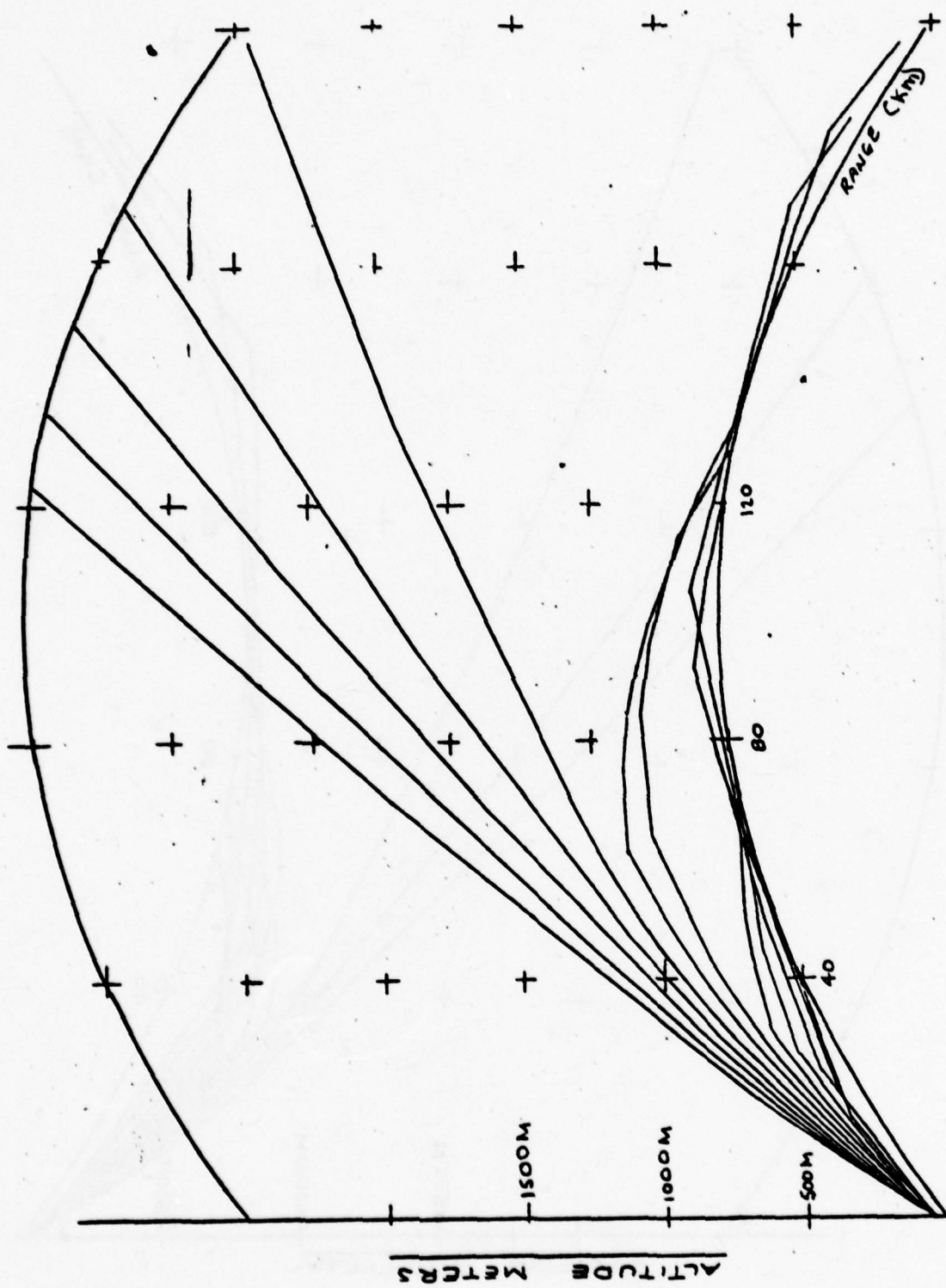


Figure (3-2) Typical Ray Trajectories for August 28

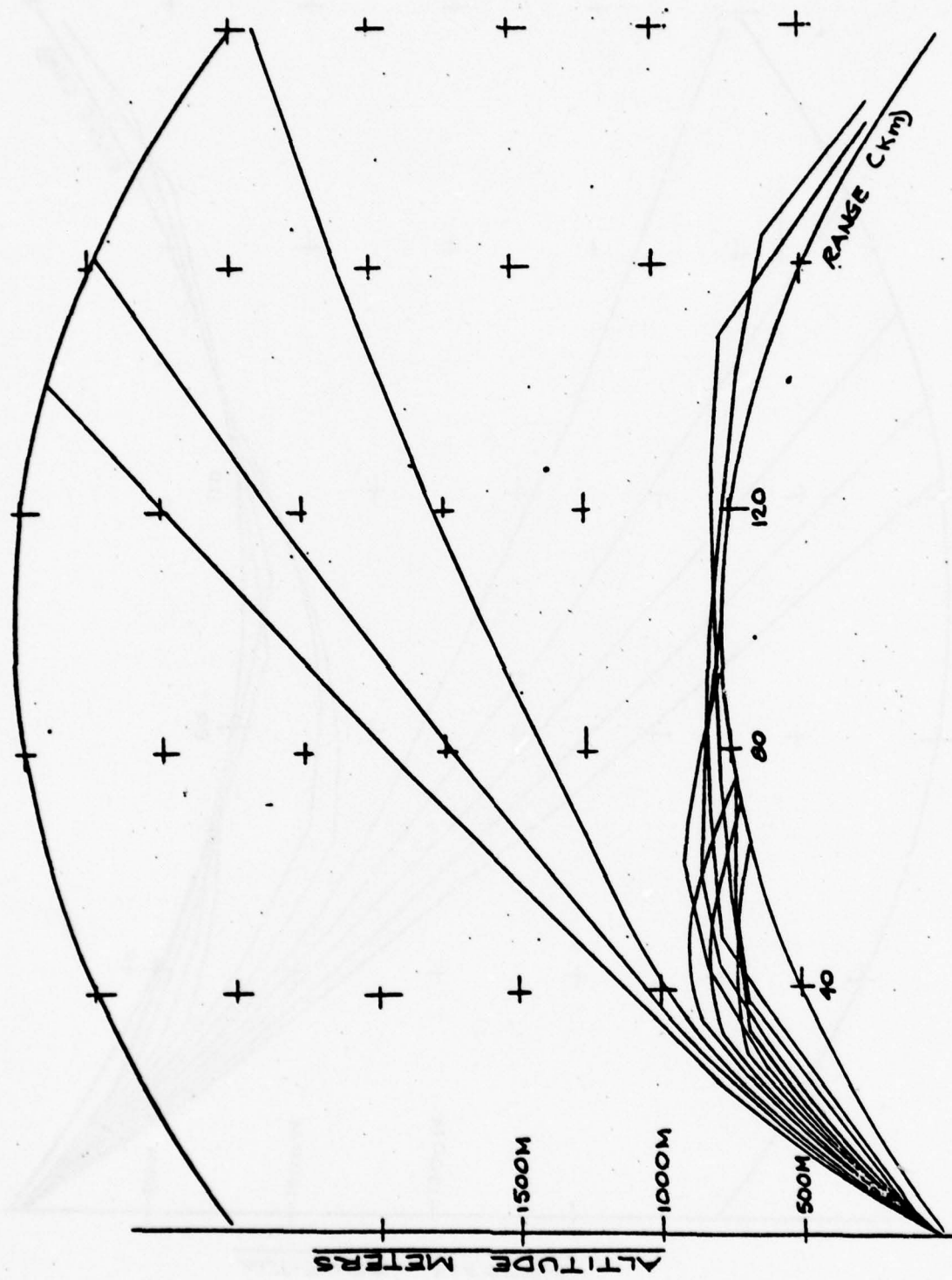


Figure (3-3) Typical Ray Trajectories for August 30

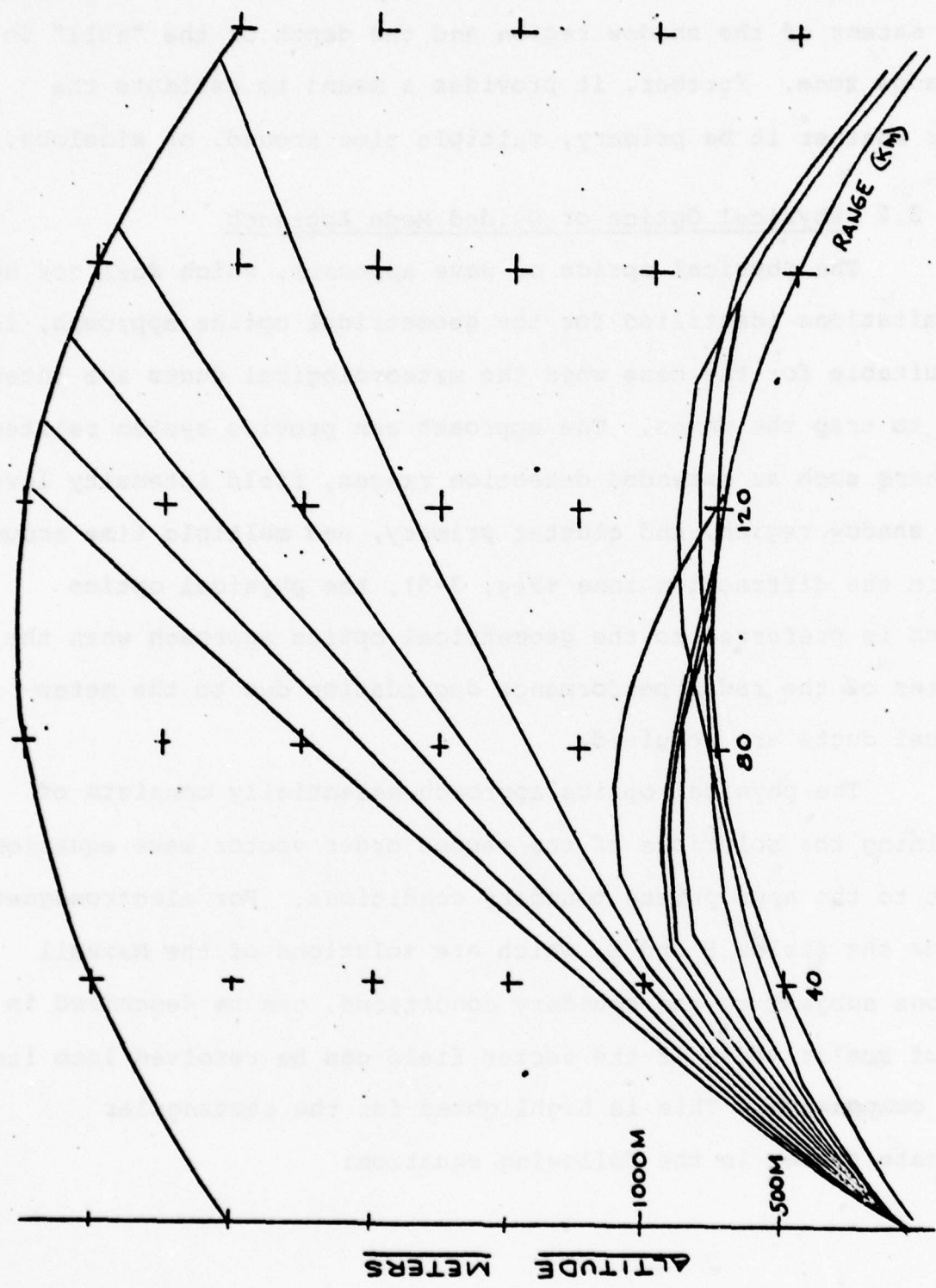


Figure (3-4) Typical Ray Trajectories for August 31

optics. The physical optics approach provides important information on the extent of the shadow region and the depth of the "null" in the shadow zone. Further, it provides a means to estimate the clutter whether it be primary, multiple time around, or sidelobe.

### 3.2 Physical Optics or Guided Mode Approach

The physical optics or wave approach, which does not have the limitations identified for the geometrical optics approach, is most suitable for the case when the meteorological ducts are intense enough to trap the waves. The approach can provide system related parameters such as extended detection ranges, field intensity levels in the shadow region, and clutter primary, and multiple time around. Thus, in the diffraction zone (Fig. 3-5), the physical optics approach is preferred to the geometrical optics approach when the estimates of the radar performance degradation due to the meteorological ducts are required.

The physical optics approach essentially consists of determining the solutions of the second order vector wave equation subject to the appropriate boundary conditions. For electromagnetic problems the fields  $\underline{E}$  and  $\underline{H}$ , which are solutions of the Maxwell equations subject to the boundary conditions, can be described in terms of scalar modes if the vector field can be resolved into its scalar components. This is highlighted for the rectangular coordinate system in the following equation:

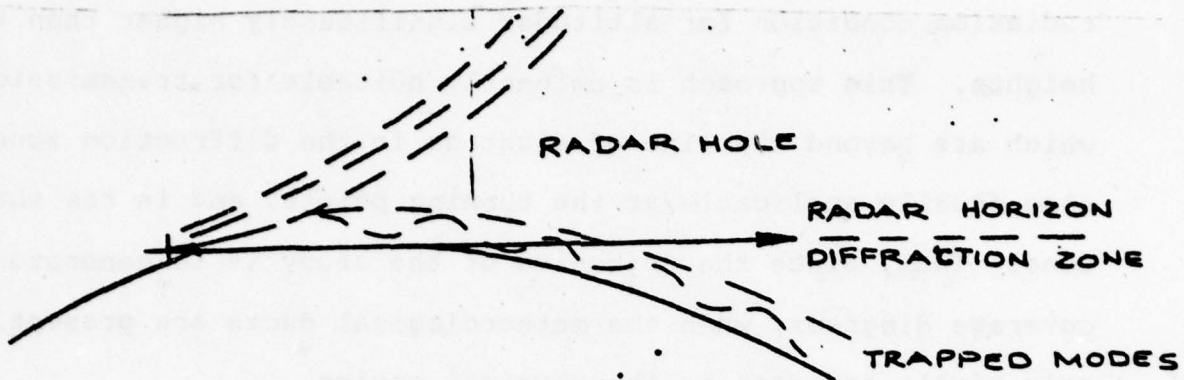


Figure (3-5) - Tropospheric Duct Propagation

$$\underline{\Phi} (\underline{r}) = \sum_i a_i \phi_i (\underline{r}) = \sum_i a_i \phi_i (T) e^{jk_{xi} x}$$

Here,  $\underline{\Phi} (\underline{r})$  is the total vector electromagnetic field and is described in terms of the summation of the characteristic modes,  $\phi_i (T)$ ; and  $T$  stands for the transverse coordinates  $y$  and  $z$  which are orthogonal to  $x$ , the direction of propagation. The longitudinal wave numbers  $k_{xi}$  are the characteristic values. The modes  $\phi_i (T)$  are functions of the transverse coordinate, and they form a complete orthonormal set. The amplitude coefficient  $a_i$  thus are determined from the source conditions with the help of the orthogonality condition. Thus implicit in this approach are the characteristics of the source generating field such as frequency, polarization, antenna height, etc. Application of the boundary condition implies

the statement of the field characteristics (a) at the ground, (b) at the different regions of the M profile, and (c) the Sommerfeld radiation condition for altitudes significantly higher than the duct heights. This approach is eminently suitable for transmission paths which are beyond the line of sight or in the diffraction zone and also equally applicable at the turning points, and in the shadow zone. Thus, since the objective of the study is to generate radar coverage diagrams, when the meteorological ducts are present, the only viable approach is the physical optics.

### 3.3 Ray Trajectories For Four Refractive Index Profiles

The geometrical optics or the ray trajectory approach involves the use of Snell's Law to identify the propagation paths. Typical ray trajectories for four days of refractive index profiles from Canton Island are shown in Figs. (3-6 to 3-9). For January and April meteorological conditions, the existence of shadow zones are clearly noticeable. This should be evident from the strength of the duct as measured by  $dN/dz$ .

For the September and December meteorological conditions, the duct has been weak and a weak shadow zone is evident. It is to be noticed that the shadow zones of January and April will not be as pronounced as is displayed if finer intervals in the trajectory angles are chosen. Based on these trajectories, one would conclude that in the shadow zone there will be a total absence of propagation paths and hence a total absence of electromagnetic power. The question which is very pertinent for system performance evaluation is how valid is this interpretation;

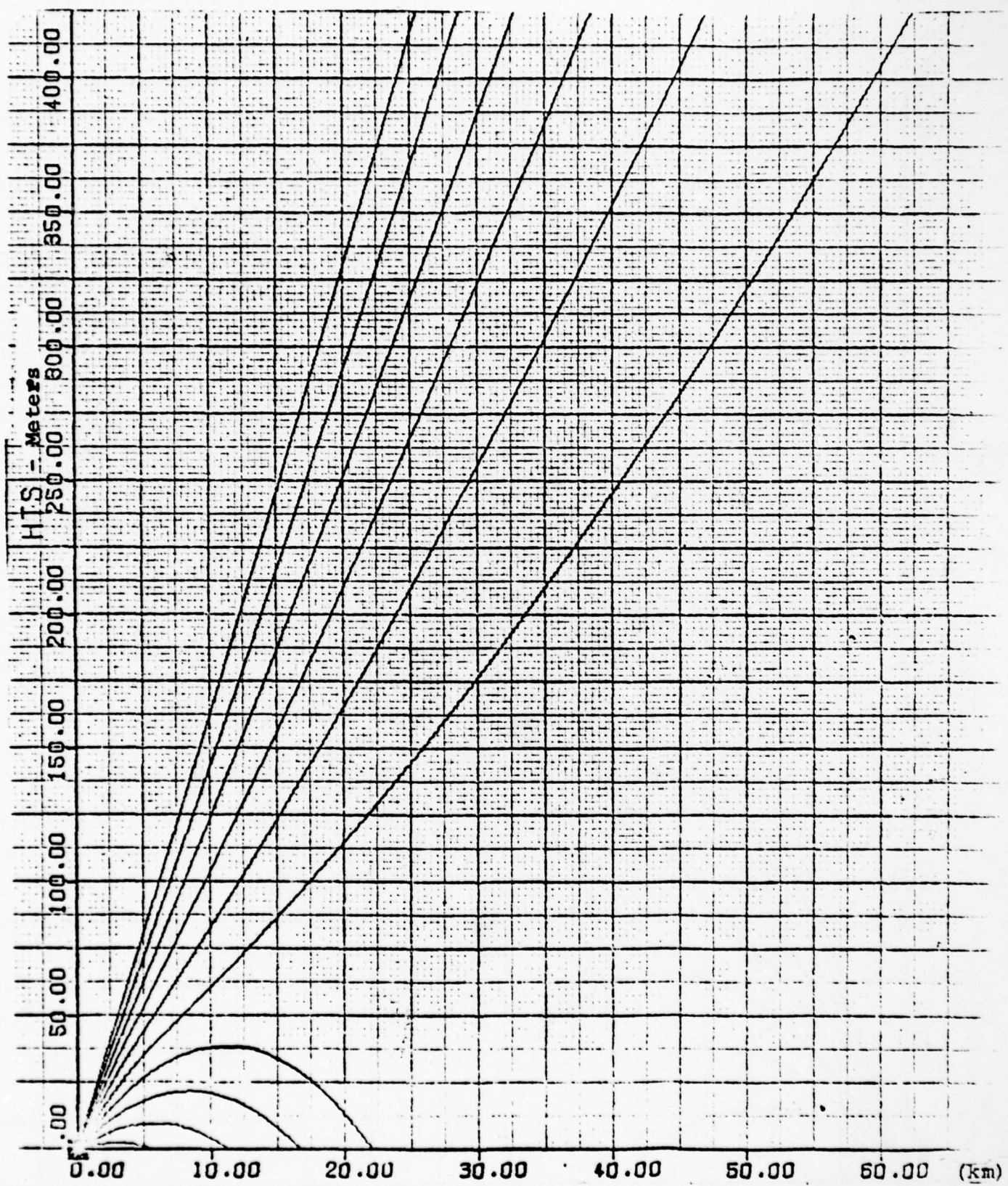


Fig. (3-6) Ray Trajectories for Canton Island - January, 1973

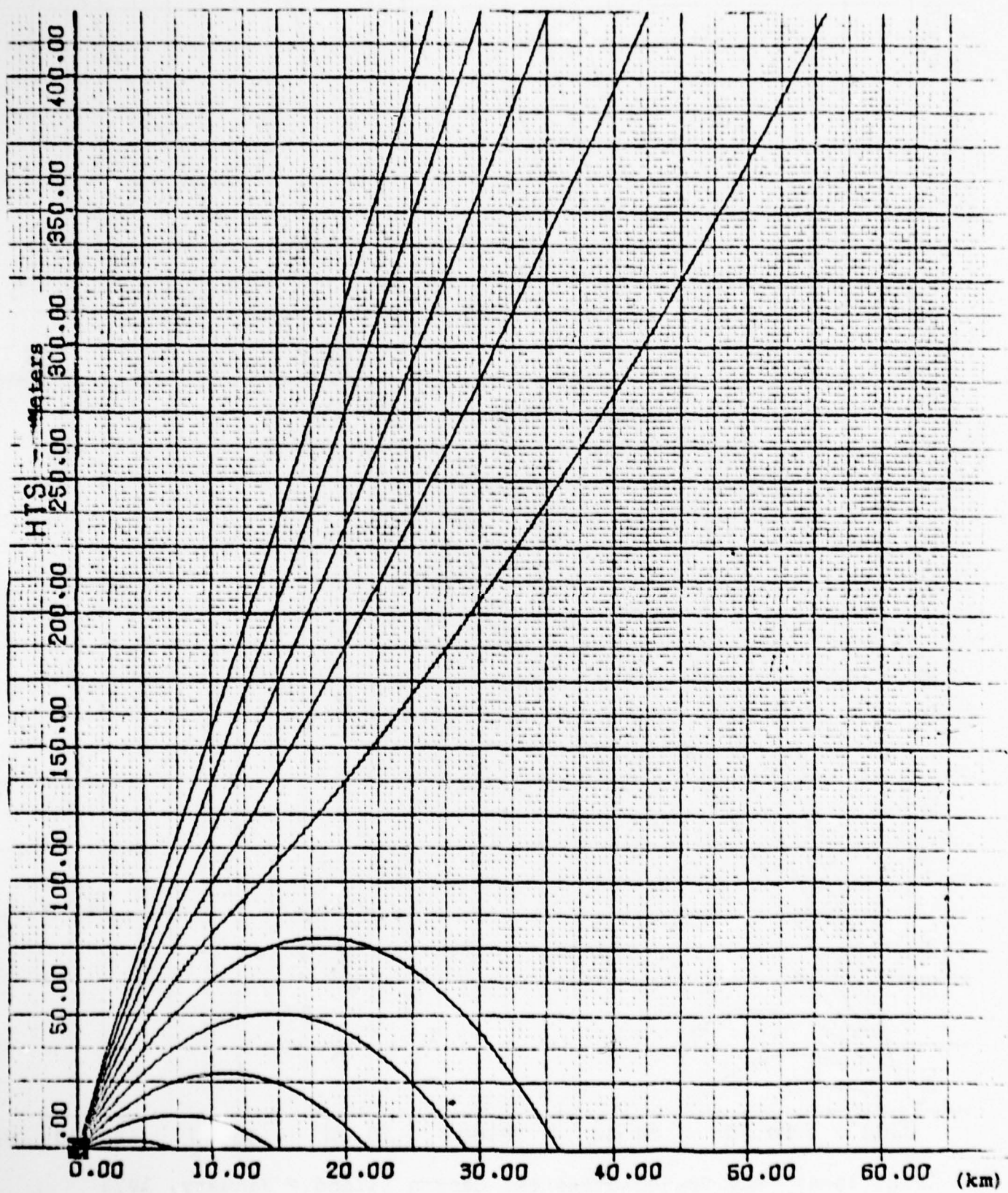


Fig. (3-7) Ray Trajectories For Canton Island - April, 1973

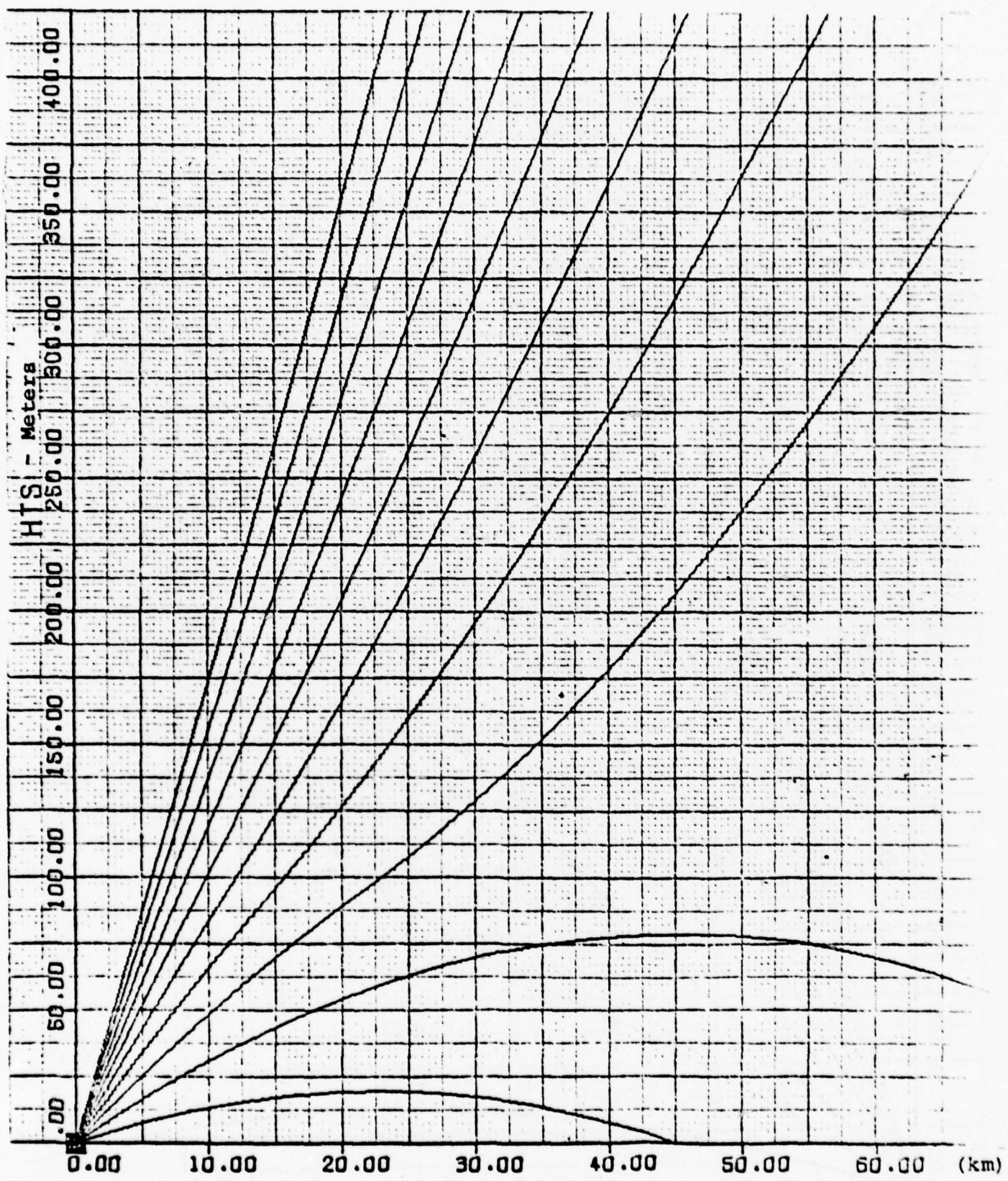


Fig. (3-8) Ray Trajectories For Canton Island - September, 1973

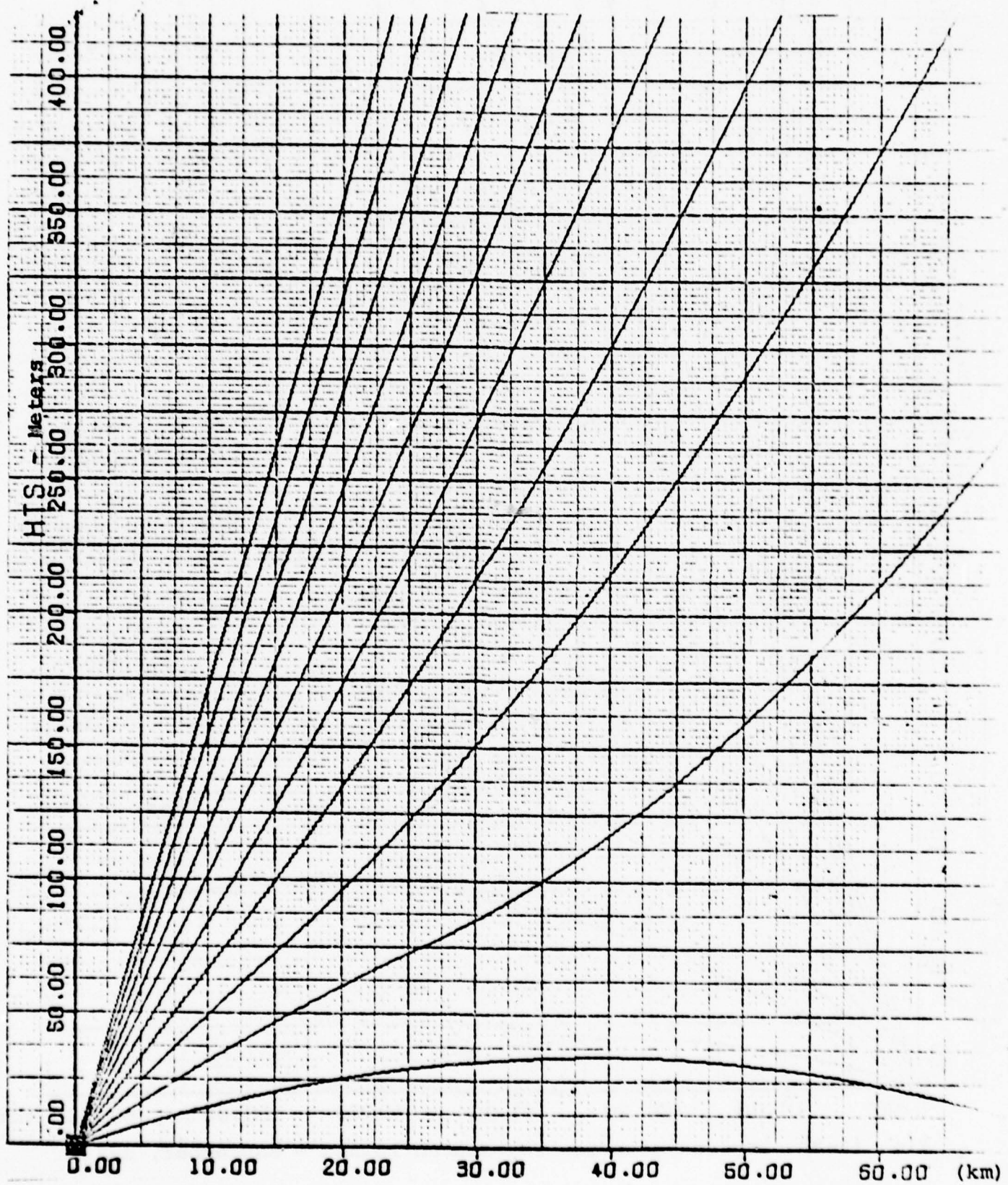


Fig. (3-9) Ray Trajectories For Canton Island - December, 1973

and is there a better way to estimate the field strength in the shadow zone.

In conclusion, it has been established that;

- a. the geometrical optics approach is not valid in the diffraction zone;
- b. it is inapplicable when the relative spacial variation of the refractive index per wavelength is larger than one;
- c. when the fractional change in the spacing between the neighboring rays in a wavelength is not less than unity, then it is not applicable.

#### 4. GUIDED MODE APPROACH - PHYSICAL OPTICS

It is thus evident that the guided mode approach is the most viable approach to establish radar performance in the diffraction zone and in the presence of meteorological ducts. The measure of the radar system performance is either (a) in terms of radar coverage diagrams depicting signal strengths or path loss as a function of ground range and altitude, or (b) the signal to noise ratio as a function of slant range. Such a performance evaluation is mandatory for the judicious hardware/software modifications to alleviate or minimize the deleterious effects of propagation degradation. Recognizing this, the goal of this phase of the program is to determine propagation behavior in the presence of bilinear and trilinear types of refractive index profiles. The important milestone of the next phase of the program is to establish the radar coverage diagrams for different meteorological conditions and for different systems parameters.

##### 4.1 Propagation Through Stratified Medium

For the propagation analysis, it was assumed that the medium is stratified in the vertical z direction. The stratification of the medium dictated by temperature, pressure and partial water vapor pressure variations with altitude is described in terms of the refractive index profile, which in turn is represented by the N-profile or the M-profile. The profiles which have been considered are the bilinear and trilinear. This is based on the evaluation of the Canton Island meteorological data for 1973.

The M-profile for January, April, September and December are produced in Fig. (4-1) and they will be considered in the numerical analysis.

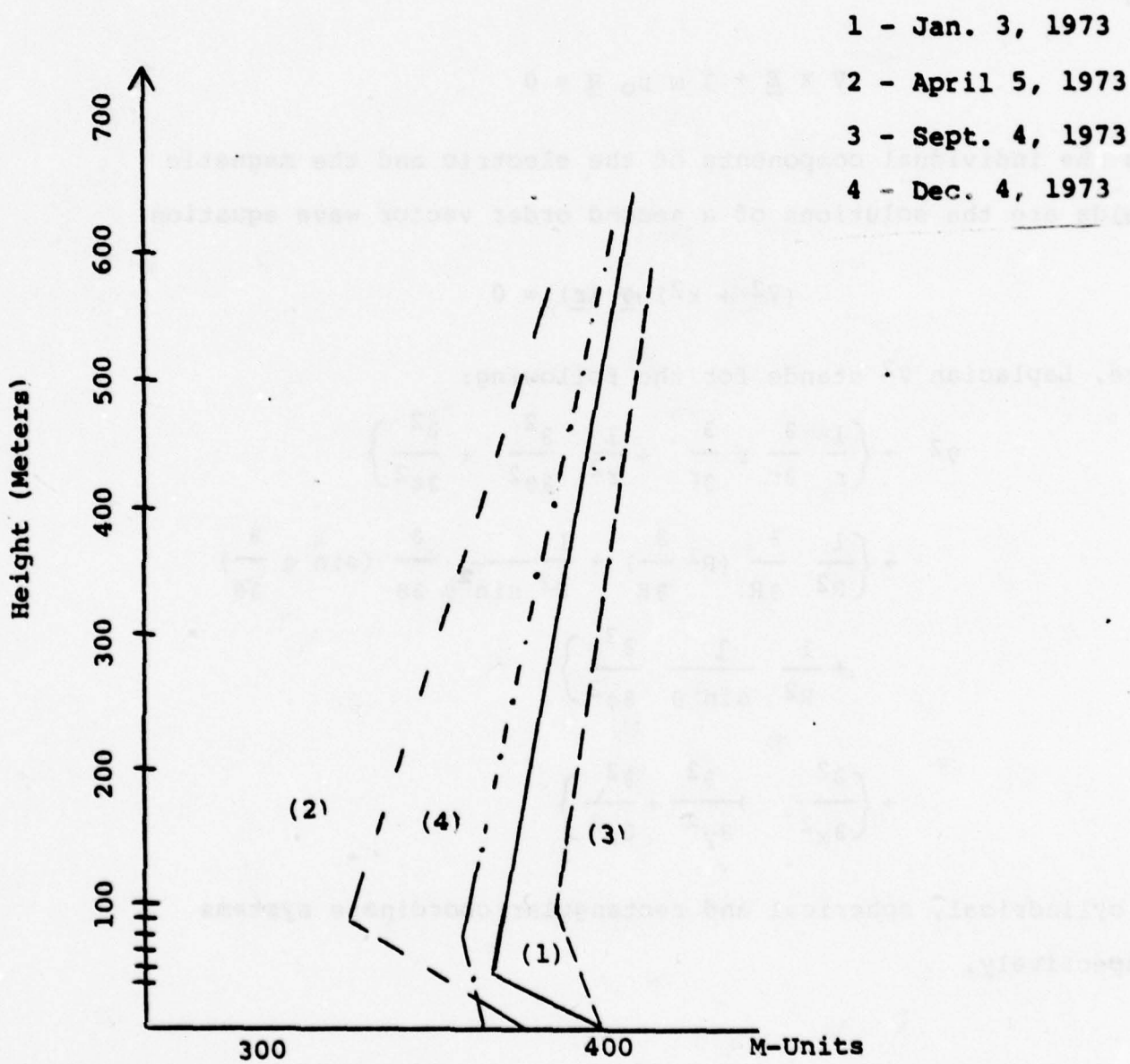


Fig. (4-1) - Canton Island Refractive Index Profiles for Four Days

**4.1.1 Propagation Through The Meteorological Duct With Bilinear M Profile**

The electromagnetic propagation through any medium is governed by Maxwell's equations.

$$\nabla \times \underline{H} - j \omega \epsilon_0 \underline{E} = 0$$

and

$$\nabla \times \underline{E} + j \omega \mu_0 \underline{H} = 0$$

and the individual components of the electric and the magnetic fields are the solutions of a second order vector wave equation

$$(\nabla^2 + k^2) \underline{\Phi} (\underline{r}) = 0$$

Here, Laplacian  $\nabla^2$  stands for the following:

$$\begin{aligned} \nabla^2 &\rightarrow \left\{ \frac{1}{r} \frac{\partial}{\partial r} r \frac{\partial}{\partial r} + \frac{1}{r^2} \frac{\partial^2}{\partial \theta^2} + \frac{\partial^2}{\partial z^2} \right\} \\ &\rightarrow \left\{ \frac{1}{R^2} \frac{\partial}{\partial R} (R^2 \frac{\partial}{\partial R}) + \frac{1}{R^2 \sin^2 \theta} \frac{\partial}{\partial \theta} (\sin \theta \frac{\partial}{\partial \theta}) \right. \\ &\quad \left. + \frac{1}{R^2 \sin \theta} \frac{1}{\partial \phi^2} \right\} \\ &\rightarrow \left\{ \frac{\partial^2}{\partial x^2} + \frac{\partial^2}{\partial y^2} + \frac{\partial^2}{\partial z^2} \right\} \end{aligned}$$

in cylindrical, spherical and rectangular coordinate systems respectively.

The wave number  $k = k_0 n$ ,  $k_0$  is the free space wave number,  $k_0 = \omega/c$ ,  $\omega$  is the angular frequency and  $c$  is the velocity of light in free space.  $n$  is the refractive index of the medium.

The vector field  $\underline{\Phi}$  stands for the  $\underline{E}$  and  $\underline{H}$  field

$$\underline{\Phi} = \begin{pmatrix} \underline{E}(r) \\ \underline{H}(r) \end{pmatrix} e^{j\omega t}$$

For a point source above ground, such as the dipole, the wave equation is more suitably described in terms of the spherical coordinate system. For the homogeneous atmosphere the mode solution of the wave equation was first obtained by Watson (18) and is given by

$$E_y = e^{j\omega t} \sum_m \frac{A_m}{x^{1/2}} e^{-jk_x m \cdot x} u_{m1}(z) u_{m2}(z)$$

Here,  $u_{m1}(z)$  and  $u_{m2}(z)$  are the height gain functions at the transmitter and the receiver, respectively; the subscript 1 stands for transmitter and 2 for the receiver. The transmitter and receiver locations have been left unspecified. For a ground radar system, the transmitter position is fixed at  $h$  and then  $u_{m1}(z) \equiv u_m(h)$  is the specified antenna characteristics.

$A_m$  are the amplitude coefficients of the modes;  $x$  is the horizontal range. Finally, the height gain function  $u_m(z)$  is the solution of the one dimensional wave equation.

$$\left\{ \frac{d^2}{dz^2} + k_0^2 \hat{n}^2 - k_x^2 \right\} E_y(z) = 0$$

The  $x$  dependence has been assumed as  $e^{-jk_x \cdot x}$  and  $E_y(z) \equiv u_m(z)$ . The  $z$  dependence will be deleted from hereon.

The refractive index  $\hat{n}$  is assumed to be stratified only in the vertical  $z$  direction. For the chosen four days of M profile

$$\frac{dM}{dz} = -p \quad z < d$$

$$= +q \quad z > d$$

$d$  is the duct width.

The scalar wave equation for  $E_y$  is thus given by

$$\left\{ \frac{d^2}{dz^2} + k_0^2 (1 + 2M(z)) - k_x^2 \right\} E_y = 0$$

Thus for the M-profile, the wave equation takes the following form:

$$M(z) = M_0 - Pz \quad z < d$$

$$M_{\min} + q(z-d) \quad z > d$$

$$\left\{ \frac{d^2}{dz^2} + B_1 - C_1 z \right\} E_y = 0 \quad z < d$$

$$\left\{ \frac{d^2}{dz^2} + B_2 + C_2 z \right\} E_y = 0 \quad z > d$$

Here  $B_1 = k_0^2 (1 + 2 M_0) - k_x^2$

$$C_1 = 2k_0^2 P$$

$$B_2 = k_0^2 (1 + 2 (M_0 - pd - qd)) - k_x^2$$

$$C_2 = 2k_0^2 q$$

The wave equations are further transformed by the following change of variables

$$\xi_< = \frac{B_1}{C_1^{2/3}} - C_1^{1/3} z$$

$$\xi_> = \frac{B_2}{C_2^{2/3}} + C_2^{1/3} z$$

Thus substituting for  $\xi_<$  in the wave equations, we have a well known Stokes equation

$$\left\{ \frac{d^2}{d\xi^2} + \xi \right\}_< E_y < = 0$$

$$\xi_<d = \xi_{1d}, \quad \xi_>d = \xi_{2d}$$

$$\xi_{1d} = \frac{B_1}{C_1^{2/3}} - C_1^{1/3} d$$

$$\xi_{2d} = \frac{B_2}{C_2^{2/3}} + C_2^{1/3} d$$

$$\xi_< = \xi_{1d} - C_1^{1/3} (z-d)$$

$$\xi_> = \xi_{2d} + C_2^{1/3} (z-d)$$

and since

$$(B_1 - C_1 d) = (B_2 + C_2 d), \quad z = d$$

$$C_1^{2/3} \xi_{1d} = C_2^{2/3} \xi_{2d}$$

Finally,

$$\xi_{<0} = \xi_{10} = \frac{B_1}{C_1^{2/3}}$$

The Stokes equation now has to be solved with the help of the following boundary conditions:

$$E_y< = E_y>, \frac{dE_y}{dz} |_< = \frac{dE_y}{dz} |_> \quad z = d$$

For perfectly conducting earth

$$E_y = 0 \quad z = 0$$

$E_y$  for  $z \gg d$  is an outgoing wave. This condition represents the Sommerfeld radiation condition. The Stokes equation is well known and it has solutions in terms of Airy Integral Functions  $A_i(\xi)$  and  $B_i(\xi)$  and they are given by

$$E_y< = a A_i(-\xi<) + b B_i(-\xi<)$$

$$E_y> = c (A_i(-\xi>) + j B_i(-\xi>))$$

Here,  $a$ ,  $b$  and  $c$  are the coefficients to be determined by applying the boundary conditions. Note that up until now, we have not introduced any modal designate.

Application of the boundary conditions lead to the following transcendental equation

$$\frac{\left\{ A_i(-\xi_{10}) - \frac{A_i(-\xi_{10})}{B_i(-\xi_{10})} \cdot B_i(-\xi_{10}) \right\} \left\{ A_i'(-\xi_{20}) + j B_i'(-\xi_{20}) \right\}}{A_i(-\xi_{20}) + j B_i(-\xi_{20})}$$

$$= - \left( \frac{p}{q} \right)^{1/3} \left\{ A_i'(-\xi_{10}) - \frac{A_i(-\xi_{10})}{B_i(-\xi_{10})} \cdot B_i'(-\xi_{10}) \right\}$$

Here the prime refers to differentiation with respect to  $\xi$ , and

$$\frac{d}{dz} |_< = \frac{d}{d\xi} \cdot \frac{d\xi}{dz} |_< = - C_1^{1/3} \frac{d}{d\xi} |_<$$

$$\frac{d}{dz} |_> = \frac{d}{d\xi} \cdot \frac{d\xi}{dz} |_> = + C_2^{1/3} \frac{d}{d\xi} |_>$$

The solutions of the transcendental equations are the eigenvalues and for the fixed frequency, the wave number  $k_{xi}$  is related to the  $i$ th eigenvalue  $\xi_{1di}$  by

$$k_{xi}^2 = k_o^2 (1 + 2 M_{min}) - \xi_{1di} \cdot C_1^{2/3}$$

$$k_{xi} \approx (k_o (1 + M_{min}) - \left( \frac{p}{q} \right)^{2/3} \cdot \frac{\xi_{1di}}{L})$$

and

$$L = \left( \frac{2 k_o}{q^2} \right)^{1/3}$$

Thus, the solutions of the transcendental equation will enable one to determine the height gain functions and the eigenwave numbers along the x axis. Thus, the field corresponding to the wave numbers are completely determined with one exception, namely, the amplitude coefficients which are determined from the specification of excitation or antenna characteristics.

#### 4.1.2 Trilinear Refractive Index Profiles

The selective meteorological data from Canton Island (Tables 2-1 through 2-12) has revealed that although, because of the nature of the measurements, majority of the cases were representable as having bilinear refractive index profiles; there were occasions when the profiles were more representable as trilinear and this in particular when the ducts were elevated. This necessitated developing an analytical propagation model for the trilinear refractive index profile. In principal, the approach is identical to the one developed for bilinear case and it entails additional boundary conditions representing matching of the transverse impedances at the intermediate regions of M-profile.

In order to display the basic features of the trilinear refractive index profile, we have reproduced in Figs. (4-2, 3, 4) some well known refractive index profiles. The Fig. (4-2) is obviously a surface duct with the bilinear M-profile, Fig. (4-3) and (4-4) are in general categorized as elevated ducts with trilinear M-profiles.

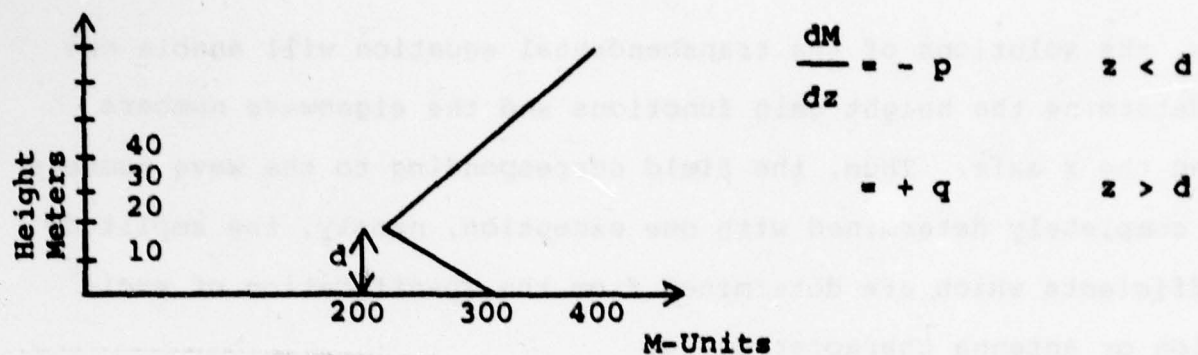


Fig. (4-2) - Surface Duct - Bilinear Profile

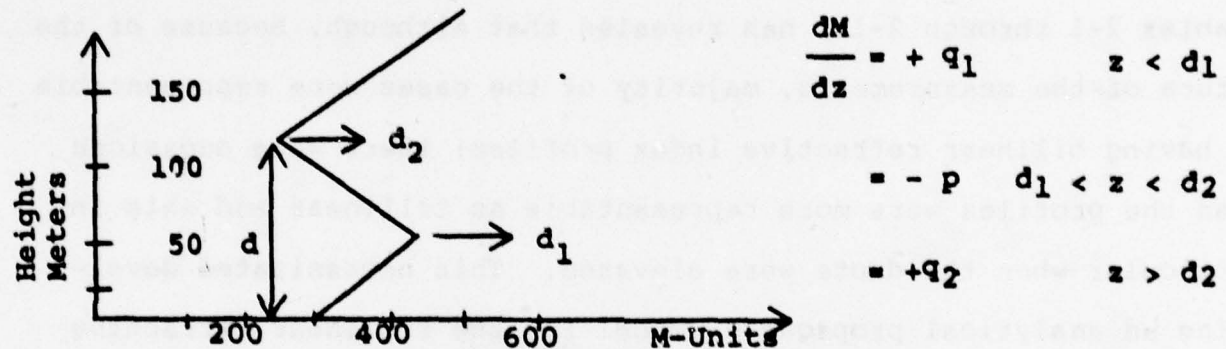


Figure (4-3) - Elevated Surface Duct - Trilinear Profile

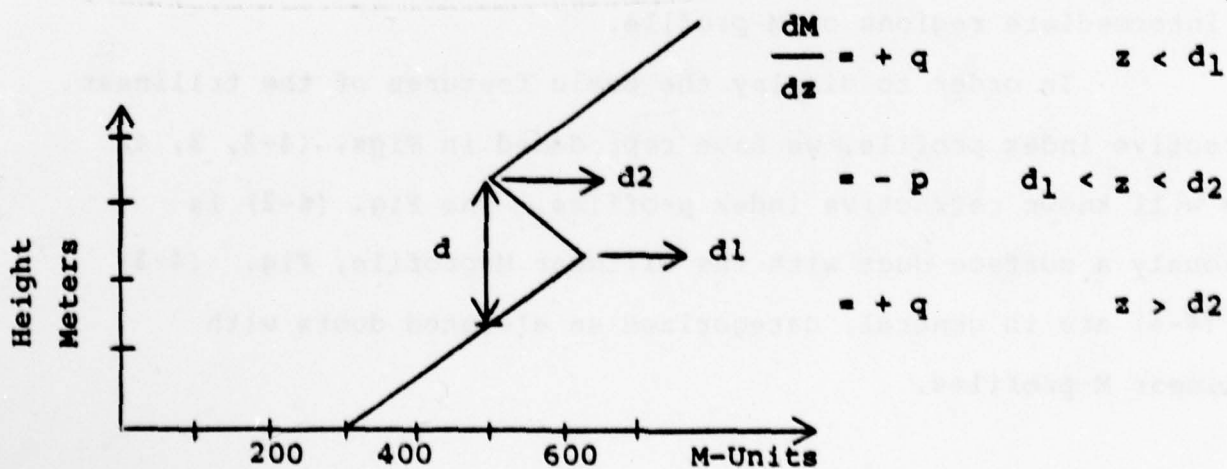


Figure (4-4) - Elevated Duct - Trilinear Profile

In all the three cases, the duct width is defined by  $d$ . In Figs. (4-3) and (4-4) note the difference in the elevated surface duct and the elevated duct. It is that at the duct apex the  $M_{min}$  is less than the  $M$  at the surface for the elevated surface duct case, and  $M_{min}$  is greater than  $M$  at the surface for the elevated duct. It is also to be recognized that in practice, the slope of the  $M$ -profile will not be that sharp, however, the measurement techniques perhaps would not provide closely spaced points to round off the  $M$  curves.

#### 4.1.3 Propagation through Ducts with Trilinear Profiles

The scalar wave equation for  $E_y$  for the trilinear refractive index profiles is given by:

$$\left\{ \frac{d^2}{dz^2} + k_o^2 [1+2M(z)] - k_x^2 \right\} E_y = 0$$

$$M(z) + M_o + q_1 z \quad z < d_1$$

$$+ M_o + q_1 d_1 - p(d_2 - d_1) + p(d_2 - z) \quad d_1 < z < d_2$$

$$+ M_o + q_1 d_1 - p(d_2 - d_1) + q_2(z - d_2) \quad z > d_2$$

or

$$\left\{ \frac{d^2}{dz^2} + B_1 + C_1 z \right\} E_y = 0 \quad z < d_1$$

$$\left\{ \frac{d^2}{dz^2} + B_2 - C_2 z \right\} E_y = 0 \quad d_1 < z < d_2$$

and

$$\left\{ \frac{d^2}{dz^2} + B_3 + C_3 z \right\} E_y = 0 \quad z > d_2$$

Here  $B_1, C_1; B_2, C_2;$  and  $B_3, C_3$  are given by

$$B_1 = k_o^2(1+2M_o) - k_x^2$$

$$C_1 = 2k_o^2 q_1$$

$$B_2 = k_o^2(1+2(M_o + q_1 d_1 + p d_1)) - k_x^2$$

$$C_2 = 2k_o^2 p$$

$$B_3 = k_o^2(1+2(M_o + q_1 d_1 - p(d_2 - d_1) - q_2 d_2)) - k_x^2$$

$$C_3 = 2k_o^2 q_2$$

Let

$$\xi_{<1} = \frac{B_1}{C_1^{2/3}} + C_1^{1/3} z \quad \frac{d\xi}{dz}|_{<} = +C_1^{1/3}$$

$$\xi_{<12>} = \frac{B_2}{C_2^{2/3}} - C_2^{1/3} z \quad \frac{d\xi}{dz}|_{<12>} = -C_2^{1/3}$$

$$\xi_{>2} = \frac{B_3}{C_3^{2/3}} + C_3^{1/3} z \quad \frac{d\xi}{dz}|_{>} = C_3^{1/3}$$

These substitutions in the wave equations lead to

$$\left\{ \frac{d^2}{d\xi^2} + \xi \right\}_{\begin{matrix} 1 \\ 2 \\ 3 \end{matrix}} E_{y_1} = 0$$

This again is the well known Spokes equation and has solutions in terms of Airy Integral functions.

Analogous to the bilinear case, the field description in the three different regions is as follows:

$$E_{y_1} = a_1 \left\{ A_i(-\xi_{<1}) - \frac{A_i(-\xi_{10})}{B_i(-\xi_{10})} B_i(-\xi_{<1}) \right\}$$

$$E_{y_2} = a_2 \left\{ A_i(-\xi_{<12}) + a_3 B_i(-\xi_{<12}) \right\}$$

$$E_{y_3} = a_4 \left\{ A_i(-\xi_{>2}) + j B_i(-\xi_{>2}) \right\}$$

The E field has to satisfy the following continuity relations:

$$\left. \begin{array}{l} E_{y_1} = E_{y_2} \\ \frac{dE_{y_1}}{dz} = \frac{dE_{y_2}}{dz} \end{array} \right\} \text{at } z = d_1$$

$$\left. \begin{array}{l} E_{y_2} = E_{y_3} \\ \frac{dE_{y_2}}{dz} = \frac{dE_{y_3}}{dz} \end{array} \right\} \text{at } z = d_2$$

These boundary conditions enable us to eliminate the different amplitude coefficients.

From now on we are specializing to the case of  $q_1 = q_2 = q$ . Consider first the continuity relations for field and its derivative at  $z = d_1$  which lead to the following equations:

$$a_1 \{ A_i(-\xi_1 d_1) - \frac{A_i(-\xi_{10})}{B_i(-\xi_{10})} \cdot B_i(-\xi_1 d_1) \} =$$

$$a_2 \{ A_i(-\xi_2 d_1) + a_3 B_i(-\xi_2 d_1) \}$$

and

$$a_1 \{ A_i'(-\xi_1 d_1) - \frac{A_i(-\xi_{10})}{B_i(-\xi_{10})} \cdot B_i'(-\xi_1 d_1) \} =$$

$$-\left(\frac{p}{q}\right)^{1/3} \cdot a_2 \{ A_i'(-\xi_2 d_1) + a_3 B_i'(-\xi_2 d_1) \}$$

or

$$\left\{ \begin{array}{l} A_i(-\xi_1 d_1) - \frac{A_i(-\xi_{10})}{B_i(-\xi_{10})} \cdot B_i(-\xi_1 d_1) \\ A_i'(-\xi_1 d_1) - \frac{A_i(-\xi_{10})}{B_i(-\xi_{10})} \cdot B_i'(-\xi_1 d_1) \end{array} \right\} =$$

$$-\left\{ \left(\frac{p}{q}\right)^{-1/3} \cdot \frac{\{ A_i(-\xi_2 d_1) + a_3 B_i(-\xi_2 d_1) \}}{\{ A_i'(-\xi_2 d_1) + a_3 B_i'(-\xi_2 d_1) \}} \right\}$$

Let the L.H.S.  $\equiv P/Q$ .

then

$$a_3 = - \left\{ \frac{A_i(-\xi_2 d_1) + \frac{p}{q} \left(\frac{p}{q}\right)^{1/3} \cdot A_i'(-\xi_2 d_1)}{B_i(-\xi_2 d_1) + \frac{p}{q} \left(\frac{p}{q}\right)^{1/3} \cdot B_i'(-\xi_2 d_1)} \right\}$$

Likewise, the continuity relations at  $z = d_2$  lead to the following

$$a_4 \{ A_i(-\xi>d_2) + jB_i(-\xi>d_2) \} =$$

$$a_2 \{ A_i(-\xi_2d_2) + a_3 B_i(-\xi_2d_2) \}$$

and  $a_4 \{ A_i'(-\xi>d_2) + jB_i'(-\xi>d_2) \} =$

$$-a_2 \left( \frac{p}{q} \right)^{1/3} \cdot \{ A_i'(-\xi_2d_2) + a_3 B_i'(-\xi_2d_2) \}$$

Thus the transcendental equation is given by

$$\left\{ \frac{A_i(-\xi>d_2) + jB_i(-\xi>d_2)}{A_i'(-\xi>d_2) + jB_i'(-\xi>d_2)} \right\} \cdot \left( \frac{q}{p} \right)^{-1/3} =$$

$$- \left\{ \frac{A_i(-\xi_2d_2) + a_3 B_i(-\xi_2d_2)}{A_i'(-\xi_2d_2) + a_3 B_i'(-\xi_2d_2)} \right\}$$

where

$$a_3 = - \frac{\left\{ A_i(-\xi_2d_1) + \left( \frac{p}{q} \right)^{1/3} A_i'(-\xi_2d_1) \right\}}{\left\{ B_i(-\xi_2d_1) + \left( \frac{p}{q} \right)^{1/3} B_i'(-\xi_2d_1) \right\}}$$

#### 4.2 The Solutions of the Transcendental Equation - The Bilinear Refractive Index Profile

The transcendental equation which is arrived at by satisfying the boundary conditions at  $z=d$ , physically represents the matching of the transverse impedances at  $z=d$ .

$$Z_{z<} = Z_{z>}$$

or equivalently  $\phi(Z) \equiv (Z_{z<} - Z_{z>}) = 0$

Here  $\frac{E_y}{H_x} \propto \frac{E_y}{\frac{dE_y}{dz}}$

and  $\mathfrak{B}_z<$ ,  $\mathfrak{B}_z>$  are the transverse impedances for  $z < d$  and  $z > d$ , respectively.

Because of the nature of the transcendental equation, a closed form solution does not exist and an iterative, numerical procedure to locate the zeros of the function  $\phi(\mathfrak{B})$  has to be adopted. Three different approaches have been explored, and they are:

- a. The Newton-Raphson Method
- b. The Secant Method
- c. The Zero Crossing Method

#### 4.2.1 The Newton-Raphson Technique

This technique, essentially, provides a procedure to obtain an approximate solution of the transcendental equation which, after several iterations, approaches the exact solution and it states

$$\mathfrak{B}_1 = \mathfrak{B}_0 - \frac{\phi(\mathfrak{B}_0)}{\phi'(\mathfrak{B}_0)}$$

Here,  $\mathfrak{B}_0$  is the first trial solution of the transcendental equation  $\phi(\mathfrak{B}) = 0$ .  $\phi'(\mathfrak{B}_0)$  is the derivative of  $\phi$  with respect to  $\mathfrak{B}_0$  and  $\mathfrak{B}_1$  is the next better solution to be used for second iteration and so on. Thus, the  $i$ th solution is obtained from  $(i-1)$ th and is

$$\mathfrak{B}_i = \mathfrak{B}_{i-1} - \frac{\phi(\mathfrak{B}_{i-1})}{\phi'(\mathfrak{B}_{i-1})}$$

If the transcendental equation has n solutions then this procedure has to be repeated n times.

The Newton-Raphson iterative technique to locate the zeros of the transcendental equation is effective only when the trial solution is reasonably close to the actual solution. The Newton-Raphson procedure thus has severe limitations.

#### 4.2.2 The Secant Method

This iterative approach is analogous to the Newton-Raphson approach and the iterative solutions are given by

$$z_i = z_{i-1} - \frac{(z_i - z_{i-1})\phi(z_{i-1})}{\phi(z_i) - \phi(z_{i-1})}$$

Note that in the limit when  $z_i$  approaches the exact solution  $z_{i-1}$ , then this expression is identical to the Newton-Raphson expression. Alternatively, if  $|z_i - z_{i-1}| < \delta$  and if  $|\phi(z_i) - \phi(z_{i-1})| < \epsilon$  then the technique is identical with the Newton-Raphson technique. Here  $\delta$  and  $\epsilon$  are very small quantities.

#### 4.2.3 The Zero-Crossing Technique

Another technique which is applicable to determine the solutions of the transcendental equation is the zero crossing of  $\phi(z)$ , when  $\phi(z)$  is plotted as a function of  $z$ . This procedure is extremely effective for the trapped modes or when the  $\xi_{ldi}$  are pure real, positive or negative numbers.

In any case, for all three cases, the computer programs for the Airy Integral Functions and the Hankel Functions are required.

#### 4.3 Numerical Analysis For Bilinear M-Profile

It was decided that four meteorological profiles will be chosen in such a fashion that the two extremes of the characteristic parameters such as the duct height and duct intensity shall be chosen.

For the 3rd of January, the intensity of the duct was close to the maximum; for the 4th of December, the duct intensity was minimum. For the 4th of September the duct height was close to the largest while January 3rd it was close to the smallest. For the 5th of April the duct was moderately intense. For all four days, the profile was describable as bilinear. Finally, in order to extract the frequency dependence, three wavelengths were chosen, and they were 10, 20 and 50 cm.

Based on the expression for the maximum wavelengths that are trapped by ducts of height  $d$ , the following observation is made:

Table (4-1) - Trapped Wavelengths

Date	$d$ (meters)	$\lambda$ max (cm)
3rd Jan.	42	22.65
5th Apr.	85	65.20
4th Sept.	94	75.82
4th Dec.	75	54.04

- a. For 10 and 20 cm wavelengths the field is trapped for all the four cases.
  
- b. For 50 cm wavelengths the field is not trapped for Jan. 3rd case, however, it is trapped for the remaining three days.

#### 4.3.1 The Zero-Crossing Technique For Trapped Modes

For the four days of M-profile data and for three wavelengths 10, 20 and 50 cm, the transcendental function  $\phi(z)$  is plotted for various real values of  $z$  varying from -5 to +5. These plots are displayed in Figs. (4-5 to 4-16). The zero-crossing values of  $z$ , or equivalently  $\xi_{ld}$ , for which  $\phi(z) = 0$  are the solutions of the transcendental equation. Consider now the January 3rd profile and  $\lambda = 10$  cm case (Fig. 4-5). The zero-crossings take place for the following  $\xi_{ld}$  values:

$$\xi_{ld} = -1.25, 0.68, 2.8, 5.25$$

First observe that the zero-crossing at -1.67 is not a true crossing as is evident from the computations for finer spacings of the  $\xi_{ld}$  values. The  $\phi(z)$  will continue to decrease approaching  $-\infty$  for  $\xi_{ld}$  values in the vicinity of -1.65. Likewise for  $\xi_{ld} \rightarrow -1.68$ , the  $\phi(z)$  will increase approach  $+\infty$ ; hence no zero-crossing for  $\xi_{ld} = -1.67$  is possible.

The first  $\xi_{ld}$  for which  $\phi(z) = 0$  is -1.25 and this negative root needs to be interpreted. Consider the field  $E_y$  associated with this root and observe how it behaves as the height increases from  $z=0$  to  $z=d$  and  $z \gg d$ .

$\lambda$  - 0.1  
 $d$  - 42.0  
 $p/a$  - 4.3

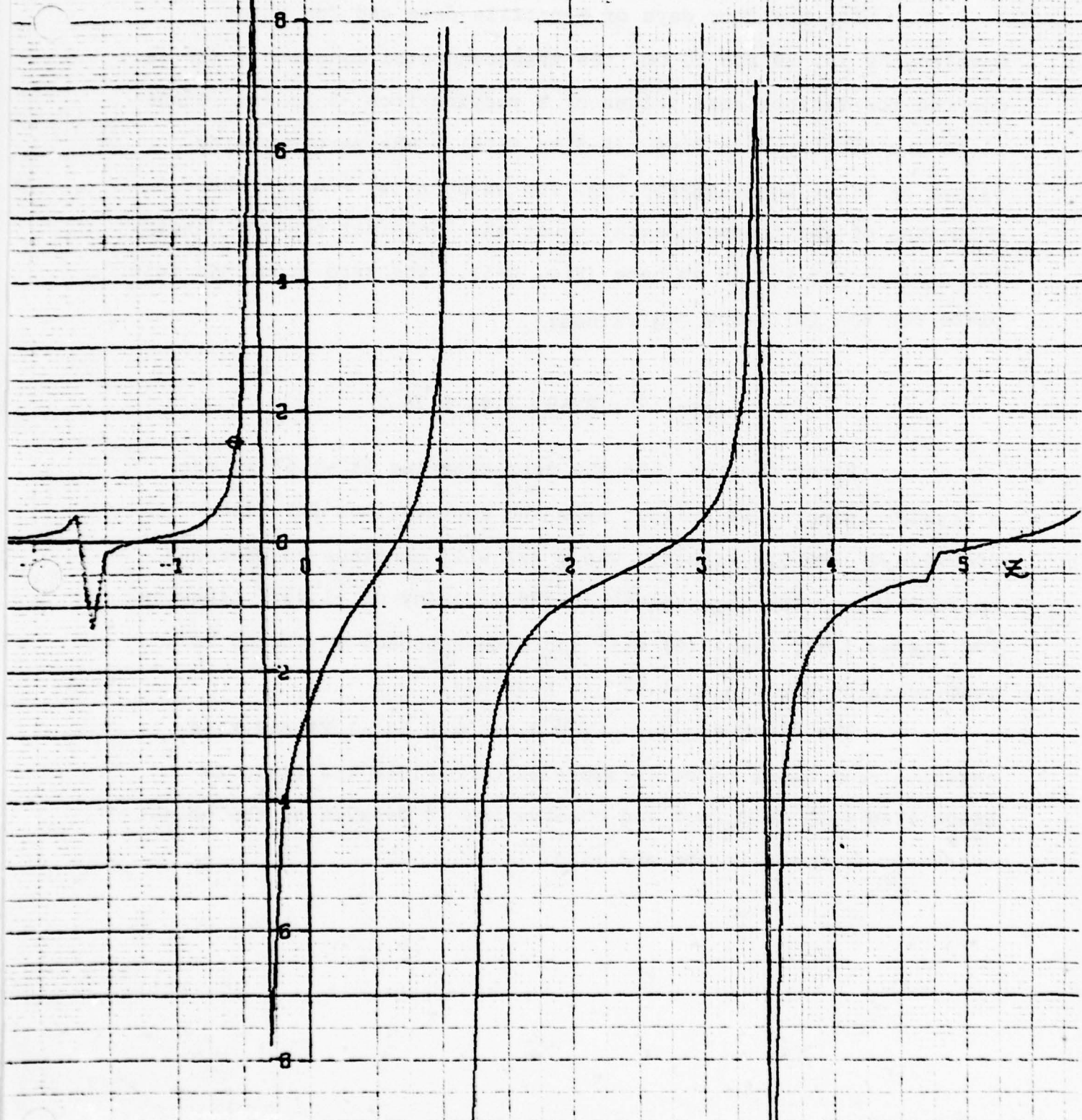


FIG. (4-5) PLOTS OF  $\phi(z)$  AS A FUNCTION OF  $z$

$\lambda = 0.2$   
 $a = 42.0$   
 $p/\tau = 4.8$

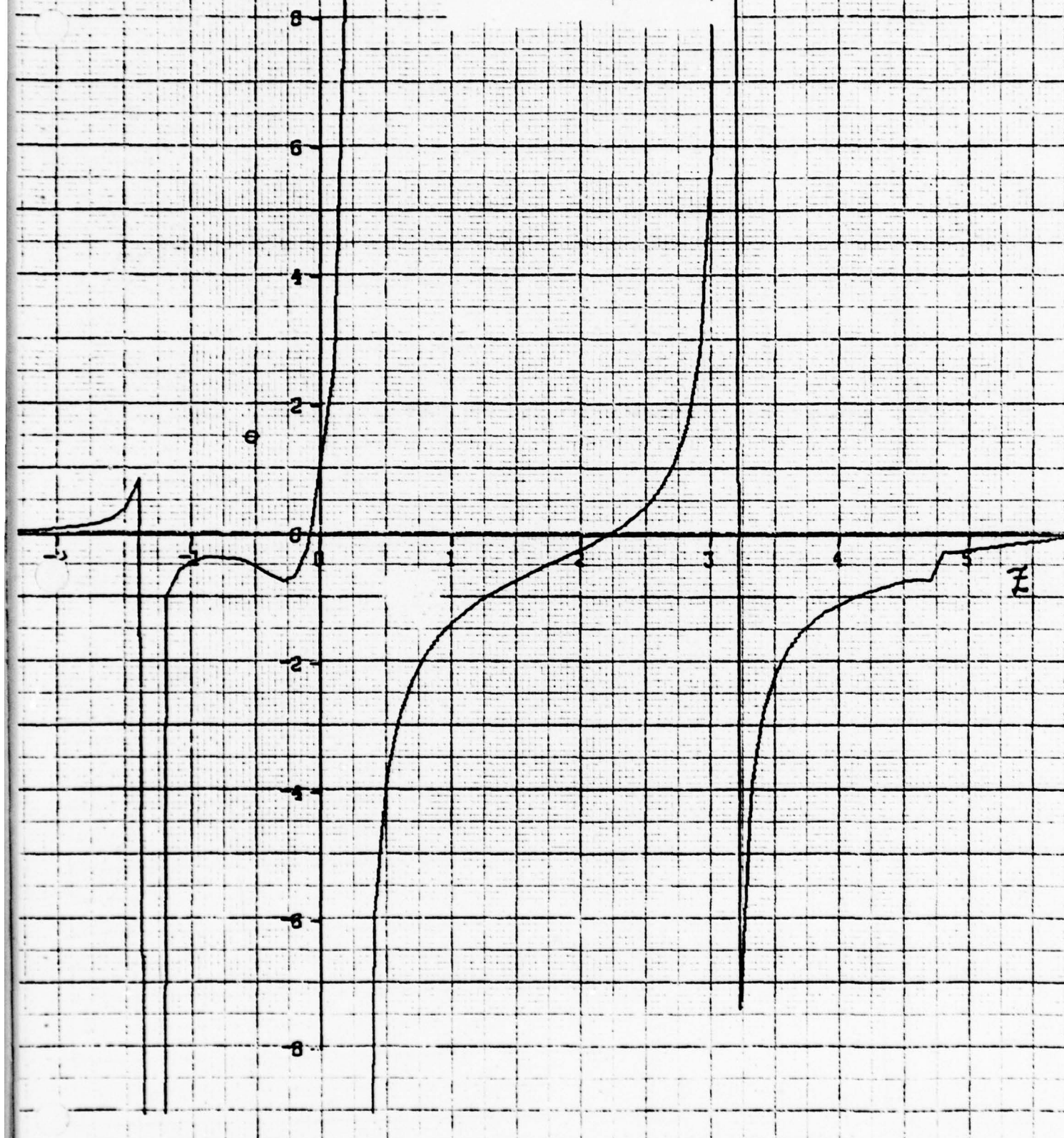


FIG. (4-6) PLOTS OF  $\psi(z)$  AS A FUNCTION OF  $z$

$\lambda$  = 0.5  
 $d$  = 42.0  
 $p/q$  = 4.8

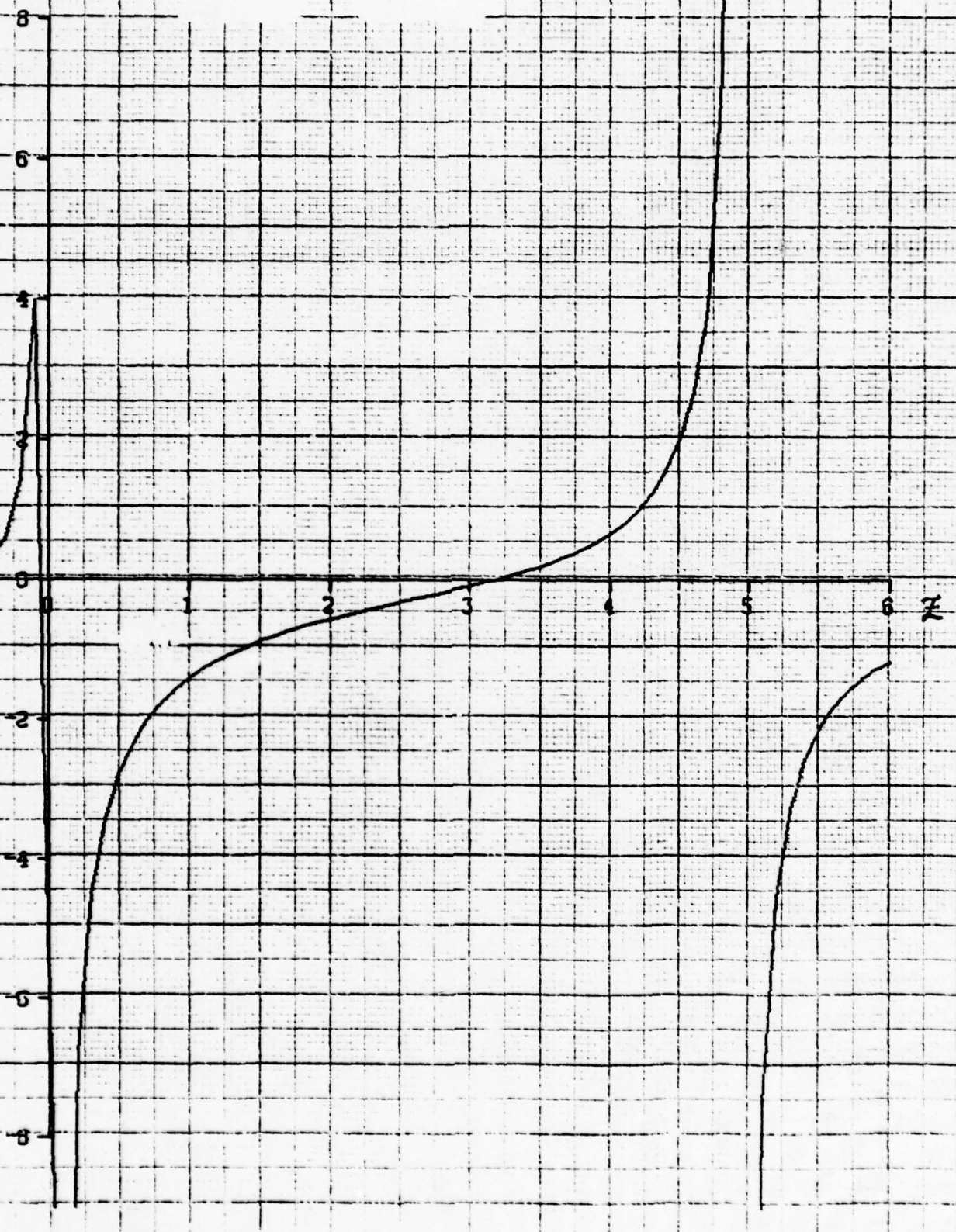


FIG. (4-7) PLOTS OF  $S(z)$  AS A FUNCTION OF  $z$

$\lambda$  - 0.1  
 $d$  - 85.0  
 $p/\alpha$  - 3.6

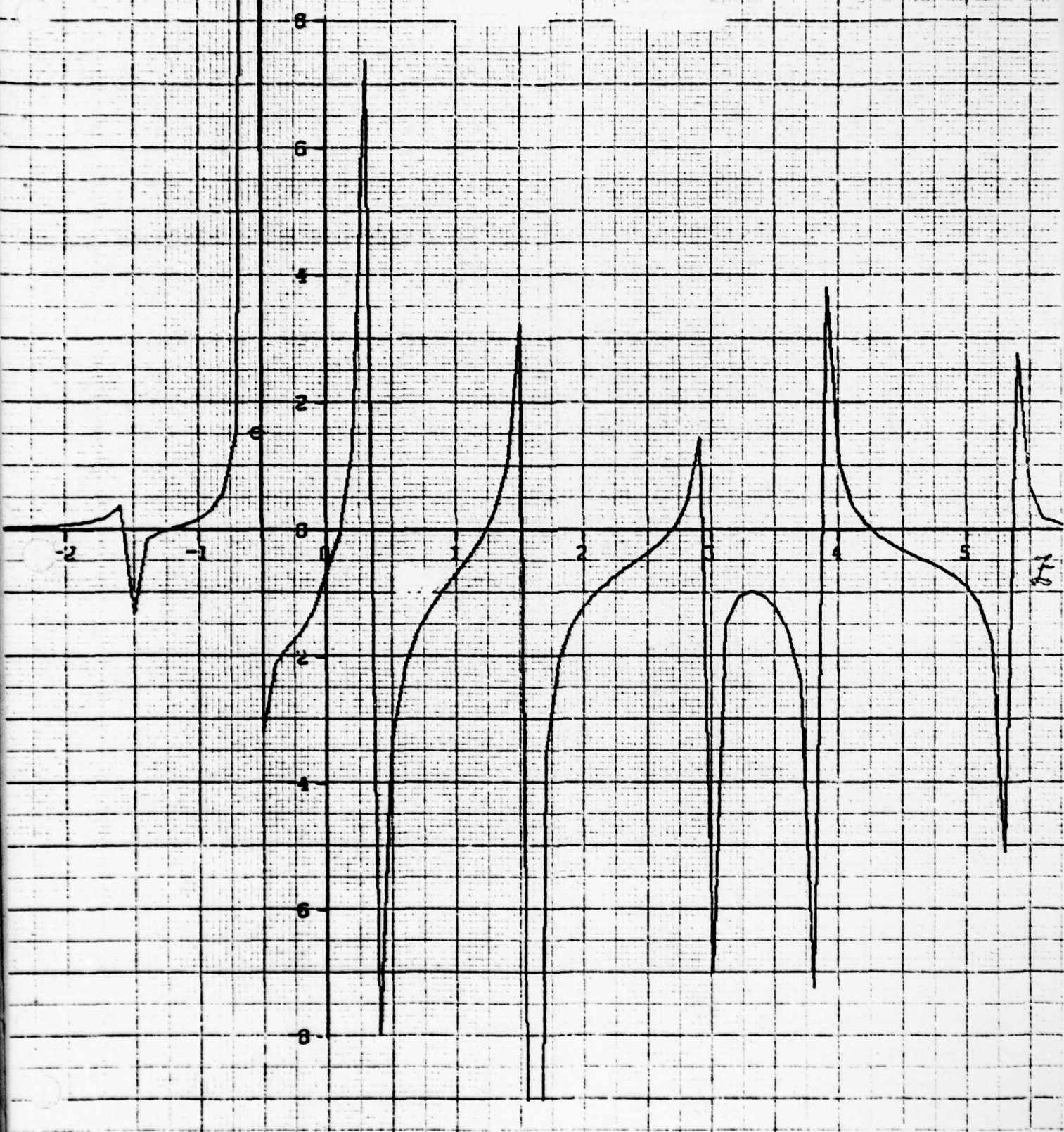


FIG. (4-8) PLOTS OF  $f(z)$  AS A FUNCTION OF  $z$

$\lambda = 0.2$   
 $d = 85.0$   
 $p/q = 3.6$

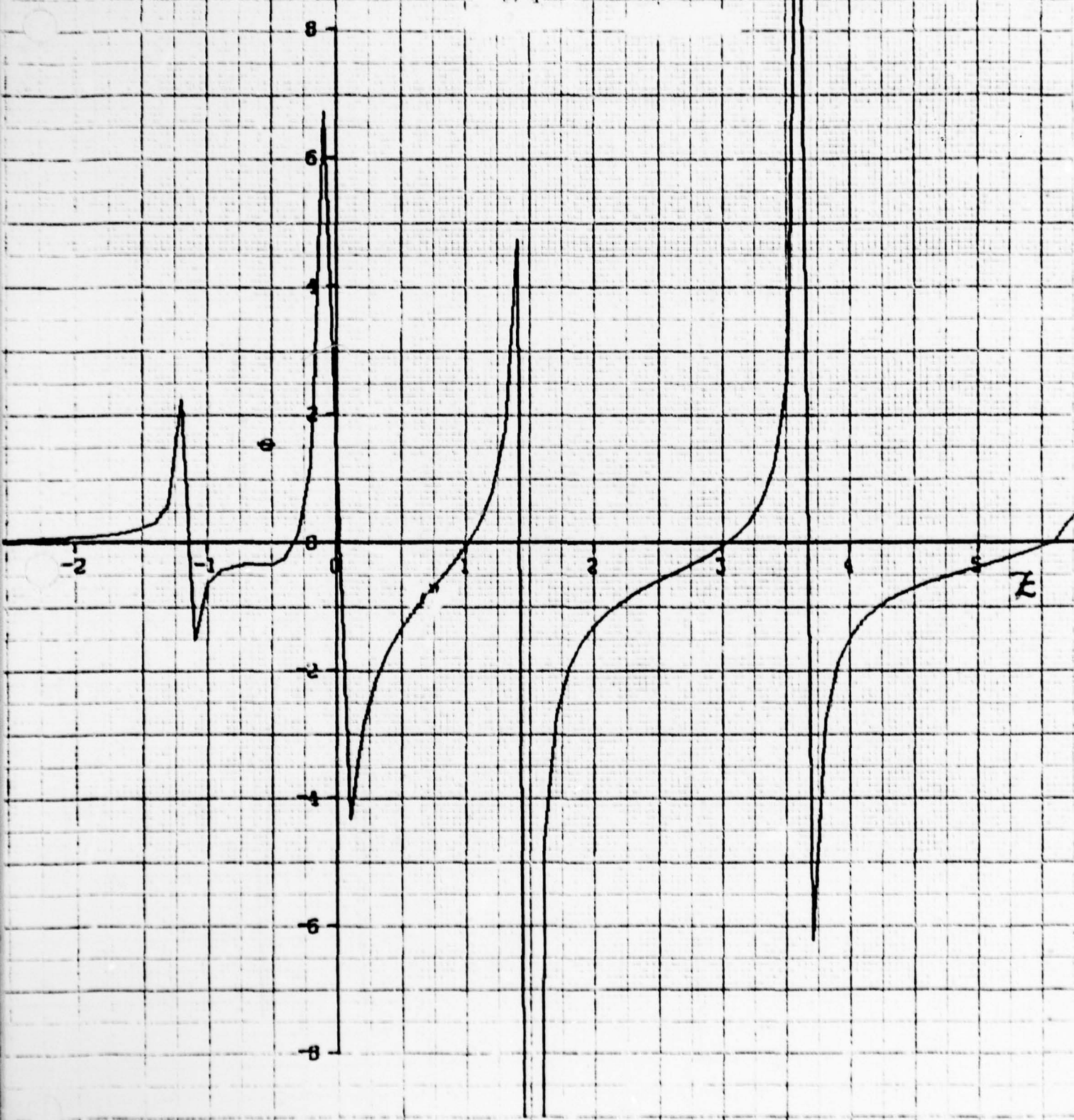


FIG. (4-9) PLOTS OF  $\Theta(z)$  AS A FUNCTION OF  $z$

67  
A - 1.5  
a - 85.0  
p/q - 3.6

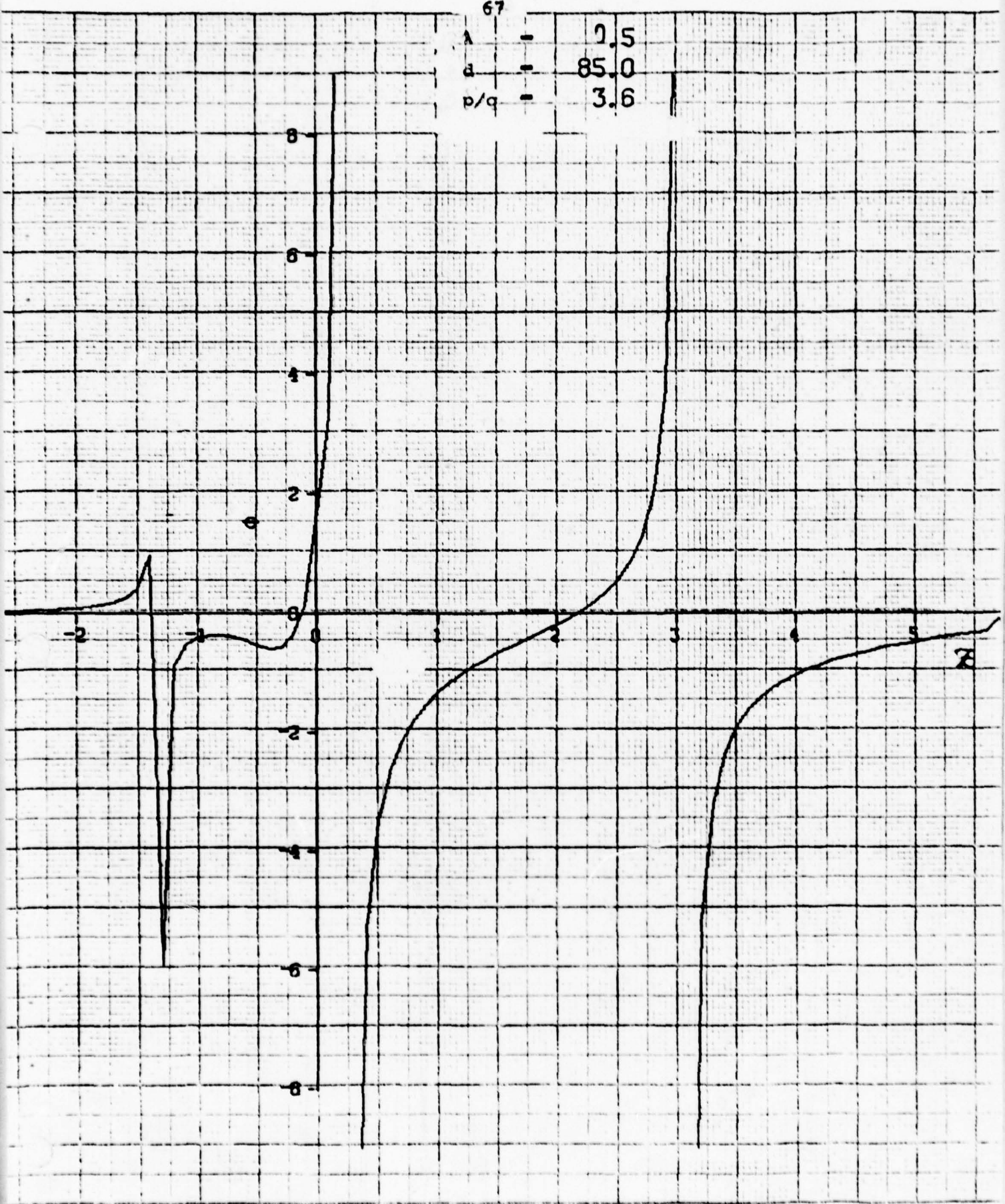
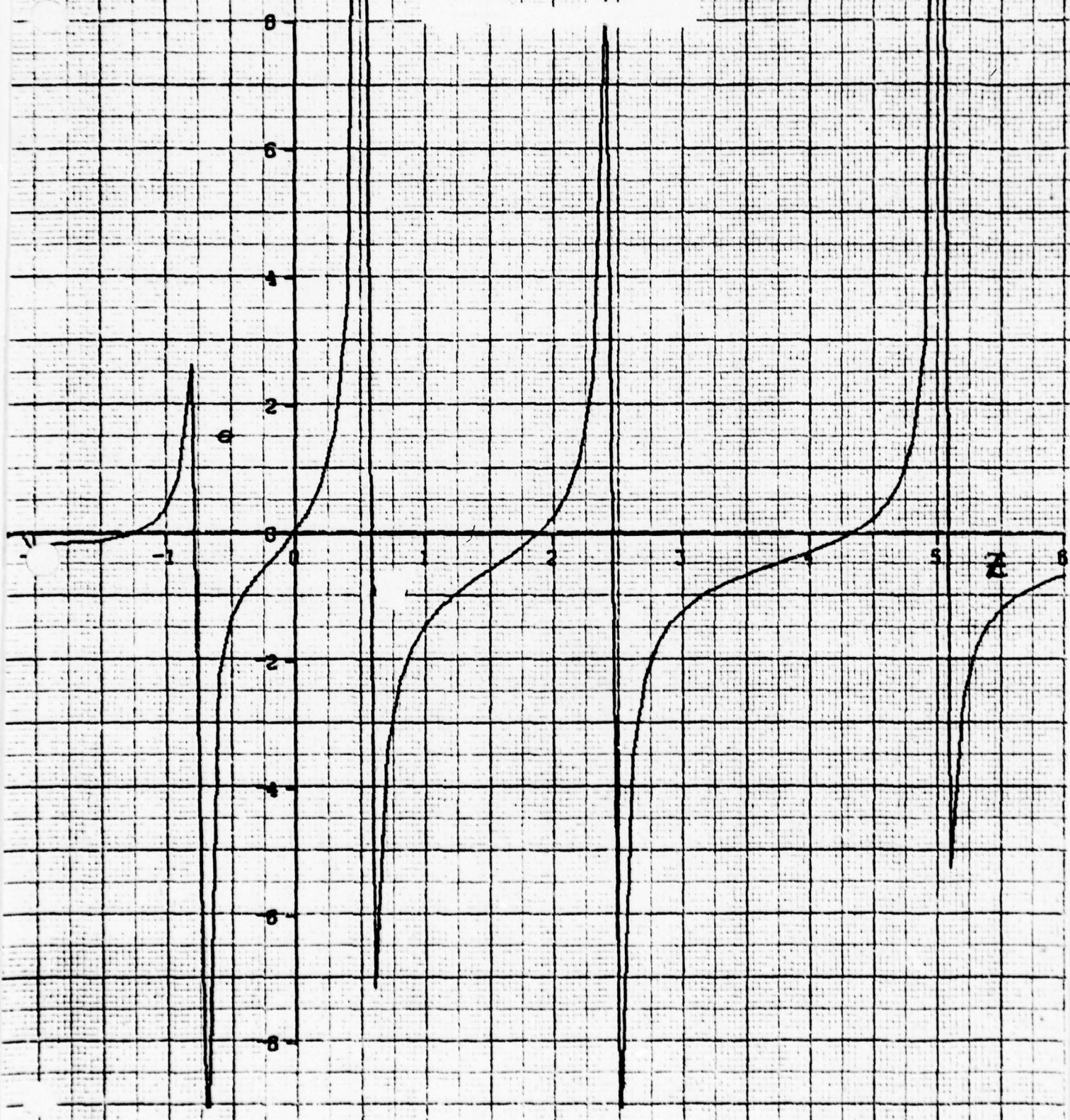


FIG. (4-10) PLOTS OF  $y(z)$  AS A FUNCTION OF  $z$

$$\begin{aligned}\lambda &= 0.1 \\ a &= 94.0 \\ p/q &= 0.6\end{aligned}$$

FIG. (4.11) PLOTS OF  $\Phi(z)$  AS A FUNCTION OF  $z$

$\lambda = 0.2$   
 $d = 94.0$   
 $p/q = 0.6$

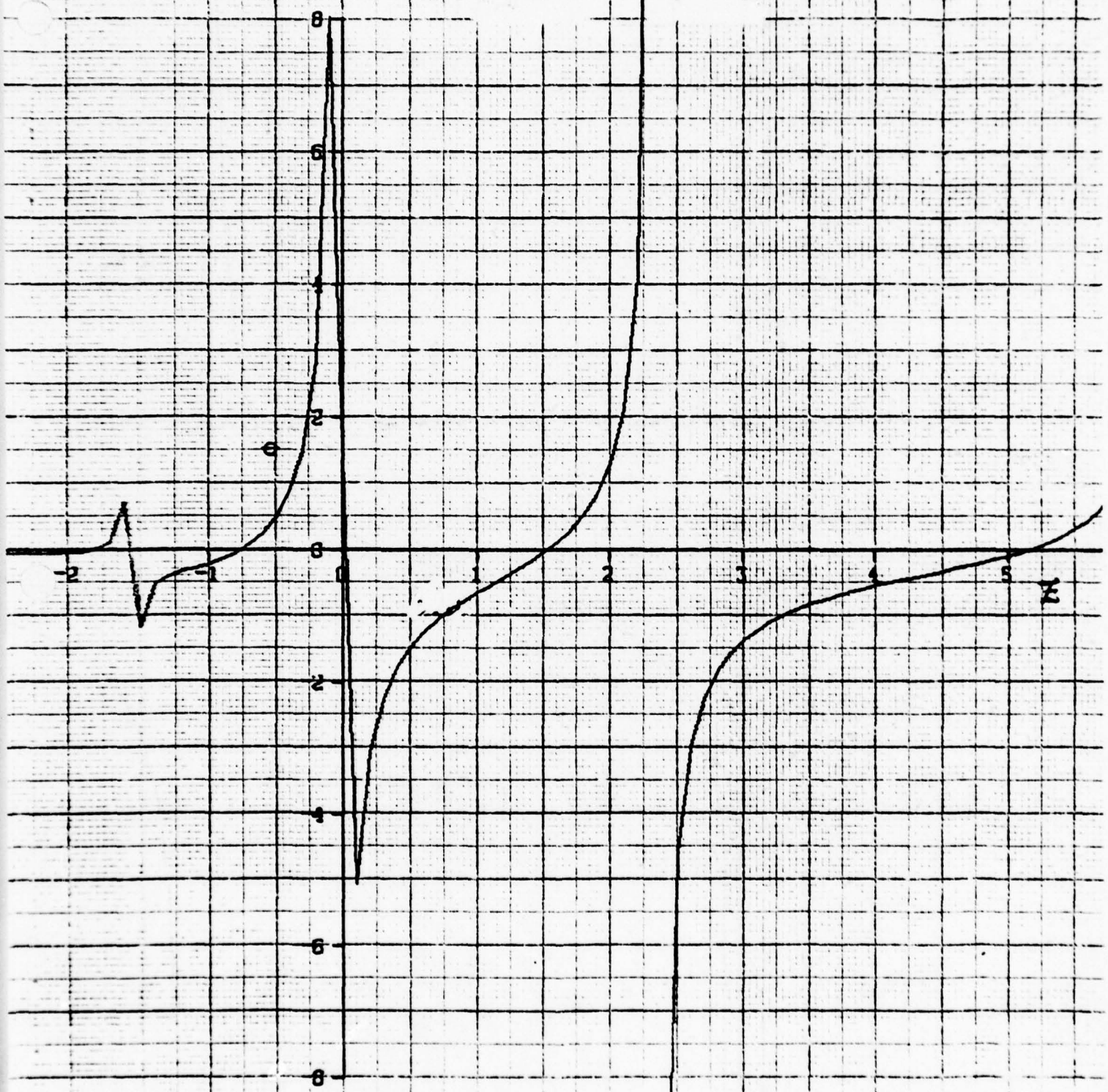


FIG. (4-12) PLOTS OF  $g(z)$  AS A FUNCTION OF  $z$

$$\begin{aligned}
 l &= 0.5 \\
 a &= 94.0 \\
 p/q &= 0.6
 \end{aligned}$$

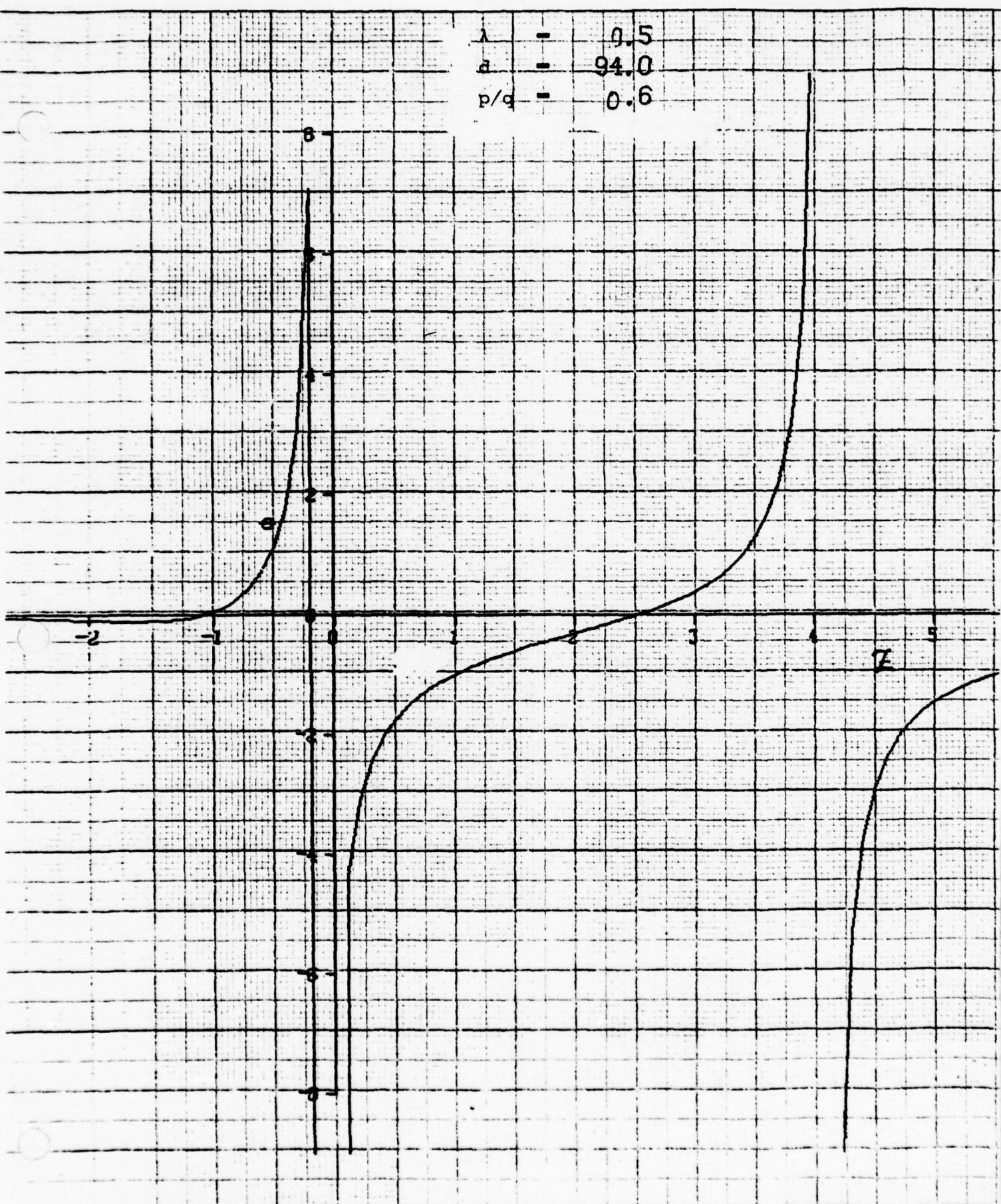


FIG. (4-13) PLOTS OF  $S(z)$  AS A FUNCTION OF  $z$

$\lambda = 0.1$   
 $d = 72.0$   
 $p/q = 0.3$

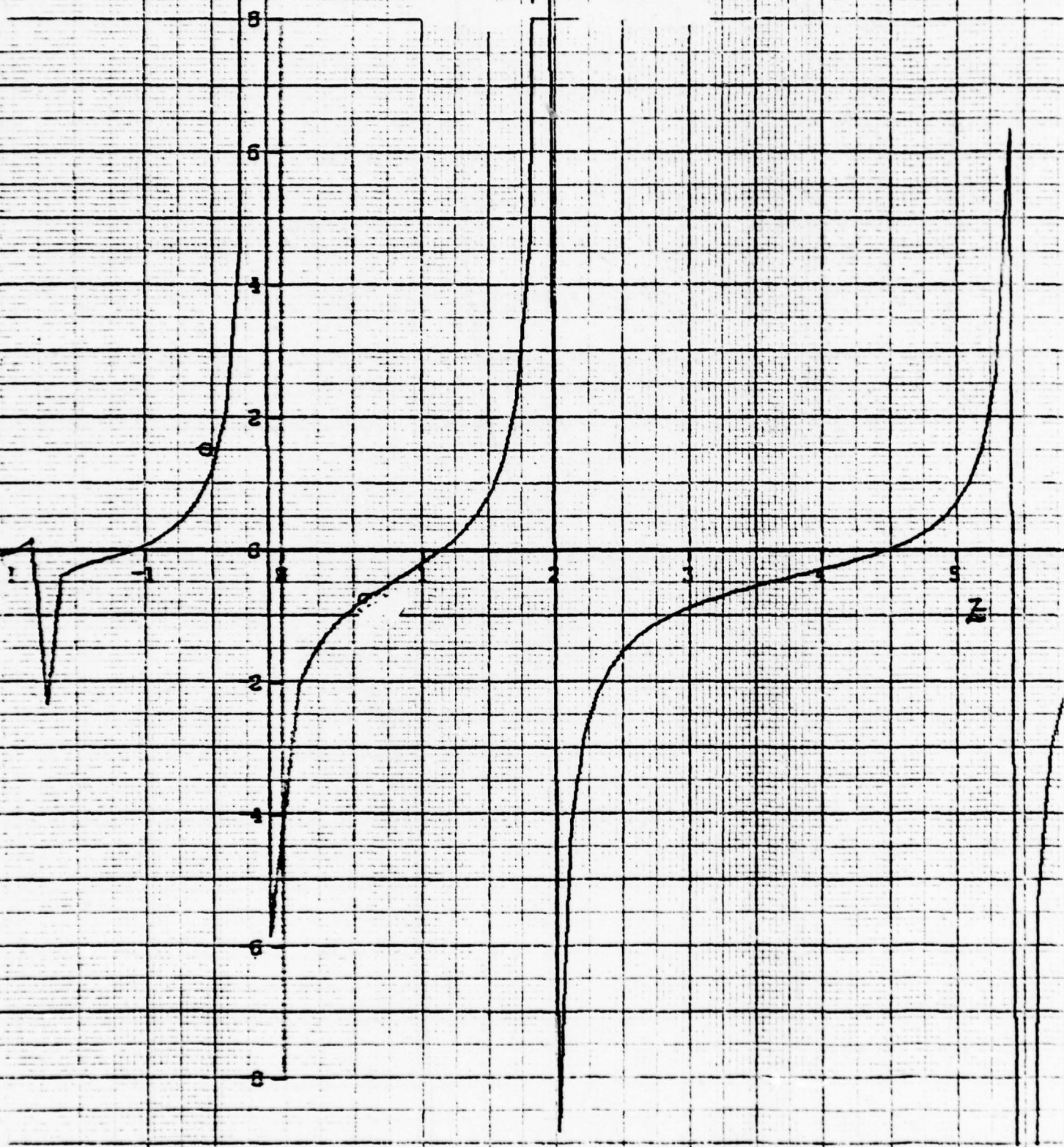
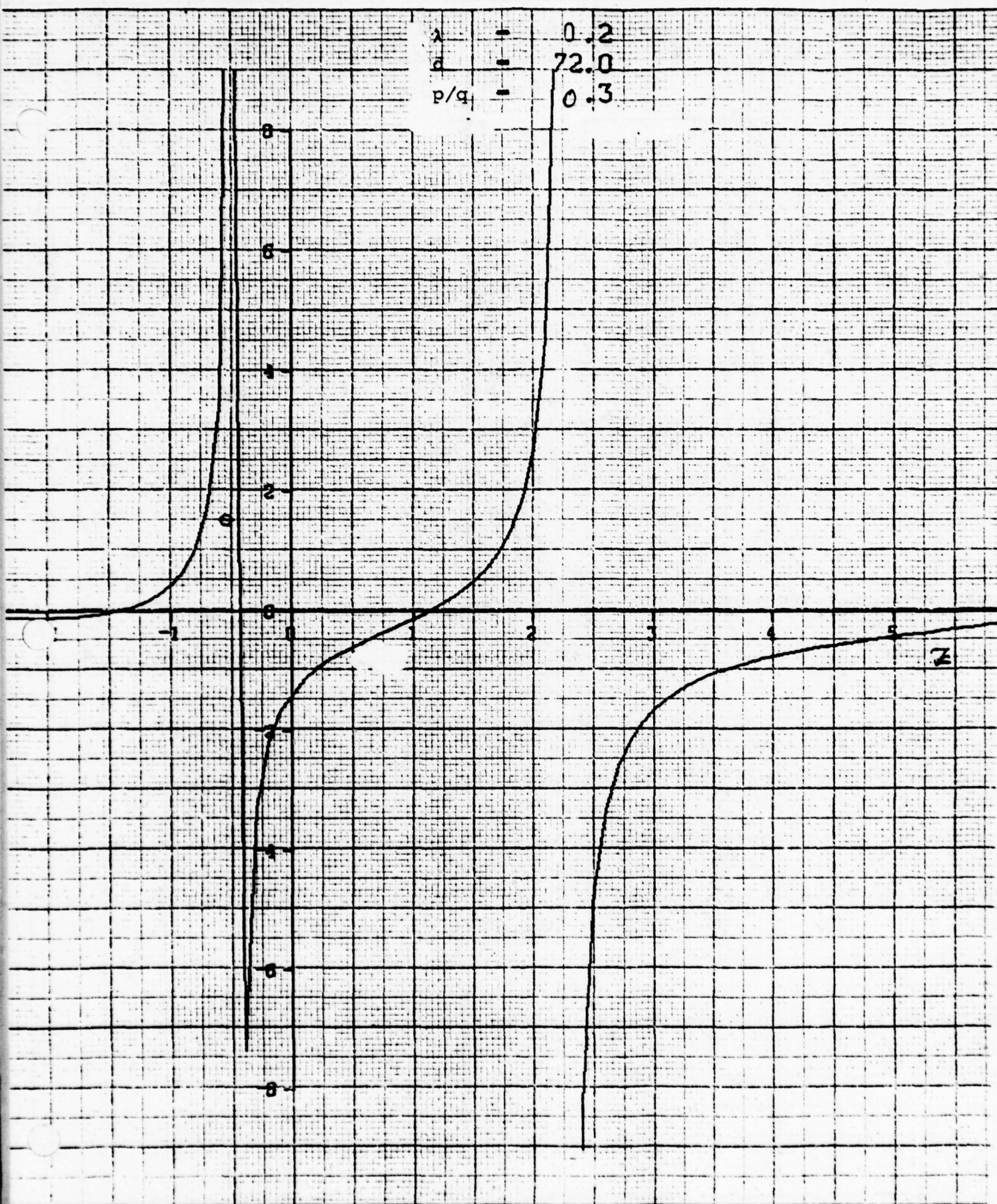


FIG. (4-14) PLOTS OF  $K(z)$  AS A FUNCTION OF  $z$

$$\begin{aligned}\lambda &= 0.2 \\ d &= 72.0 \\ p/q &= 0.3\end{aligned}$$

FIG. (4-15) PLOTS OF  $f(z)$  AS A FUNCTION OF  $z$

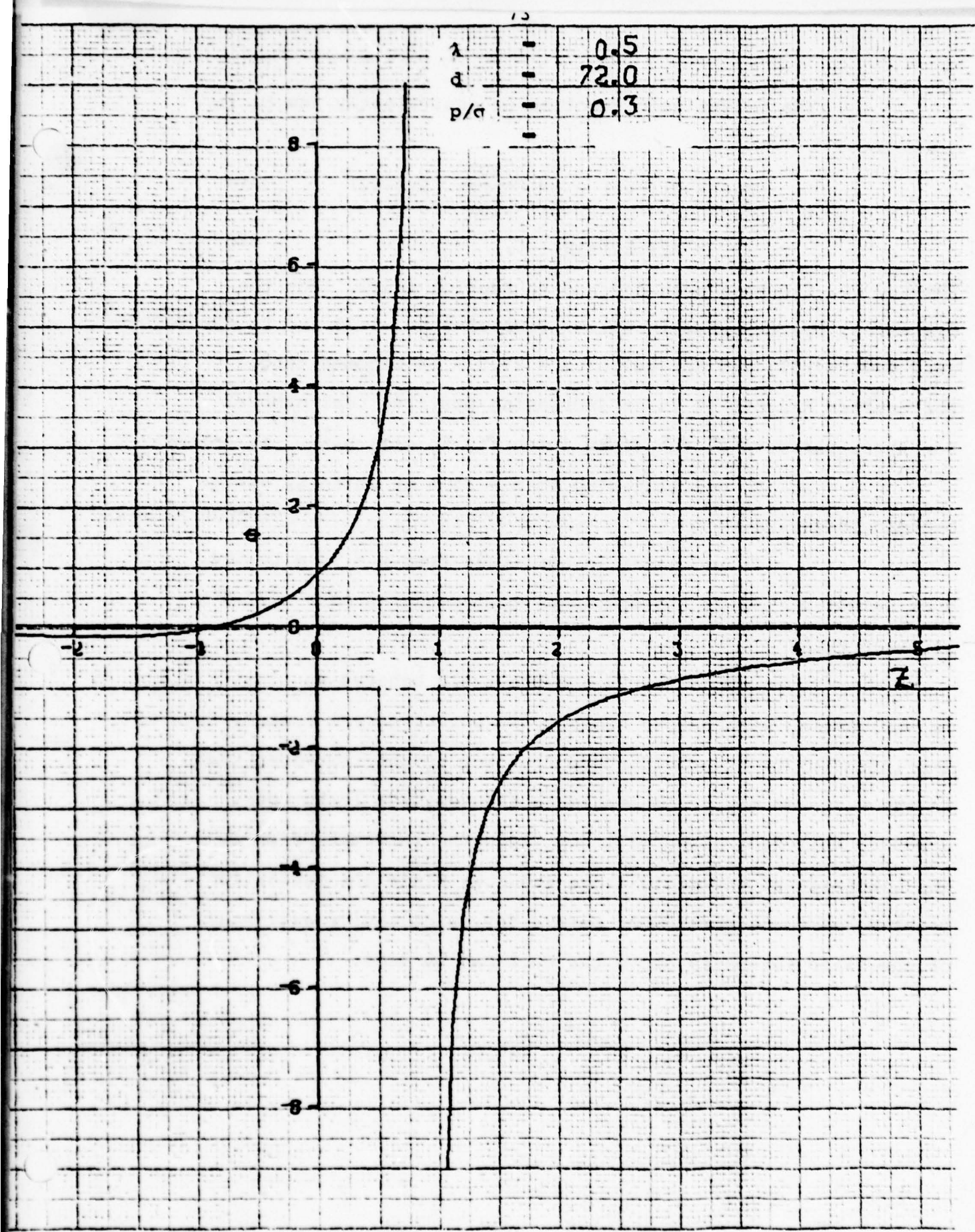


FIG. (4-16) PLOTS OF  $f(z)$  AS A FUNCTION OF  $z$

The height gain function or equivalently the  $E_y$  is given by

$$E_{y<} = A_i(-\xi<) - \frac{A_i(-\xi_{10})}{B_i(-\xi_{10})} \cdot B_i(-\xi<) \quad z < d$$

$$= A_i(-\xi>) + jB_i(-\xi>) \quad z > d$$

The  $\xi<$ ,  $\xi>$ ,  $\xi_{10}$  have been defined in Section 4.1.1. For the  $\xi_{10}$  value, the  $\xi<$  range in values from +5.9 to -1.25 and  $\xi>$  approaches zero from -3.57; and for height  $z = 77.8$  m it becomes zero.

For greater heights it is an increasing positive real number.

For these parameters, the field intensity  $E_y$  will behave as follows:

a.  $E_y$  oscillates up to  $z = 35$  m at which  $\xi<$  starts becoming negative.

b. It increases in amplitude from  $z = 35$  m to the duct height  $z = 42$  m. It continues to increase up to  $z = 77.8$  m at which  $\xi>+0$

c. Beyond  $z = 77.8$  m the field behaves as if it is attenuating with height since  $\xi>$  is positive real number.

The intensity of the field above the duct height is higher than in the duct and may be construed as the dominant leaky mode. However, this fact alone will not yield the information as to the intensity of the field above the duct since the excitation problem has to be worked out before any quantitative estimates of the field intensity above the duct can be made.

#### 4.3.2 The Leaky Modes

Up until now we sought solutions of the transcendental equation which were positive or negative real numbers. The determination of the solutions of the transcendental equation for complex values is much more involved and time consuming, and the resources of this contract do not permit detailed analysis. Nonetheless, some already developed approximate expressions are used to determine the complex eigenvalues or solutions characterizing leaky modes.

The expression which is used to determine the leaky modes is given by (2)

$$\begin{aligned} A_m = & \left\{ \xi_m + g + \frac{1}{12} Sg^4 - \frac{1}{90} S\xi_m g^6 \right. \\ & + \frac{(13S^2-5S)}{1260} g^7 + \frac{1}{1260} S\xi_m^2 g^8 \\ & \left. + \dots \dots \right\} \end{aligned}$$

Here,  $g = \frac{d}{H}$ ,  $H = (k_0^2 q)^{-1/3}$ ,  $S = 1 - s^3$ ,  $s^3 = -\frac{p}{q}$  and  $\xi_m$  are the zeros of the Hankel function of second kind and one third order and are given by

$$\begin{aligned} \xi_1 &= -1.169+j2.025 \\ \xi_2 &= -2.044+j3.54 \\ \xi_3 &= -2.76+j4.78 \end{aligned}$$

The expression for the eigenvalue  $A_m = a_m + jB_m$  is valid for small values of  $g$  ( $g < 1$ ). That is, the duct height is comparable to the scale height  $H$  and for these values of  $g$  the eigenvalues approach the zeroes of the Hankel function of the second kind and one third order.

Recognizing that for  $\lambda=100$  cm the field will not be trapped by any of the ducts;  $\lambda=100$  cm was chosen for calculations. Thus for  $\lambda=100$  cm and for two days of duct profile, the complex eigenvalues are presented in the table as follows:

Table (4-2) Eigenvalues for Leaky Modes

$\lambda=100$ cm	Jan.	Dec.
	$g = 0.545$	$g = 0.6646$
A <sub>1</sub>	-0.574+j2.02	-0.48+j2.021
2	-1.448+j3.53	-1.354+j3.53
3	-2.163+j4.78	-2.07+j4.77

Use of the same equation for  $\lambda=50$  cm leads to results which do not appear to be valid. For  $\lambda=50$  cm,  $g = 1.378$  for Jan. 3rd duct and  $g=1.476$  for Dec. 4th duct and thus the expression for  $g > 1$  does not seem to hold.

#### 4.4 The Height Gain Functions for the Trapped Modes

As discussed before, the variation of the field with height, also termed the height gain function, will reveal whether or not there exists field outside the duct. For this reason, height gain functions for individual modes have been computed and they are shown in Figs. (4-17 through 4-53).

The height gain functions are the plots of modal E field i.e., they are the plots of the following expressions:

$$E_{y<} = A_i(-\xi<) - \frac{A_i(-\xi_{10})}{B_i(-\xi_{10})} \cdot B_i(-\xi<) \quad z < d$$

$$E_{y>} = A_i(-\xi>) + j B_i(-\xi>) \quad z > d$$

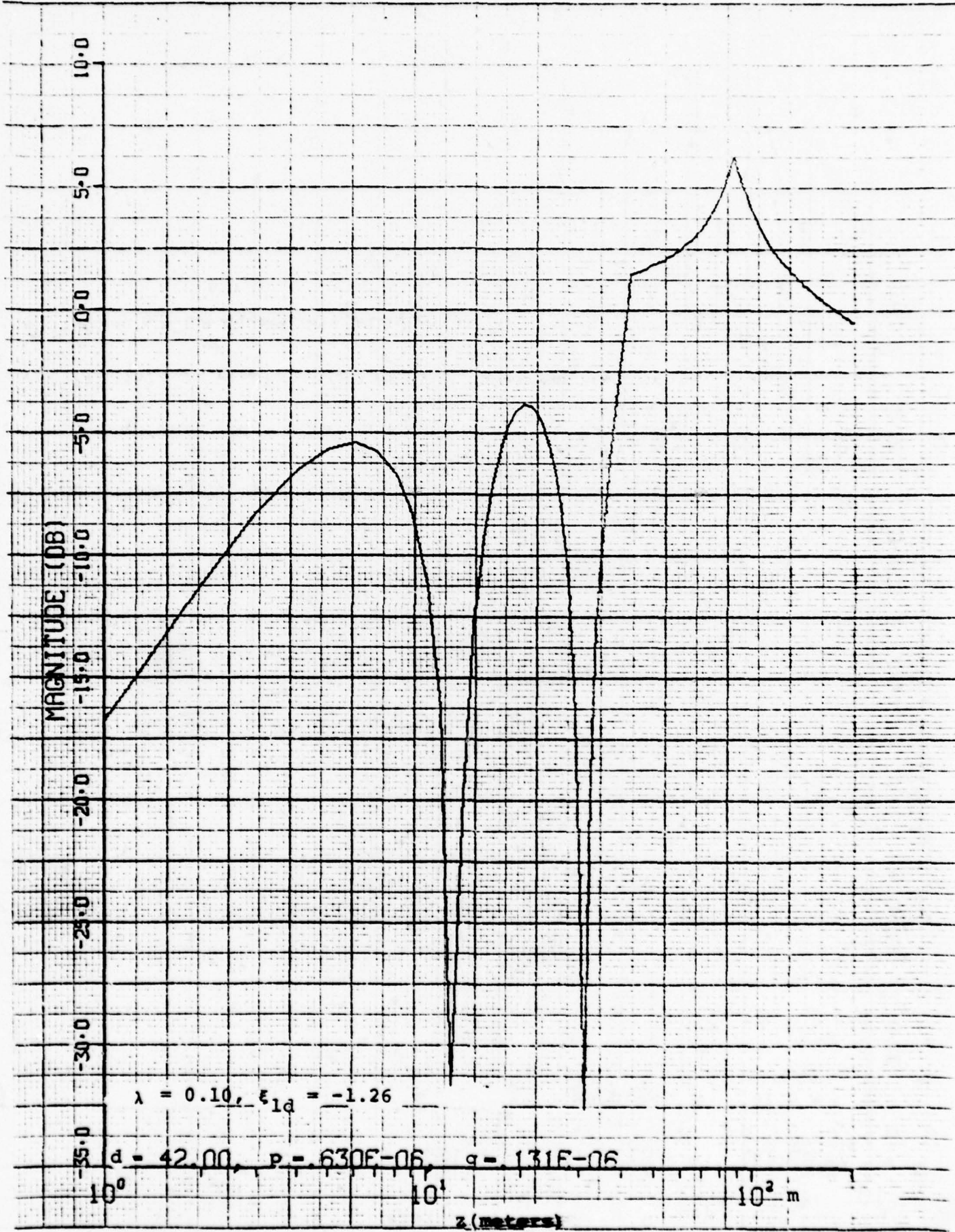


Fig. (4-17) Height-Gain Functions - January

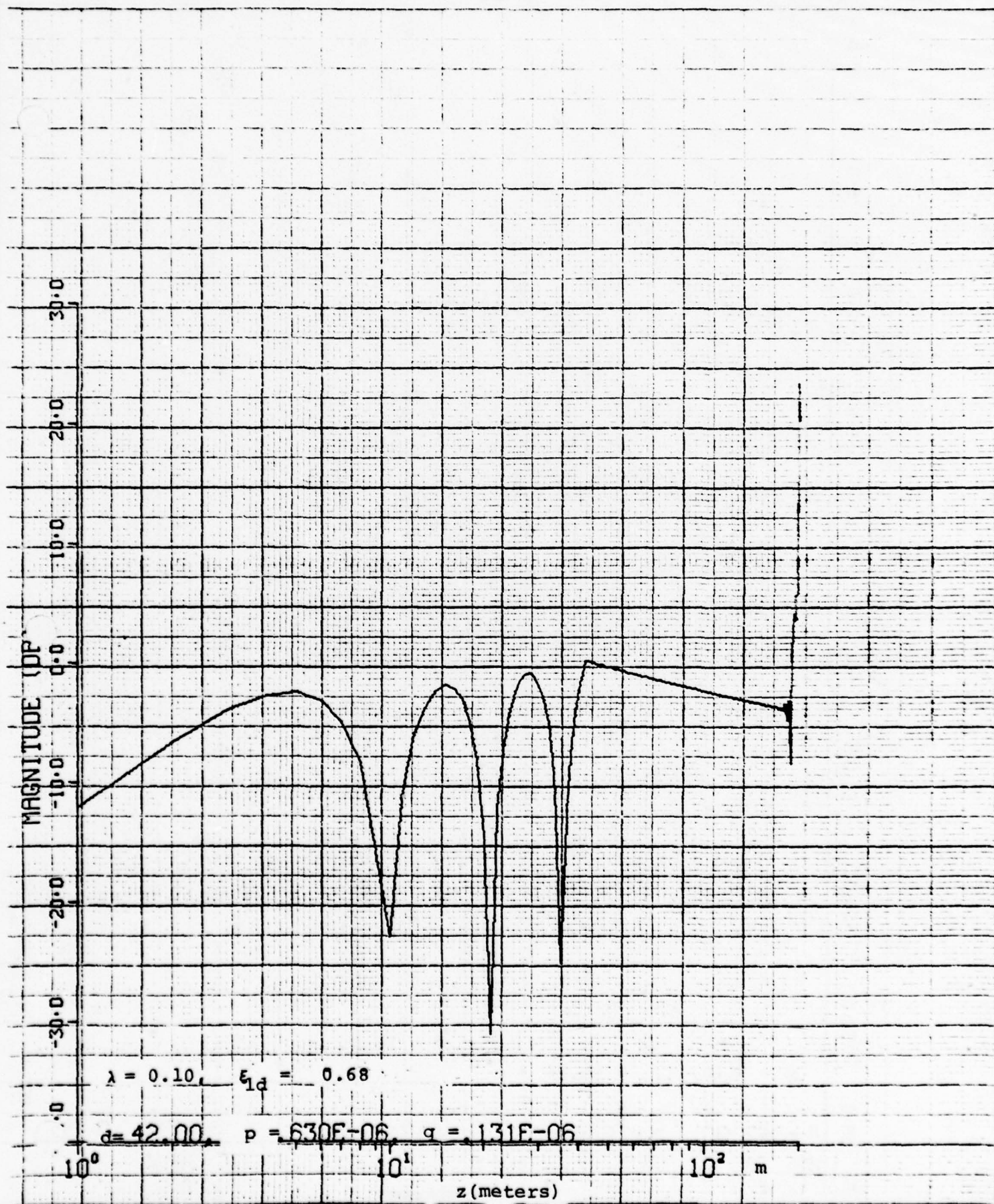


Fig. (4-18) Height-Gain Functions - January

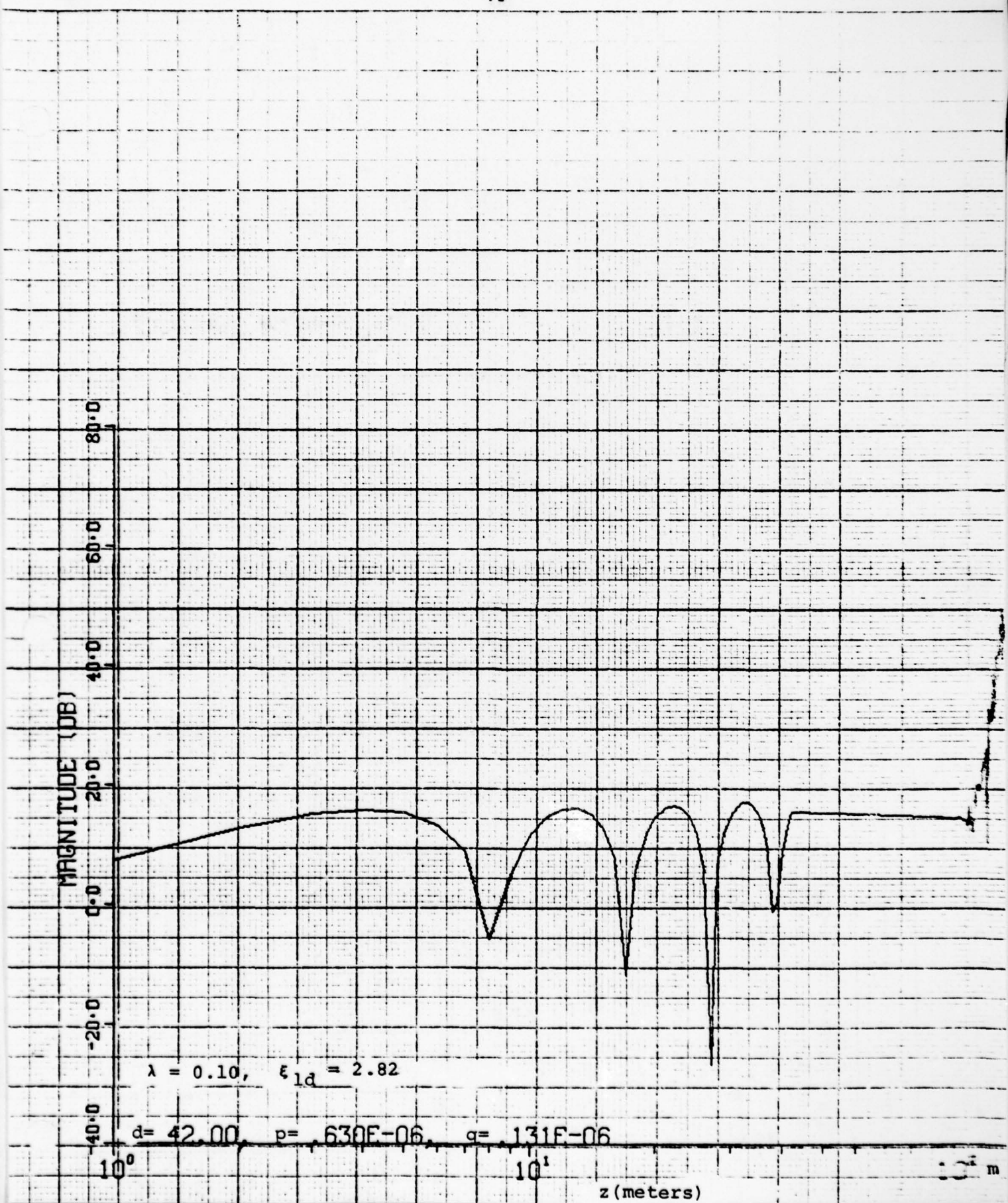
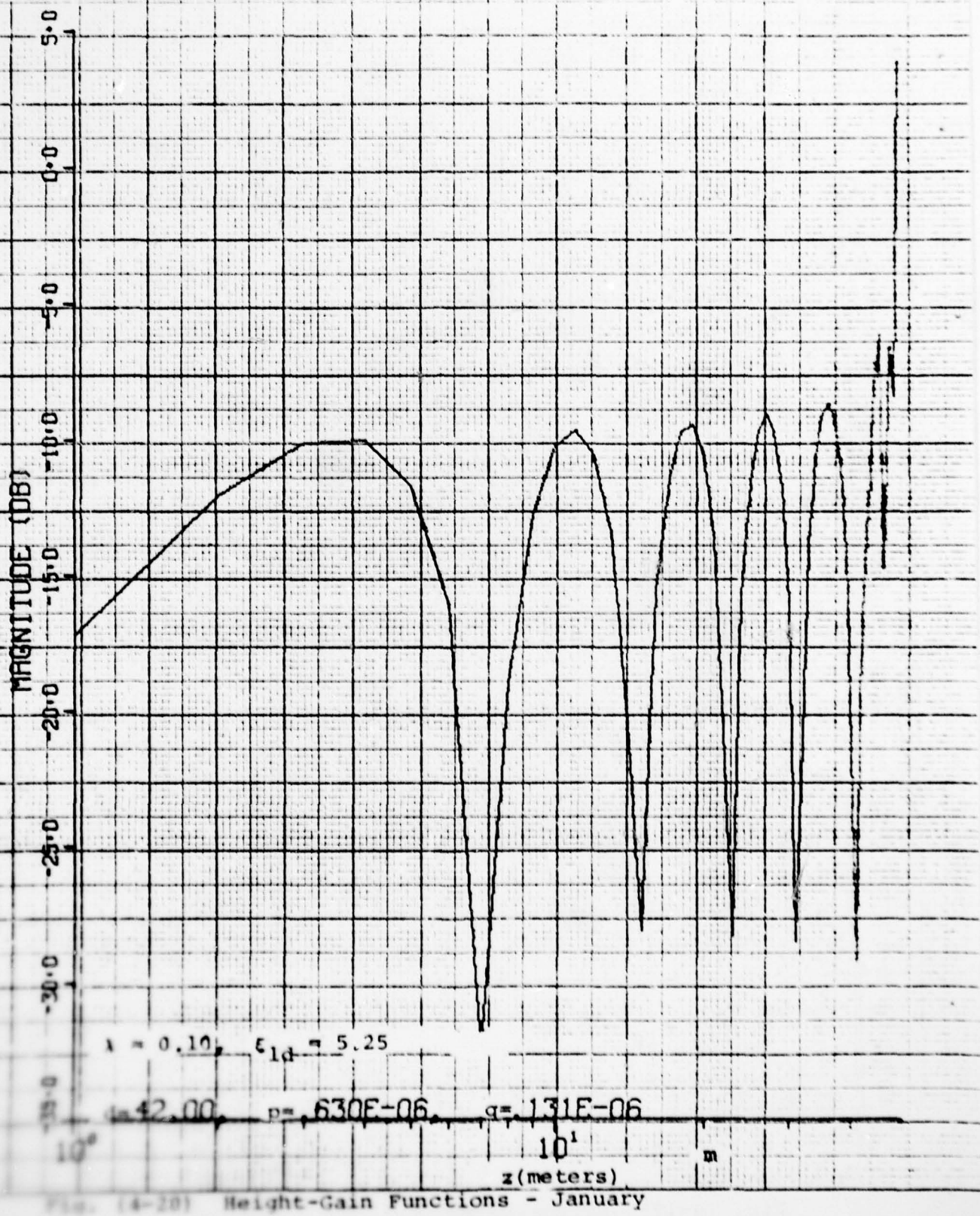


Fig. (4-19) Height-Gain Functions - January



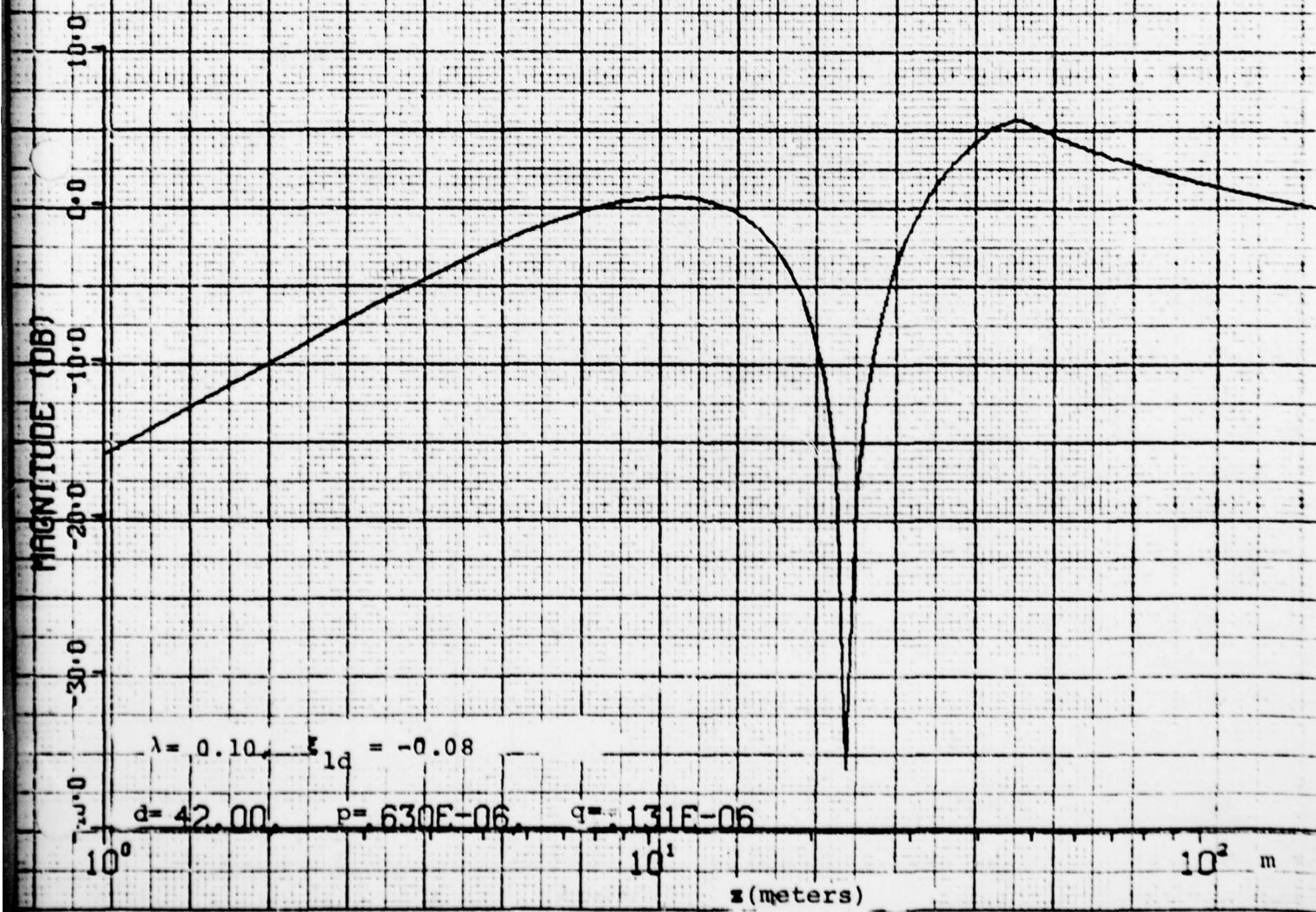


Fig. (4-21) Height-Gain Functions - January

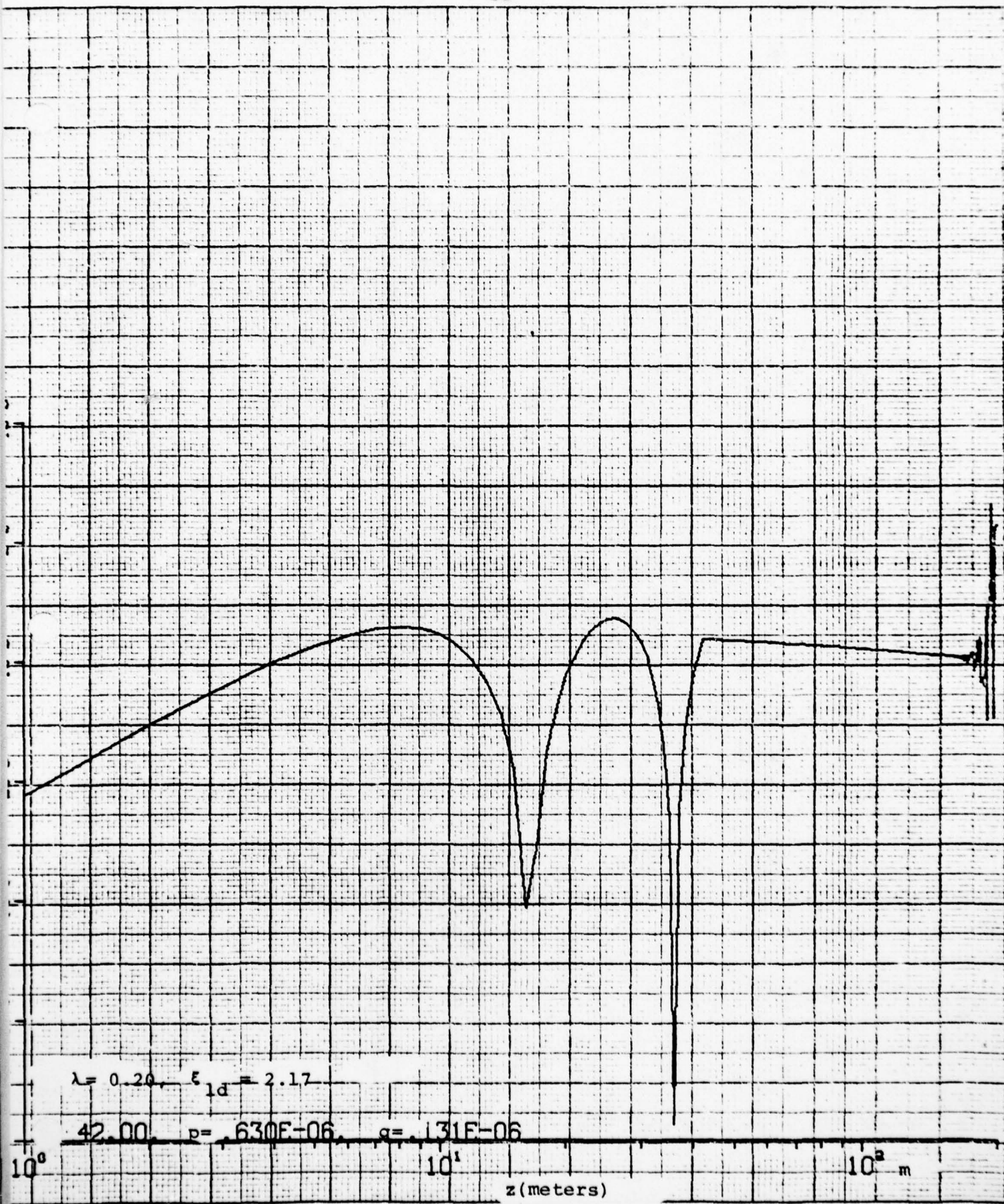


Fig. (4-22) Height-Gain Functions - January

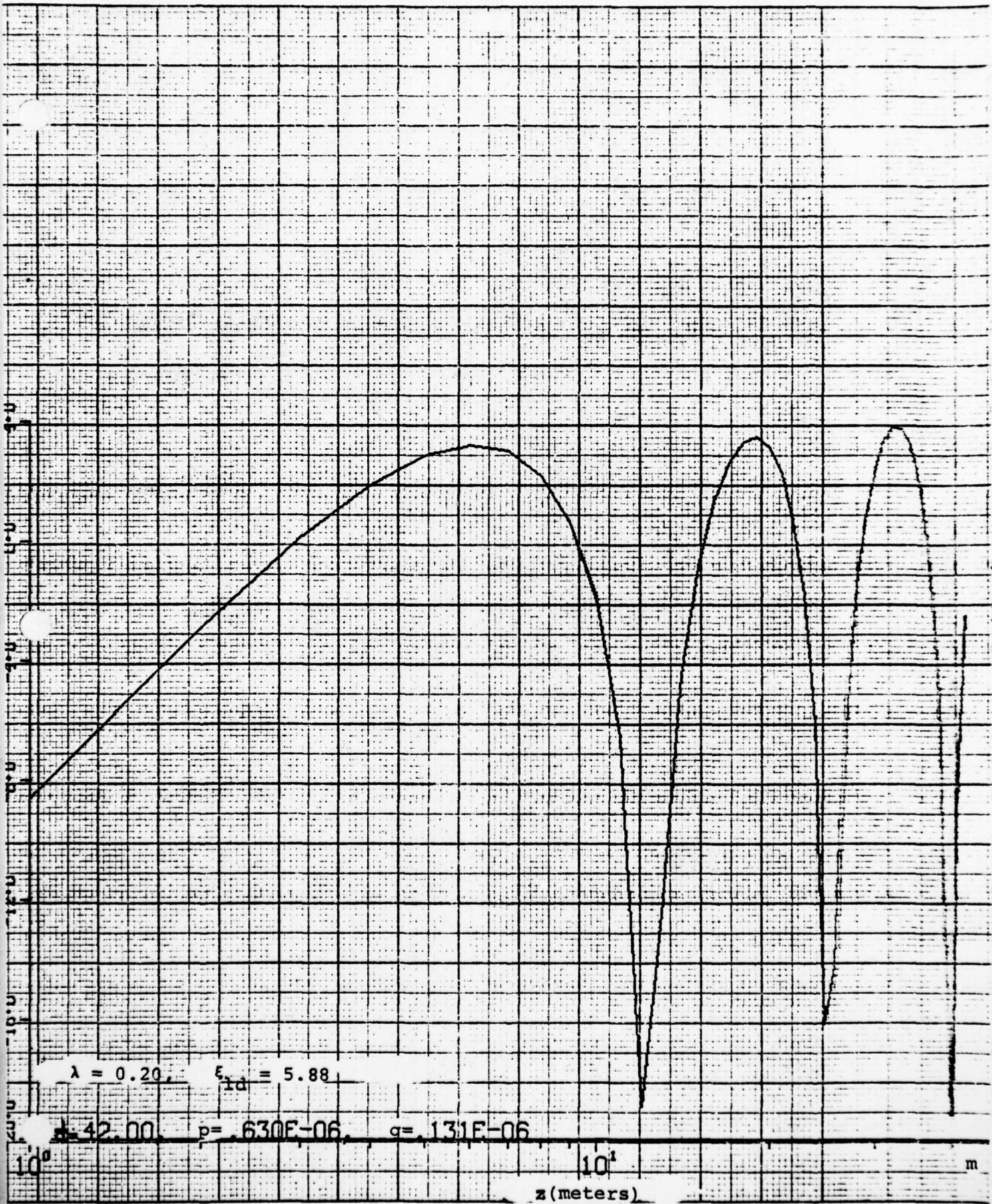


Fig. (4-23) Height-Gain Functions - January

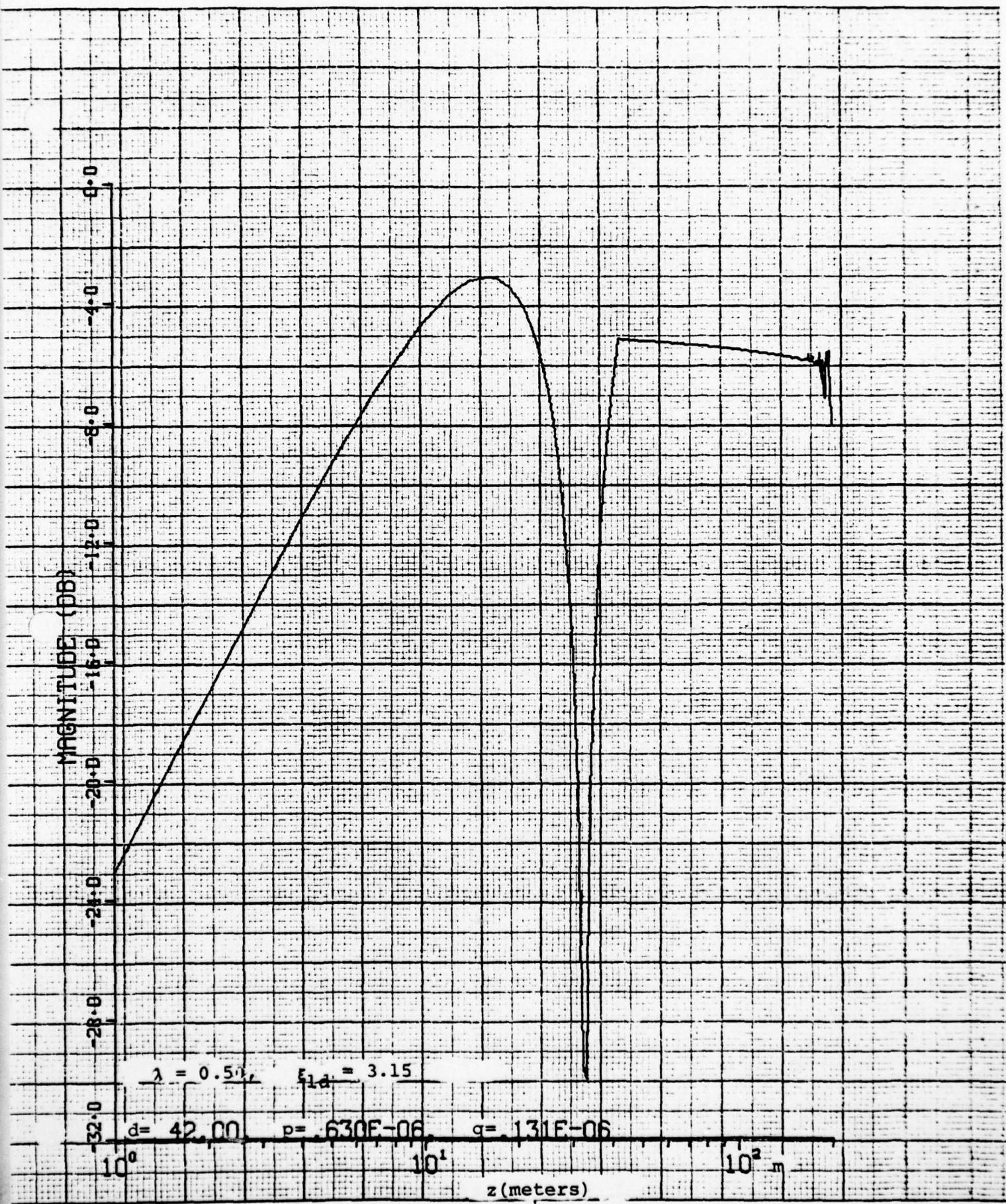


Fig. (4-24) Height-Gain Functions - January

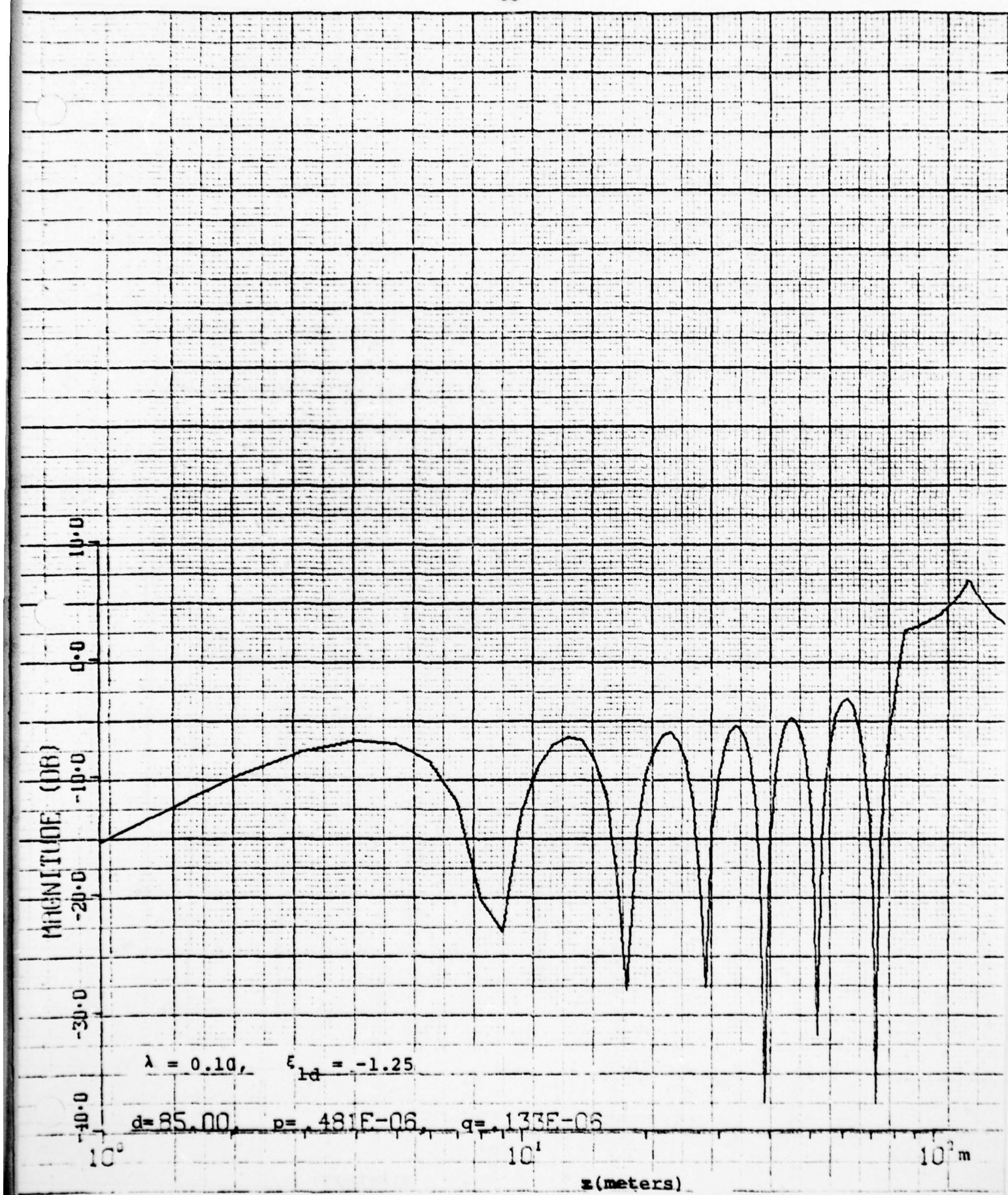


Fig. (4-25) Height-Gain Functions - April

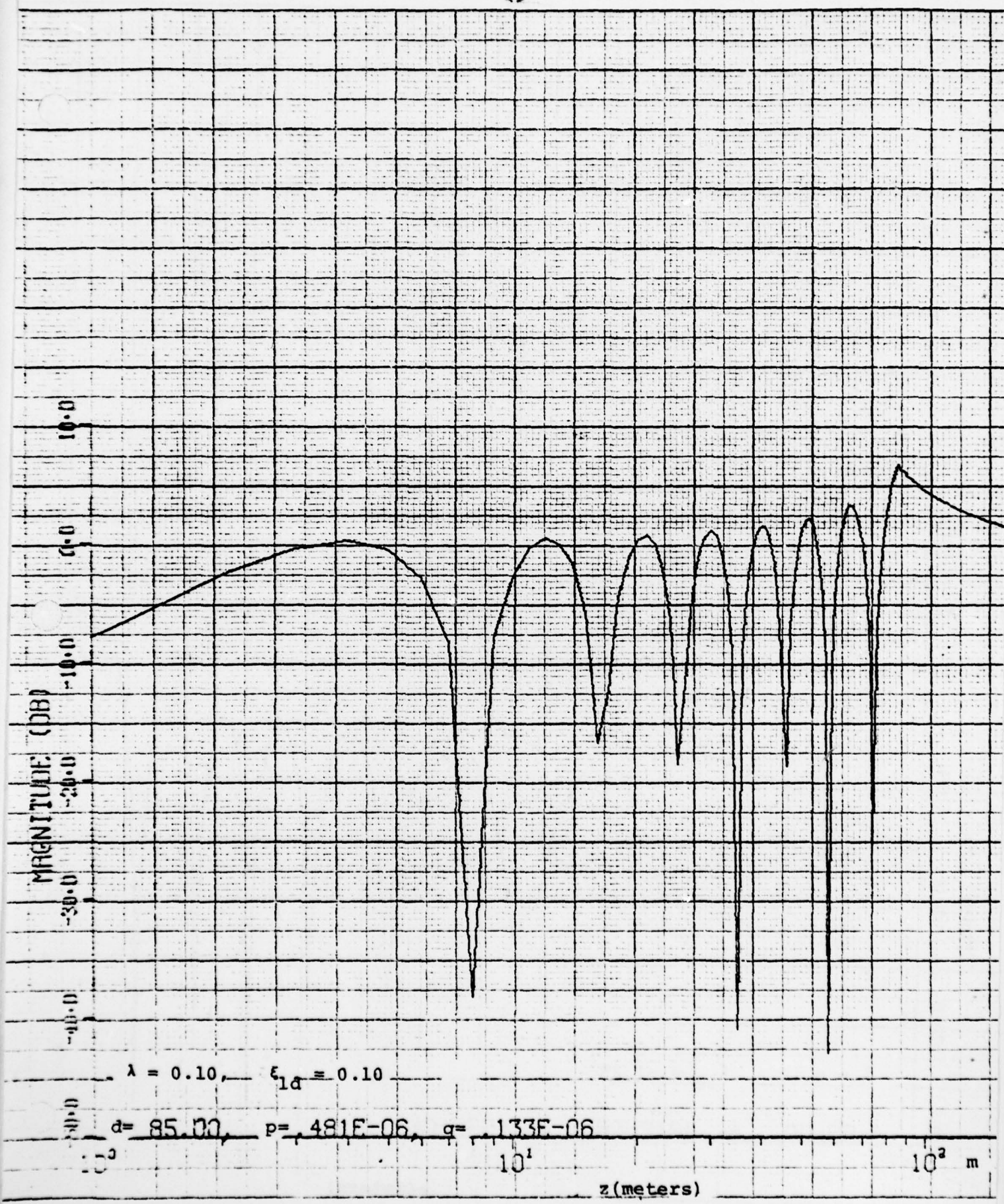


Fig. (4-26) Height-Gain Functions - April

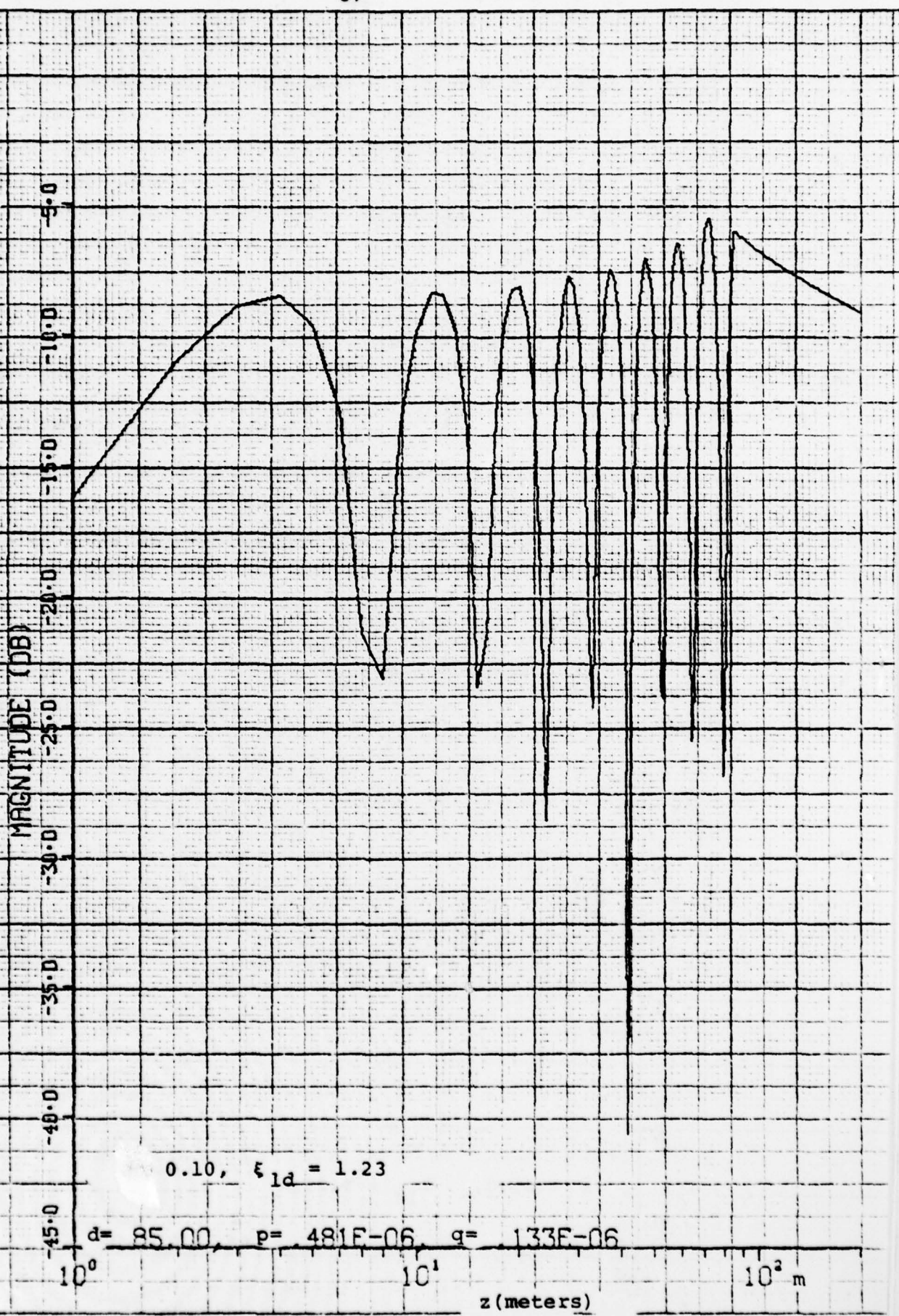


Fig. (4-27) Height-Gain Functions - April

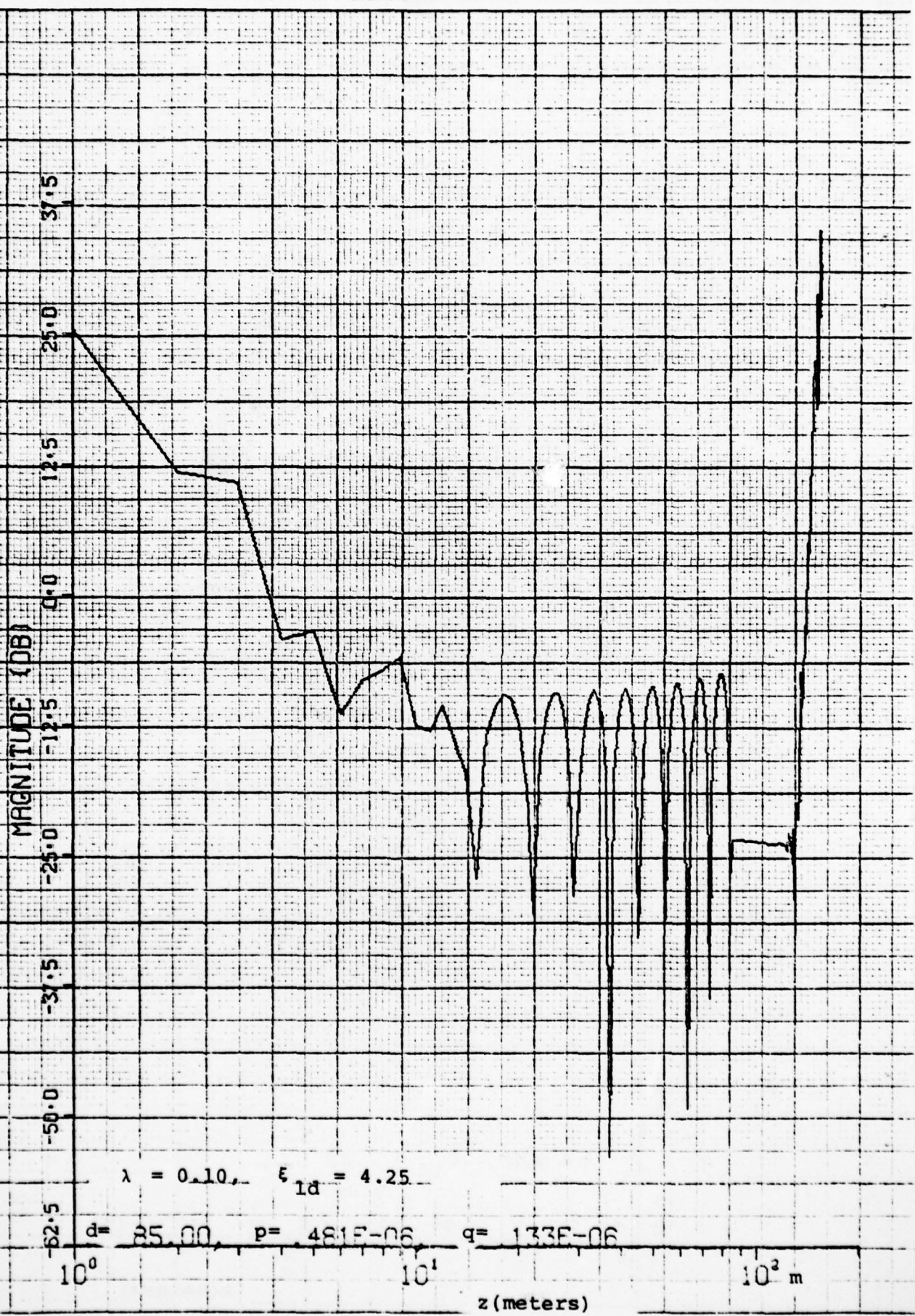


Fig. (4-28) Height-Gain Functions - April

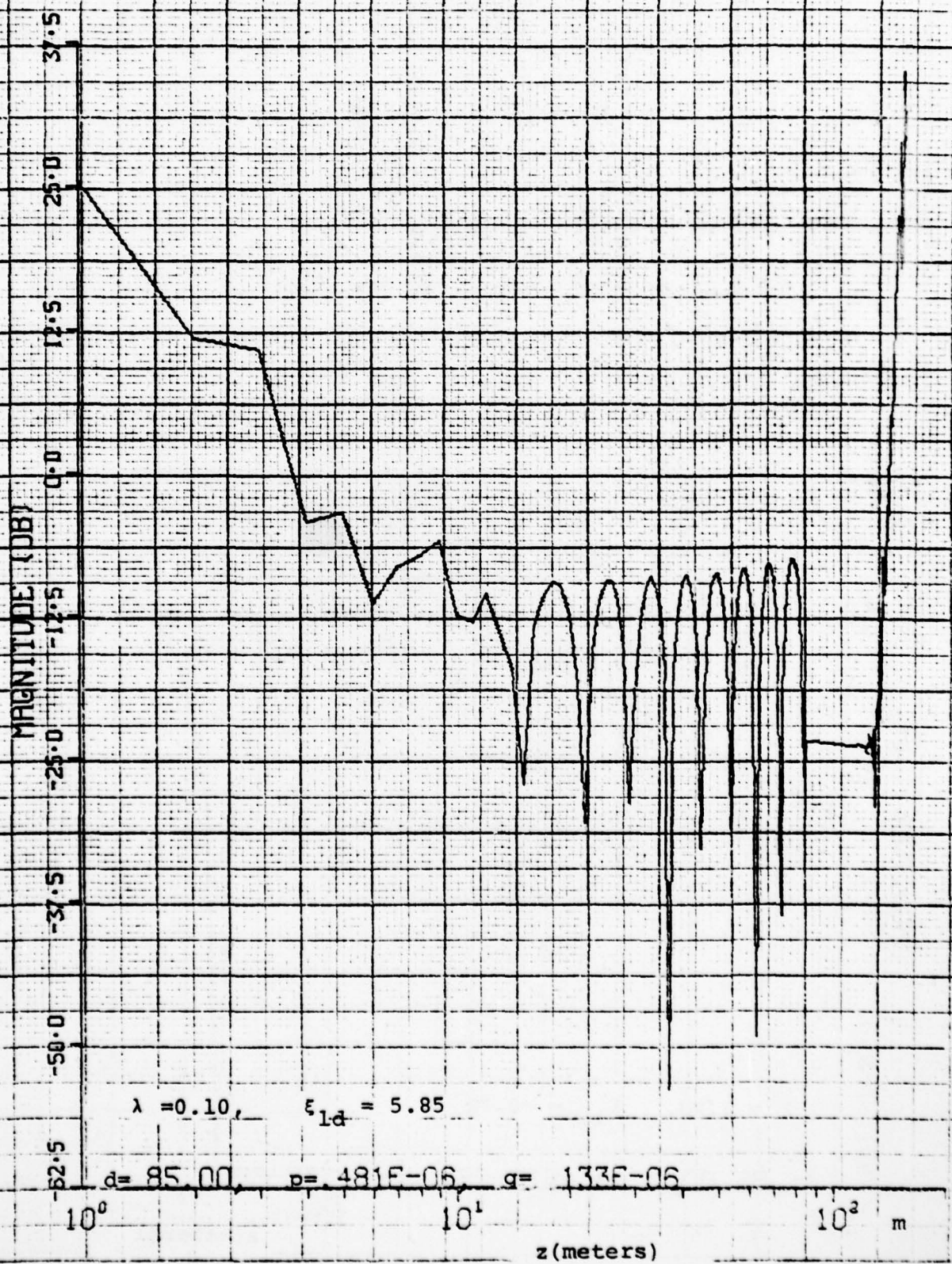


Fig. (4-29) Height-Gain Functions - April

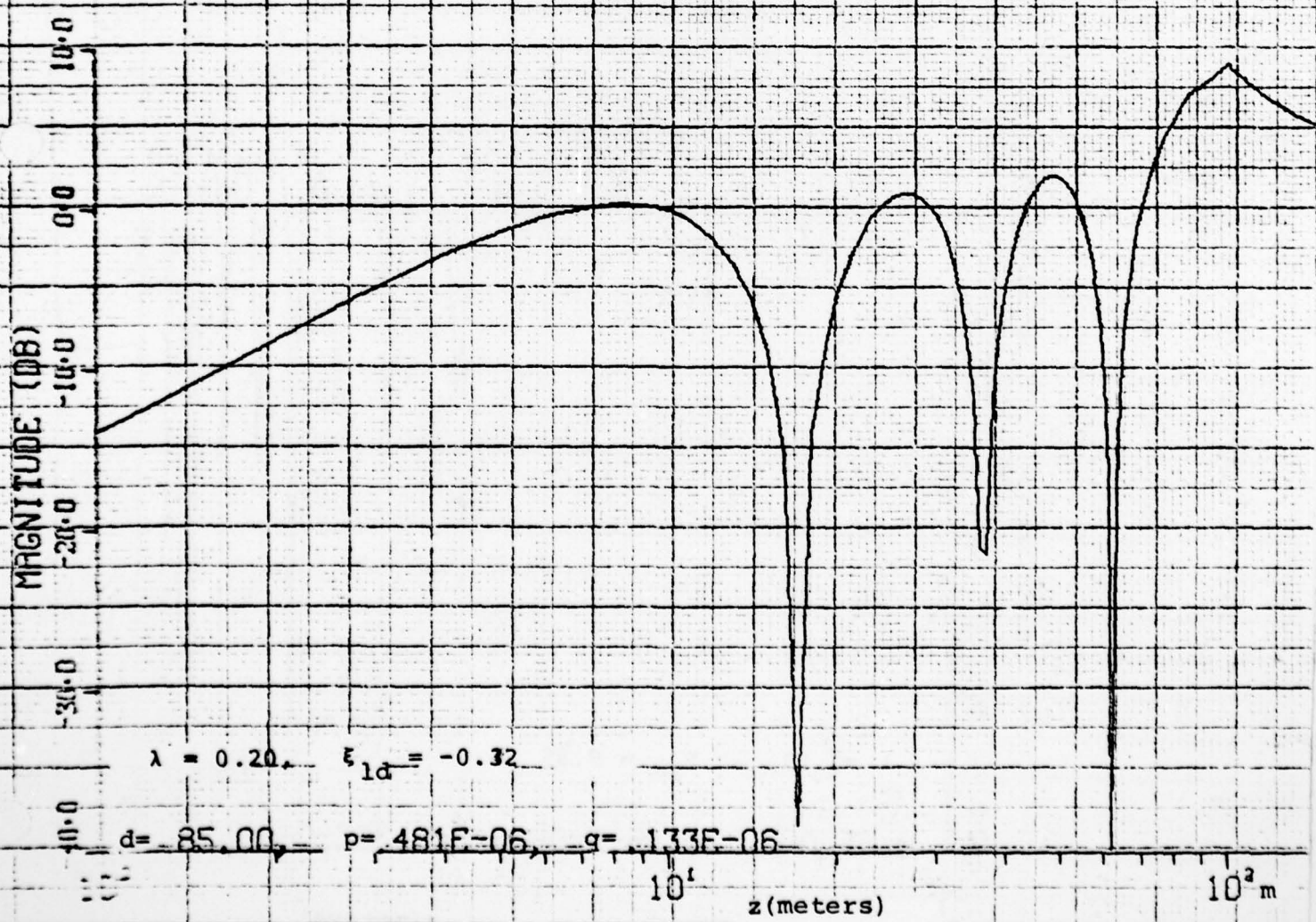


Fig. (4-30) Height-Gain Functions - April

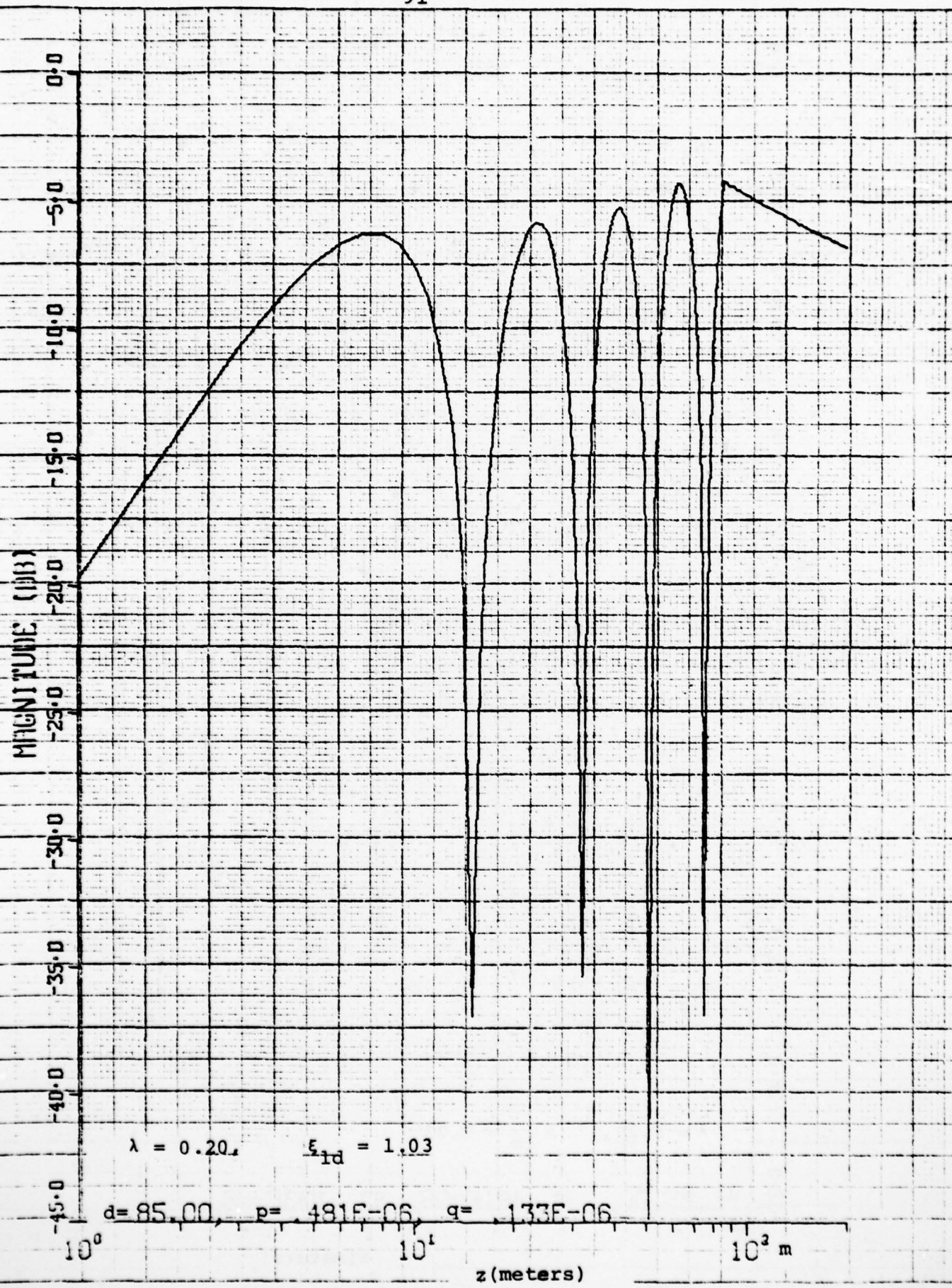


Fig. (4-31) Height-Gain Functions - April

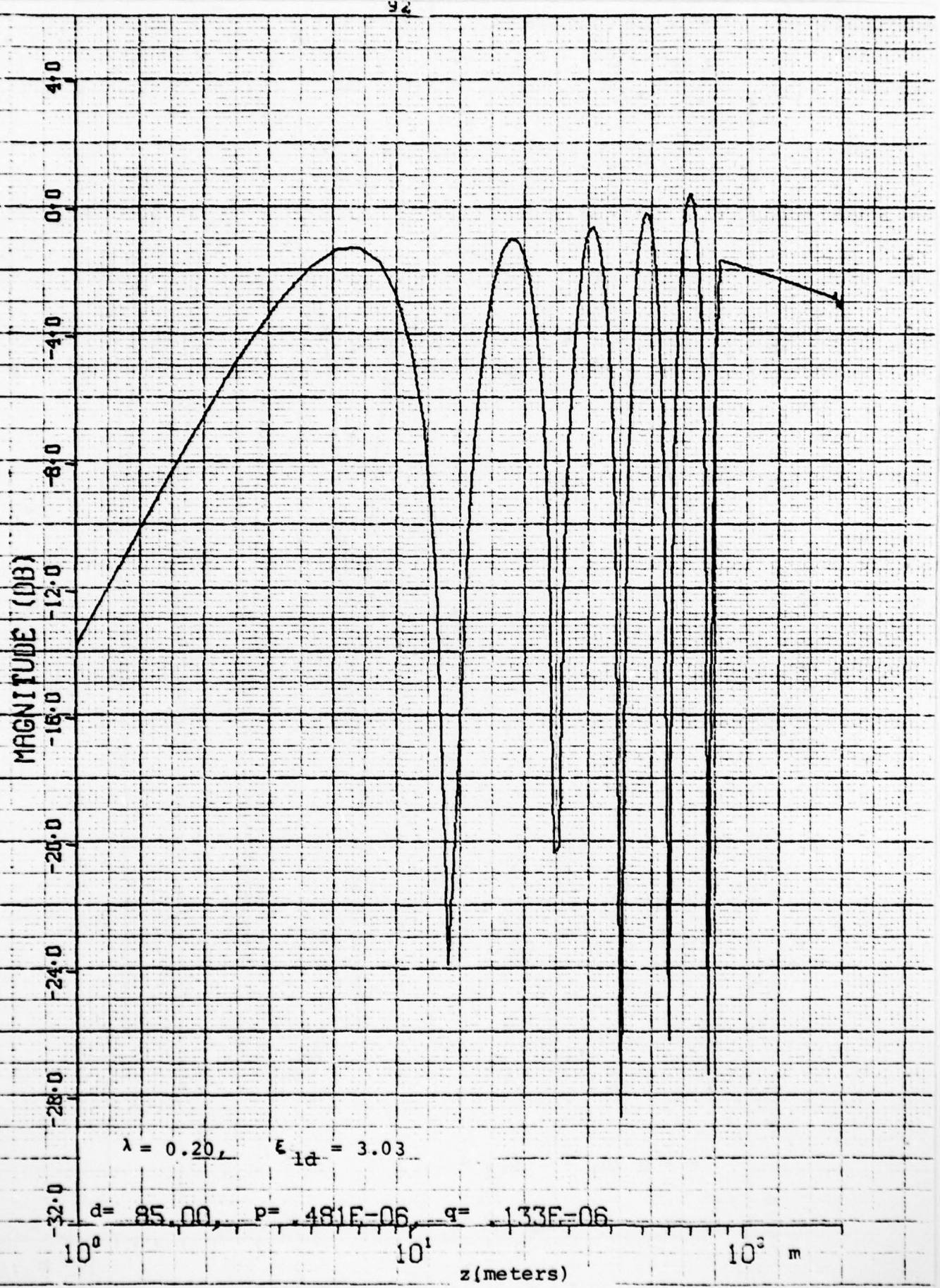


Fig. (4-32) Height-Gain Functions - April

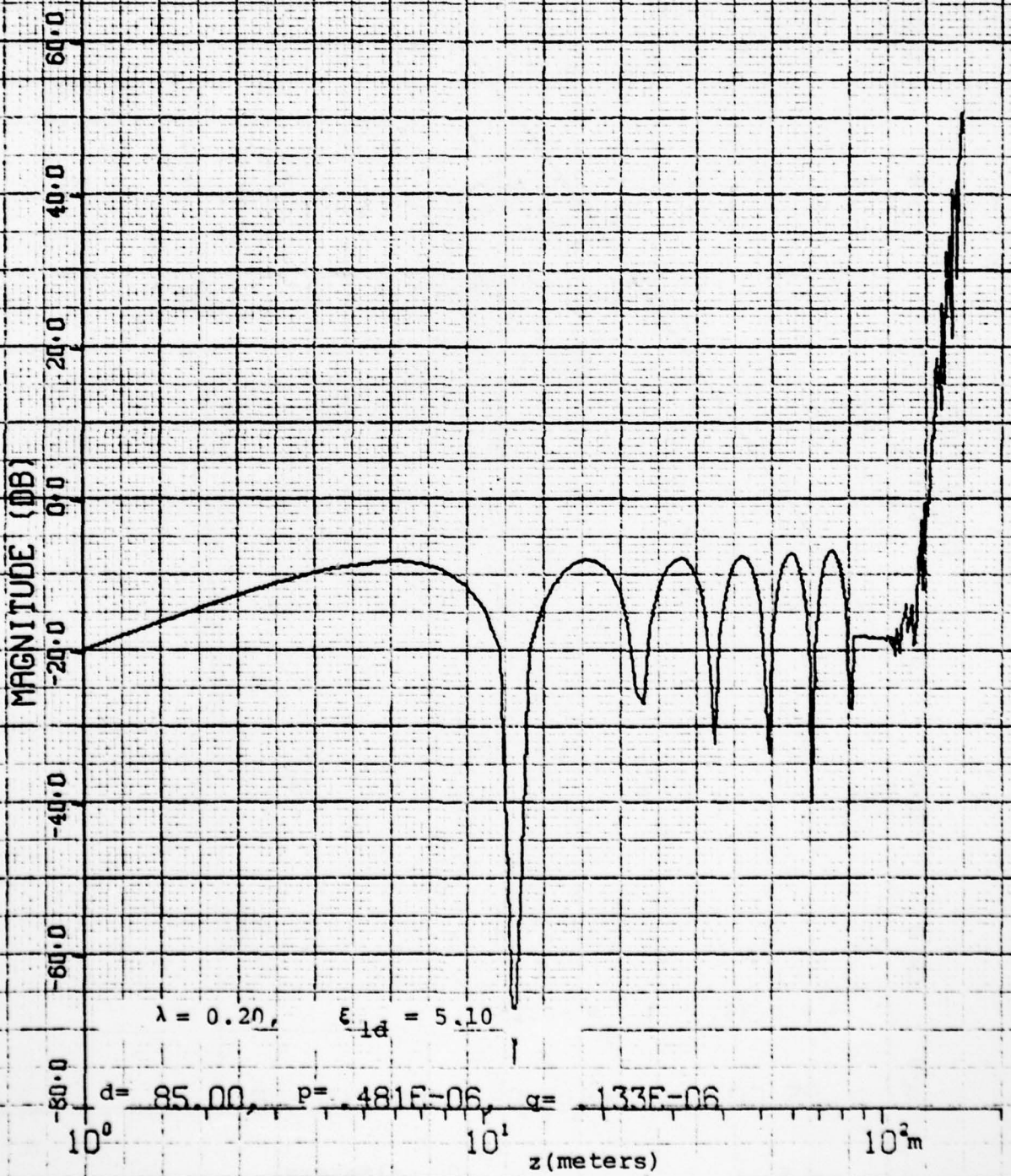


Fig. (4-33) Height-Gain Functions - April

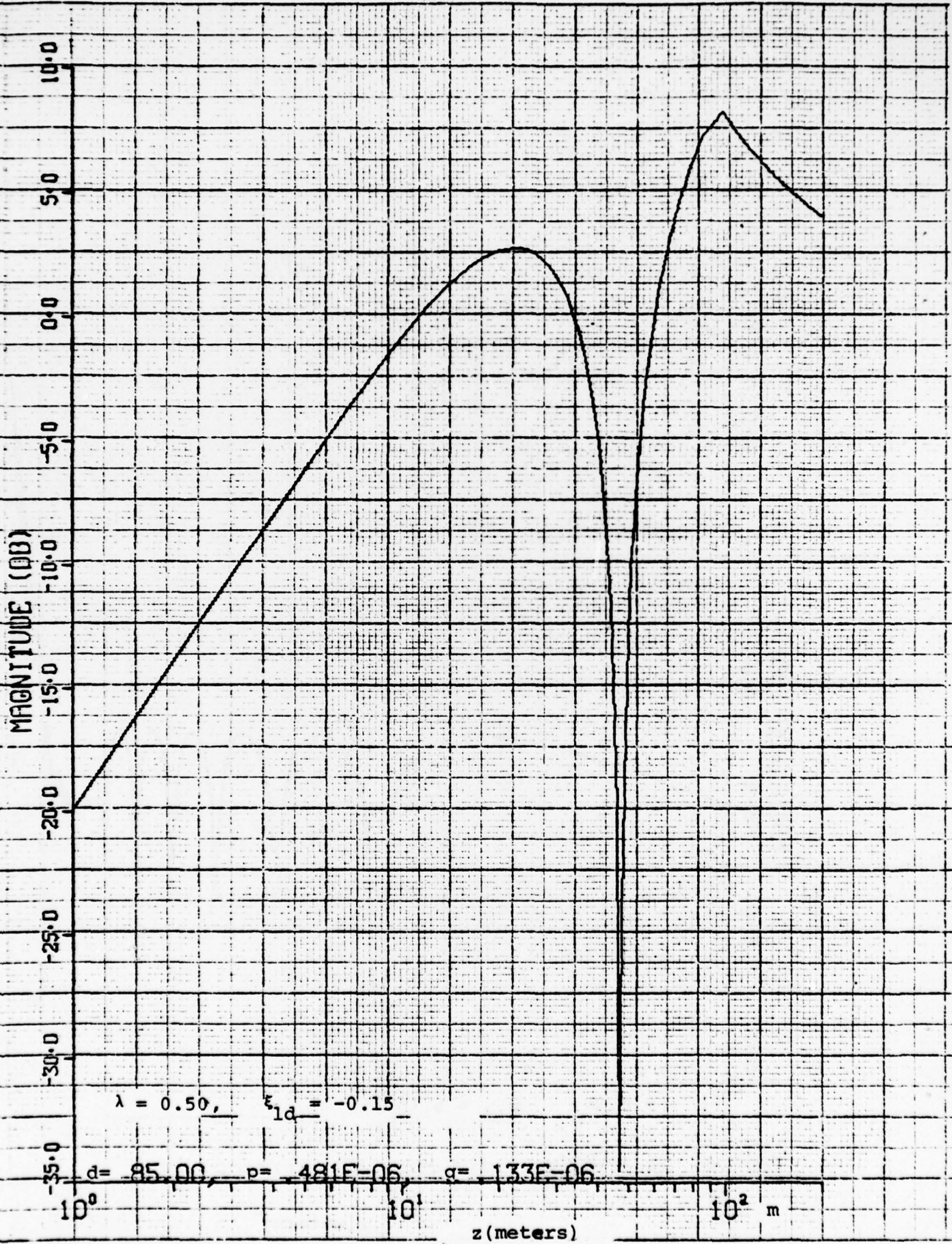


Fig. (4-34) Height-Gain Functions - April

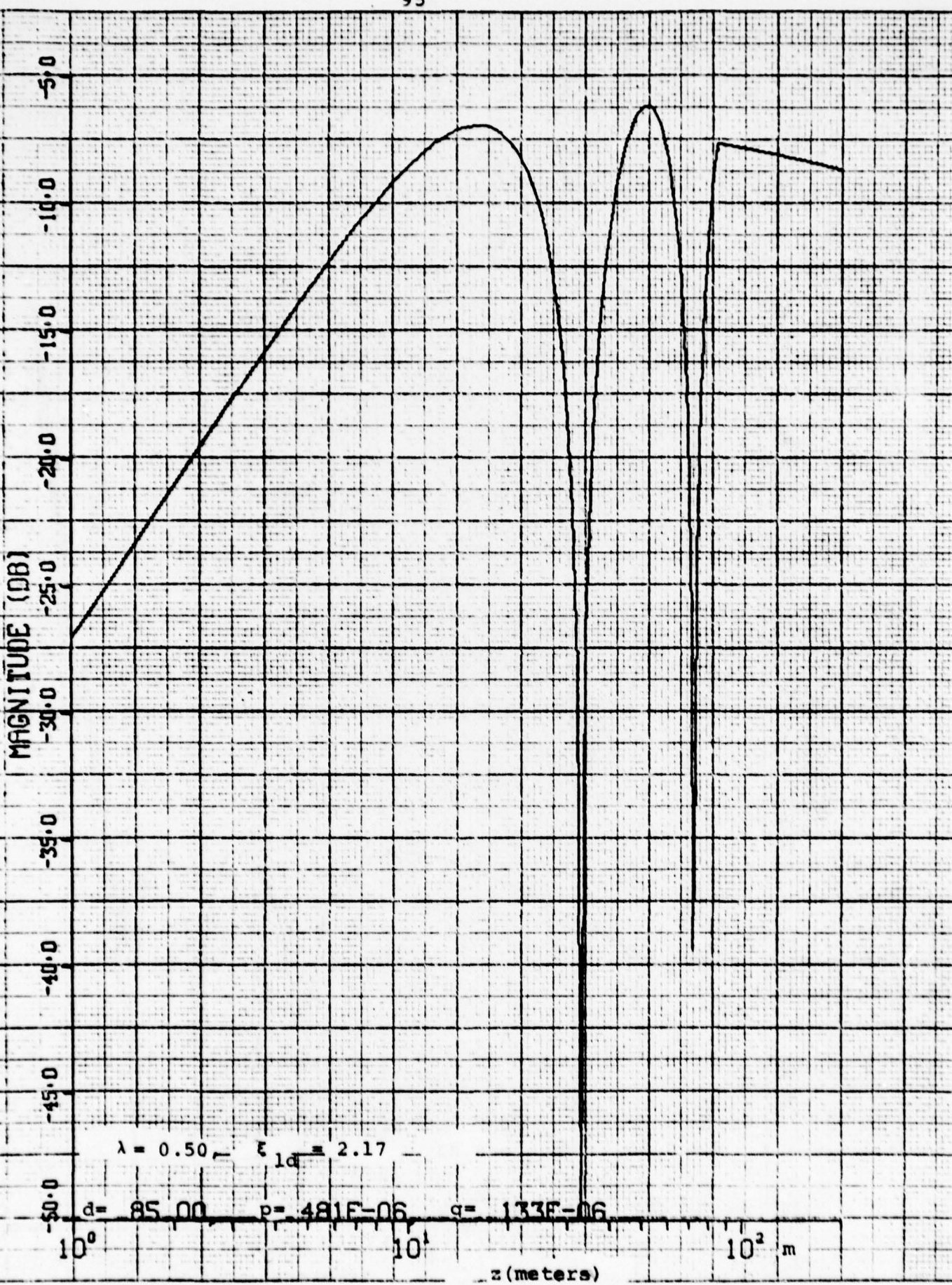


Fig. (4-35) Height-Gain Functions - April

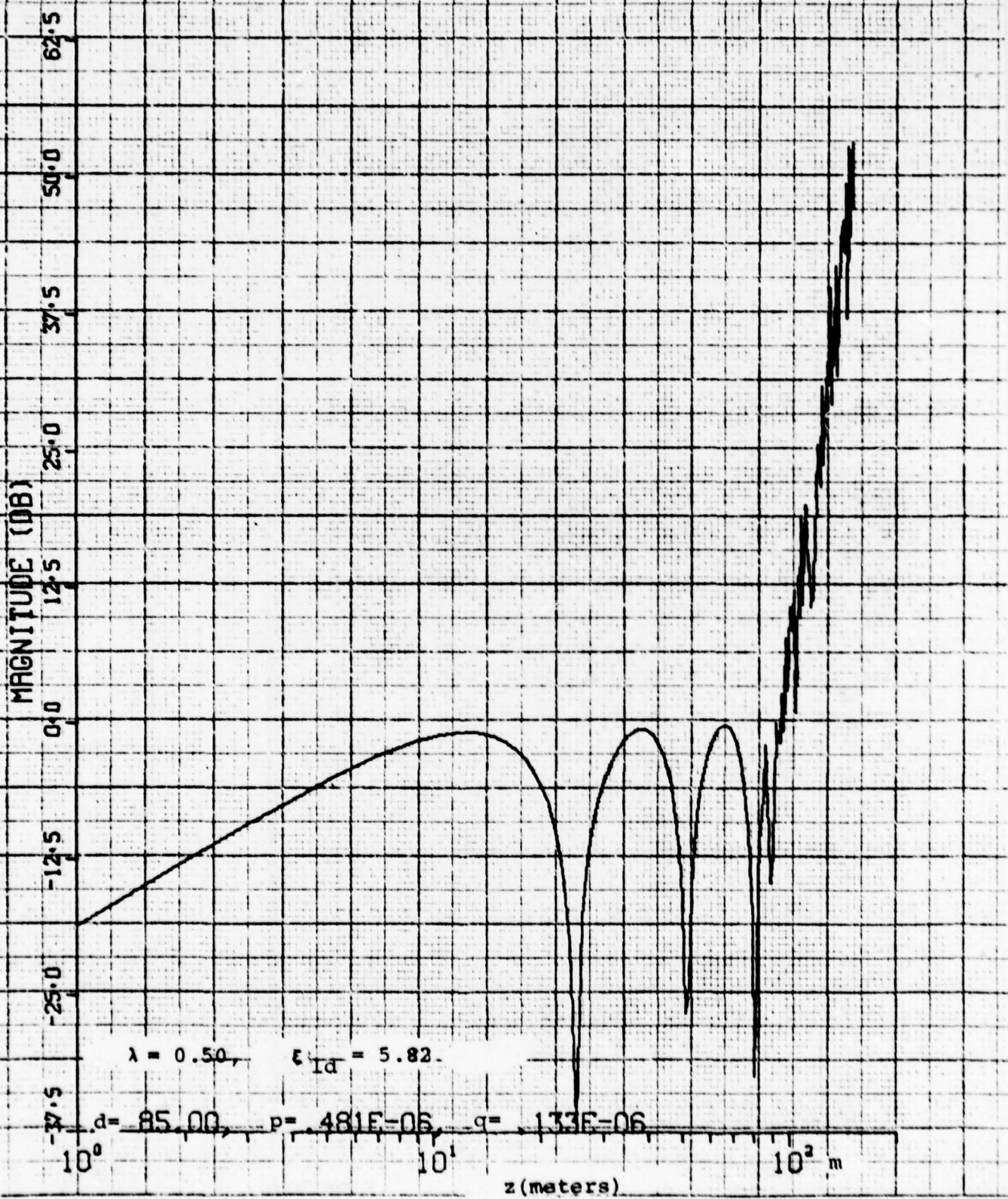


Fig. (4-36) Height-Gain Functions - April

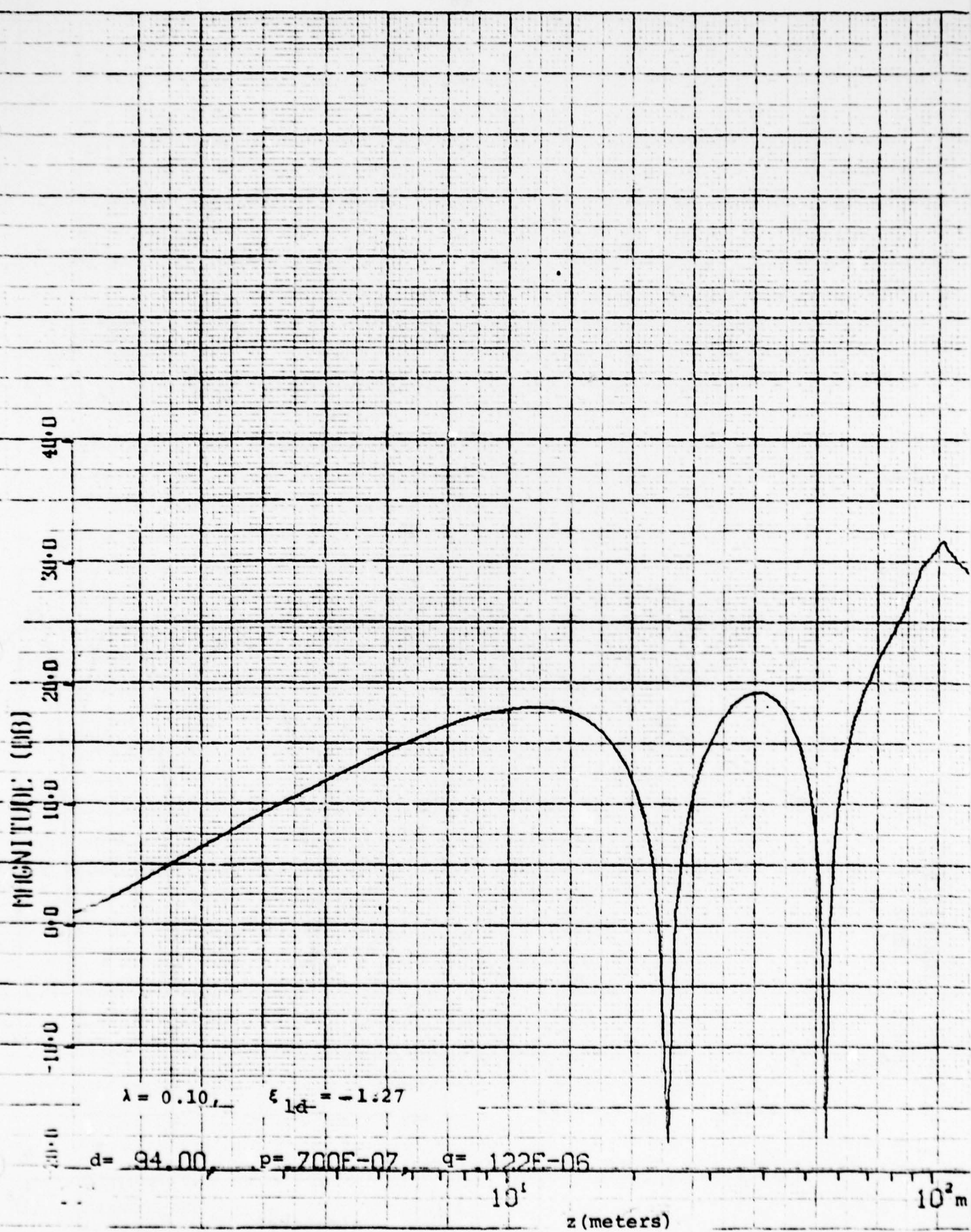


Fig. (4-37) Height-Gain Functions - September

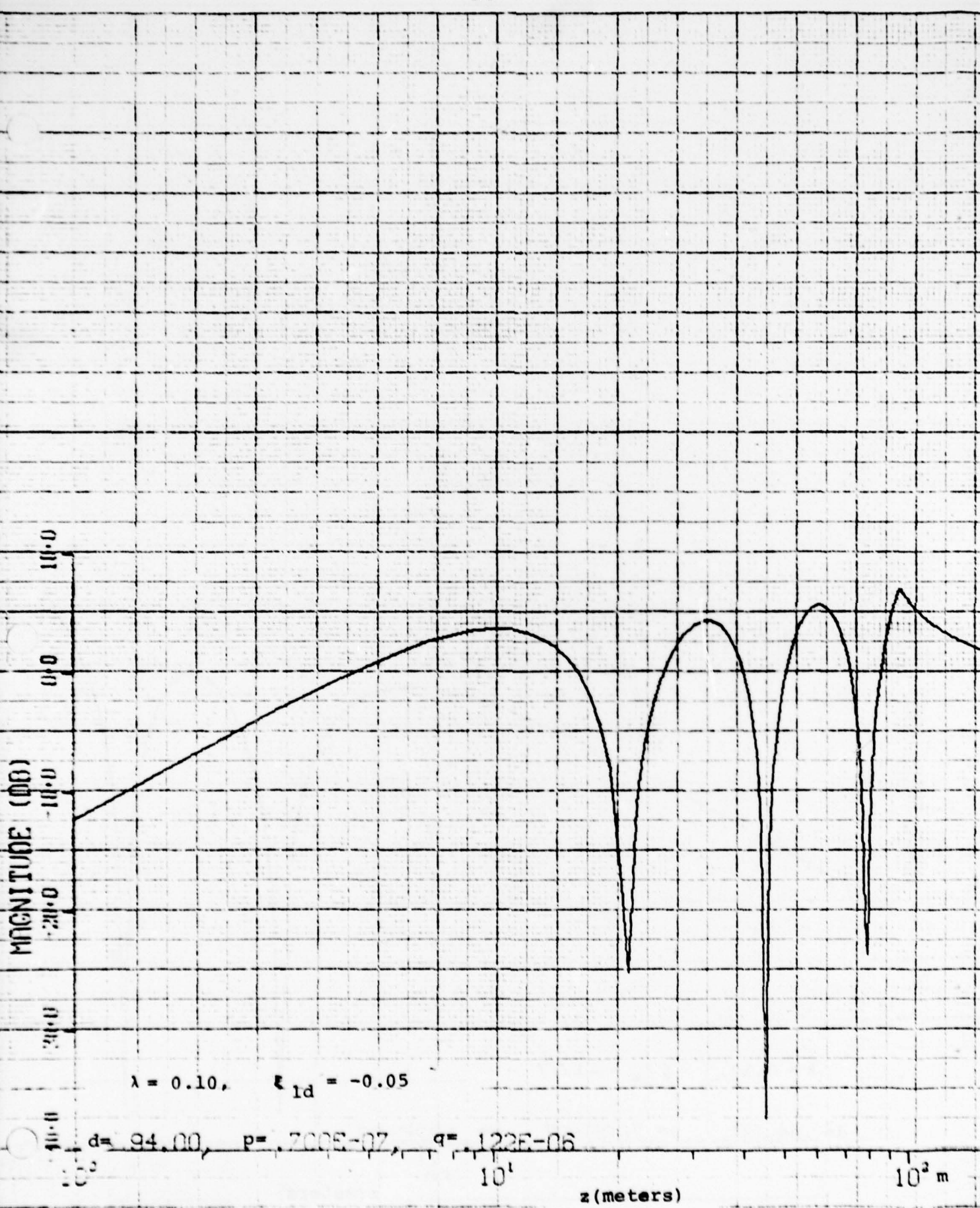


Fig. (4-38) Height-Gain Functions - September

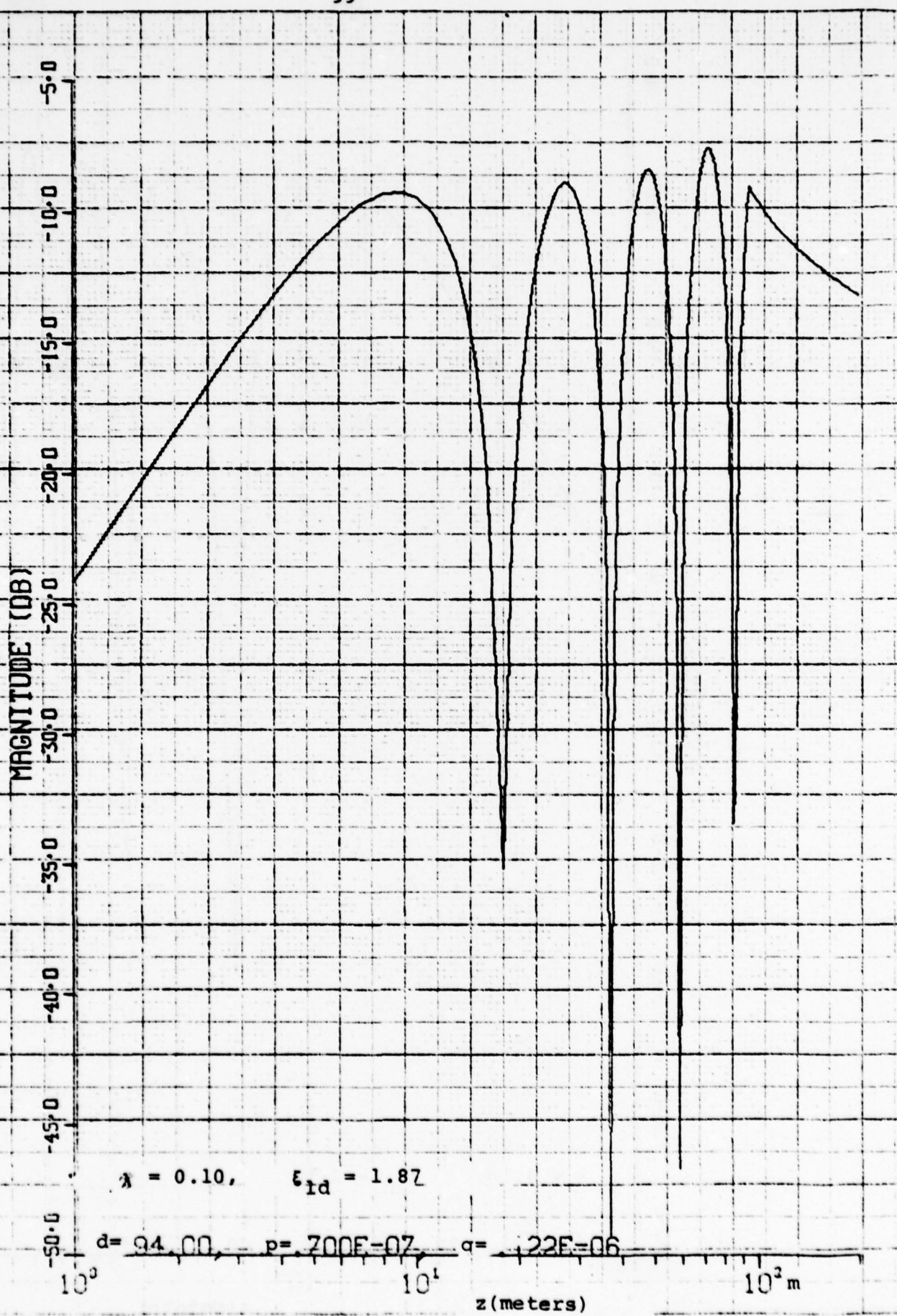


Fig. (4-39) Height-Gain Functions - September

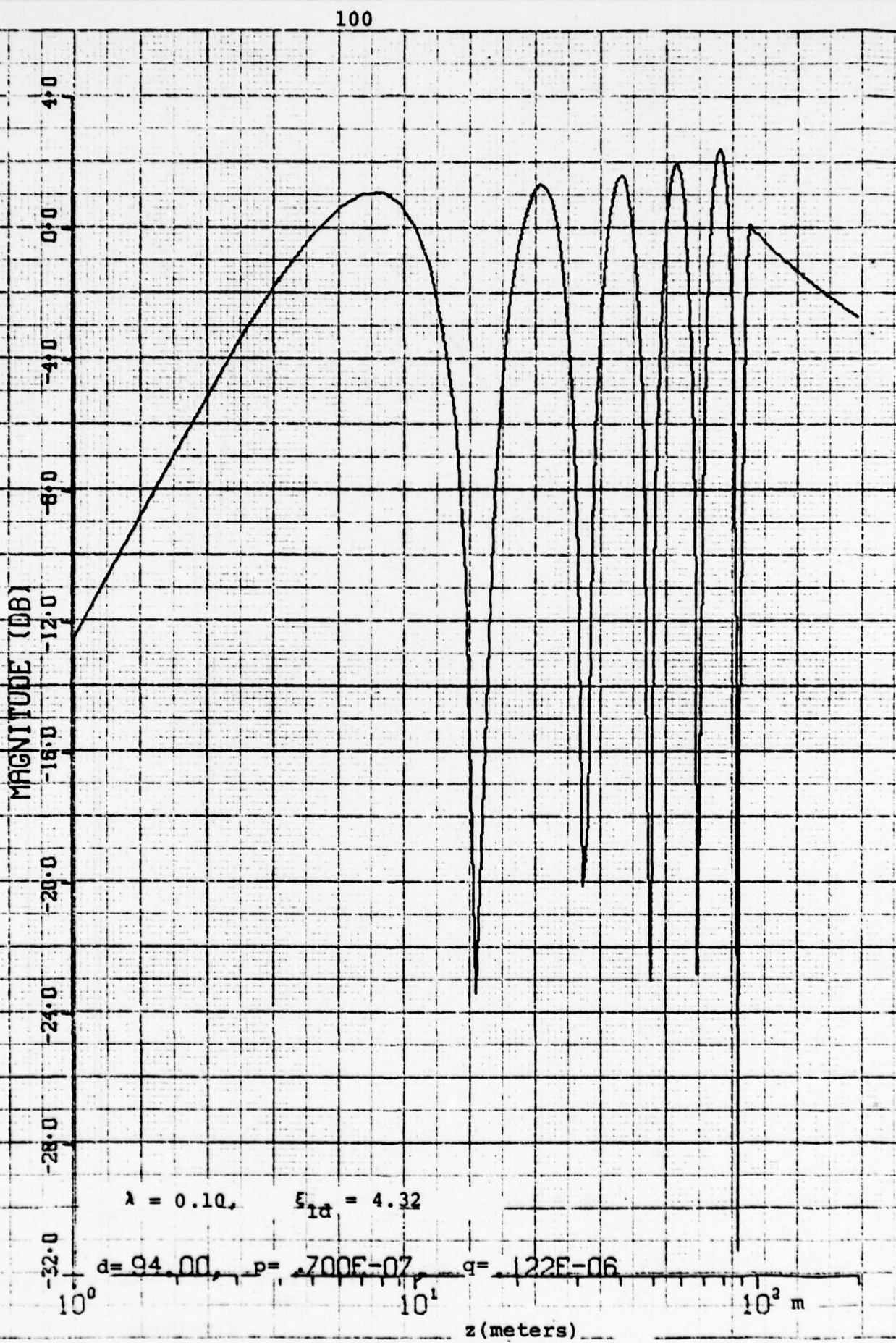


Fig. (4-40) Height-Gain Functions - September

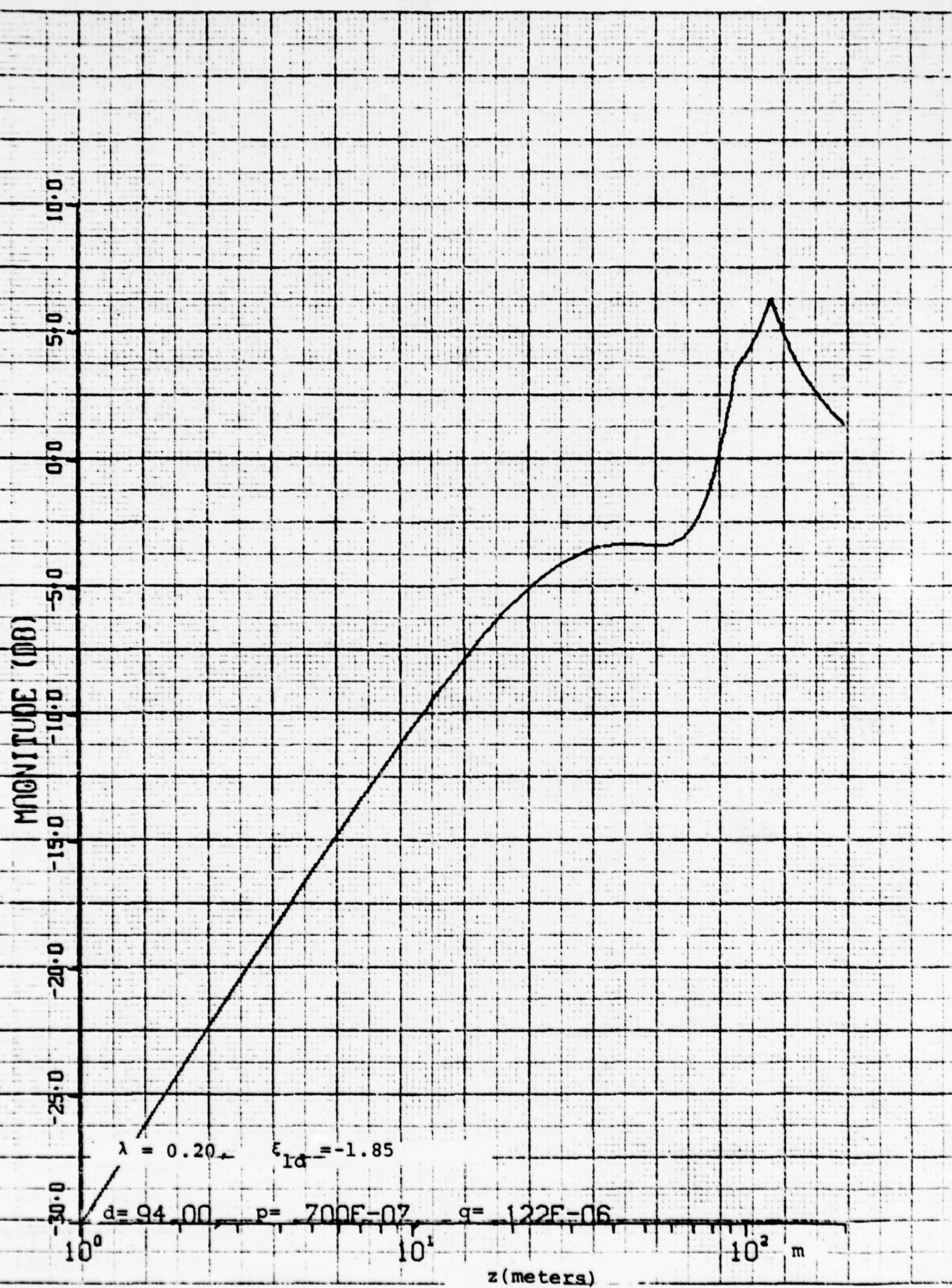


Fig. (4-41) Height-Gain Functions - September

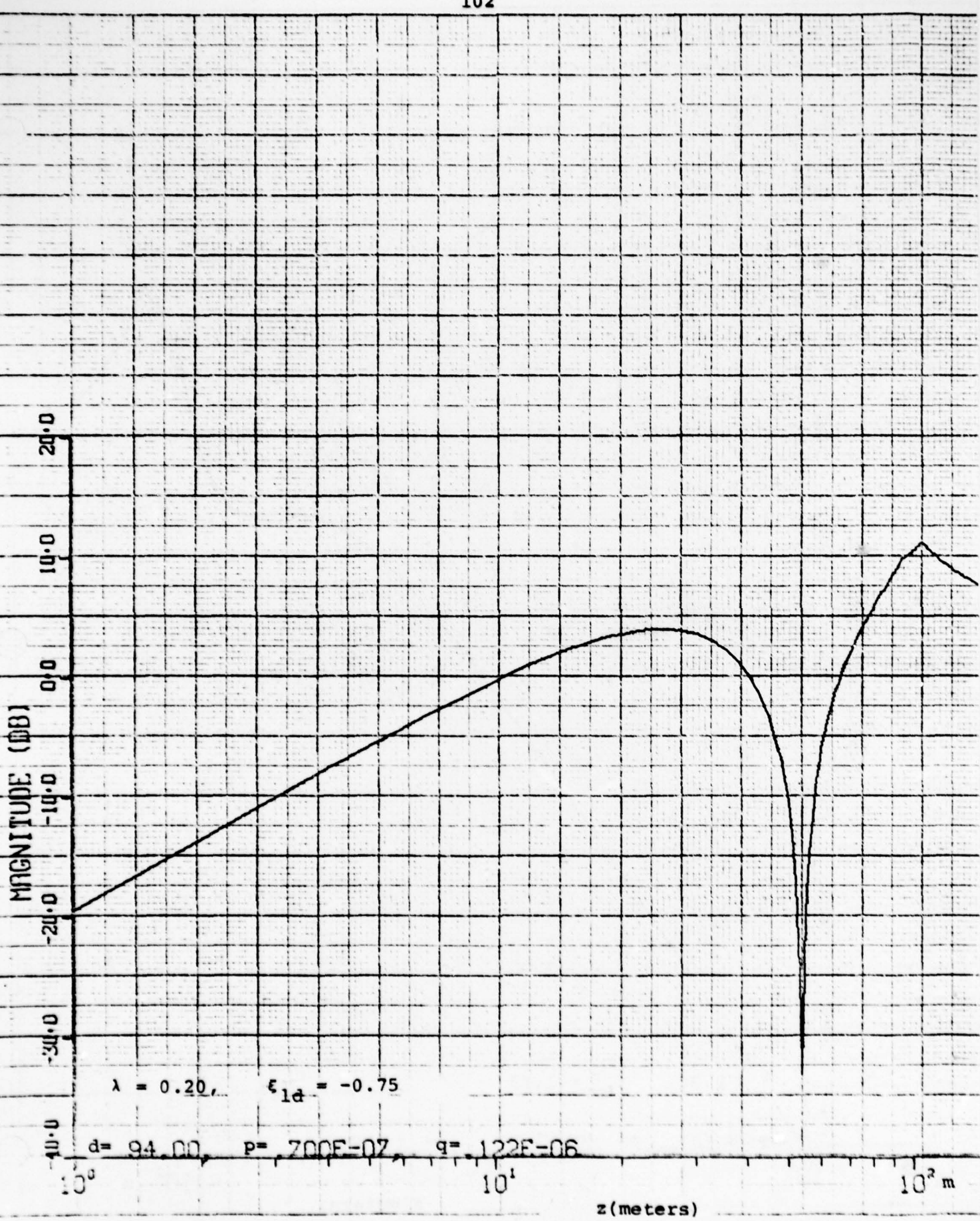


Fig. (4-42) Height-Gain Functions - September

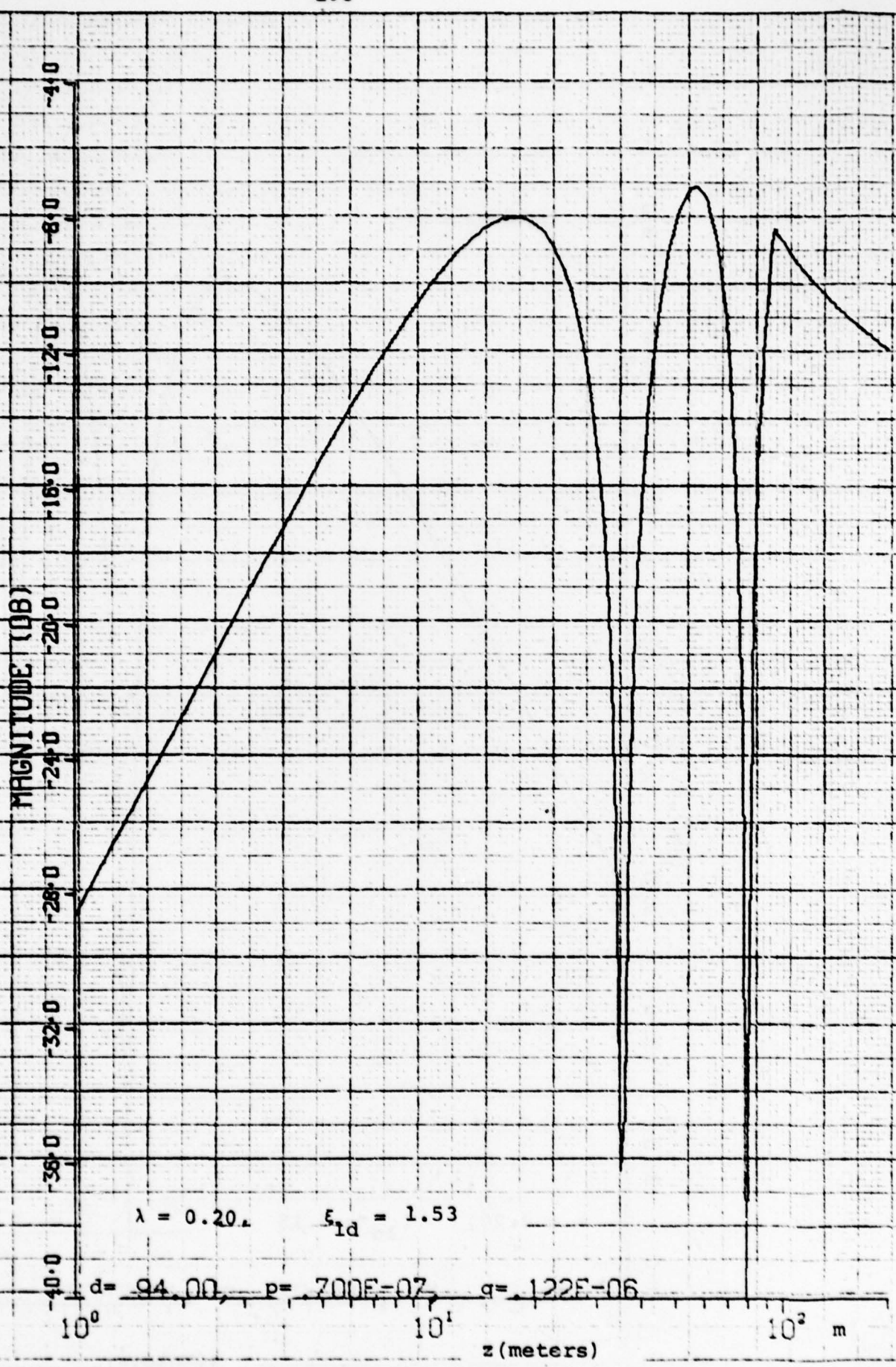


Fig. (4-43) Height-Gain Functions - September

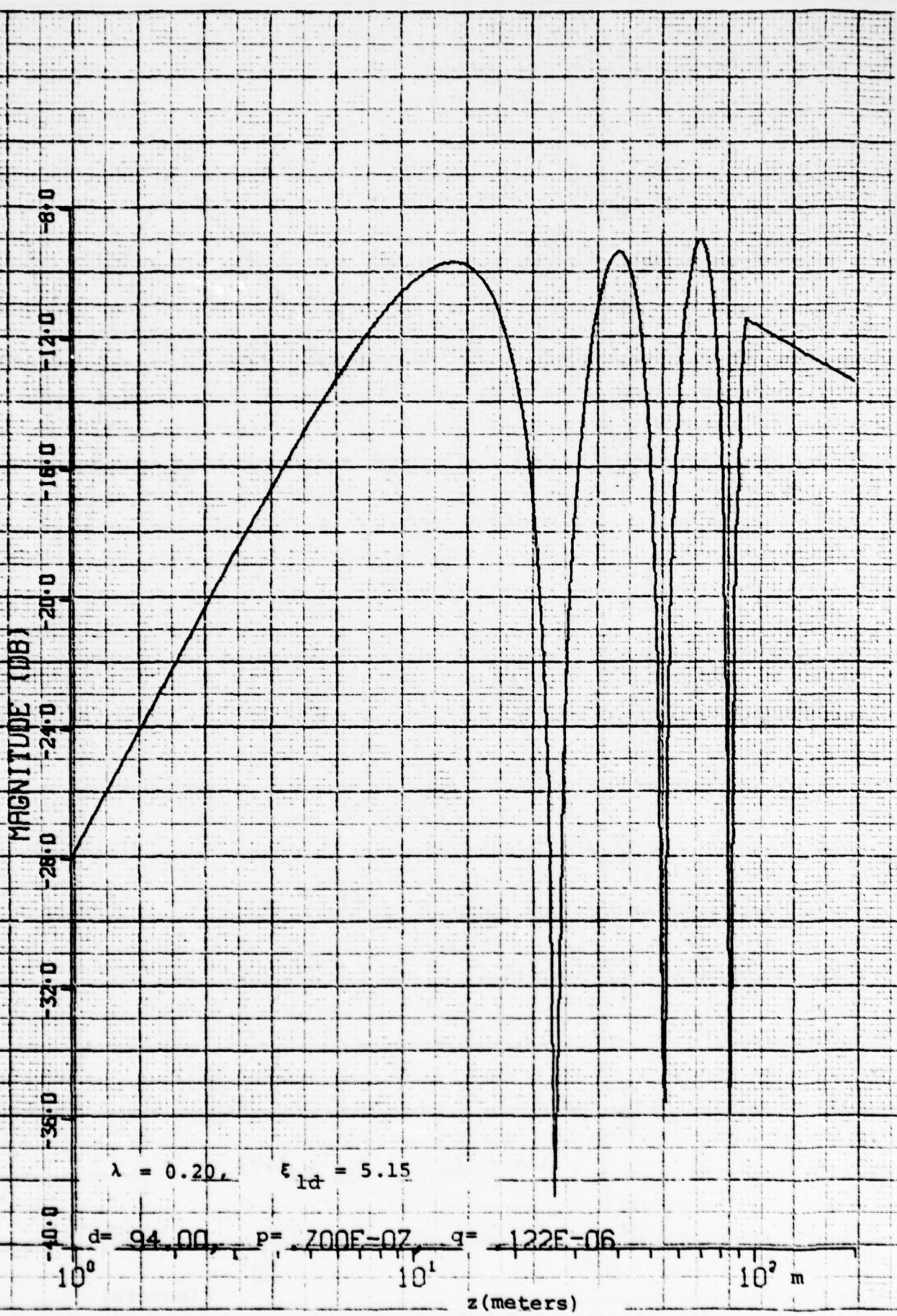


Fig. (4-44) Height-Gain Functions - September

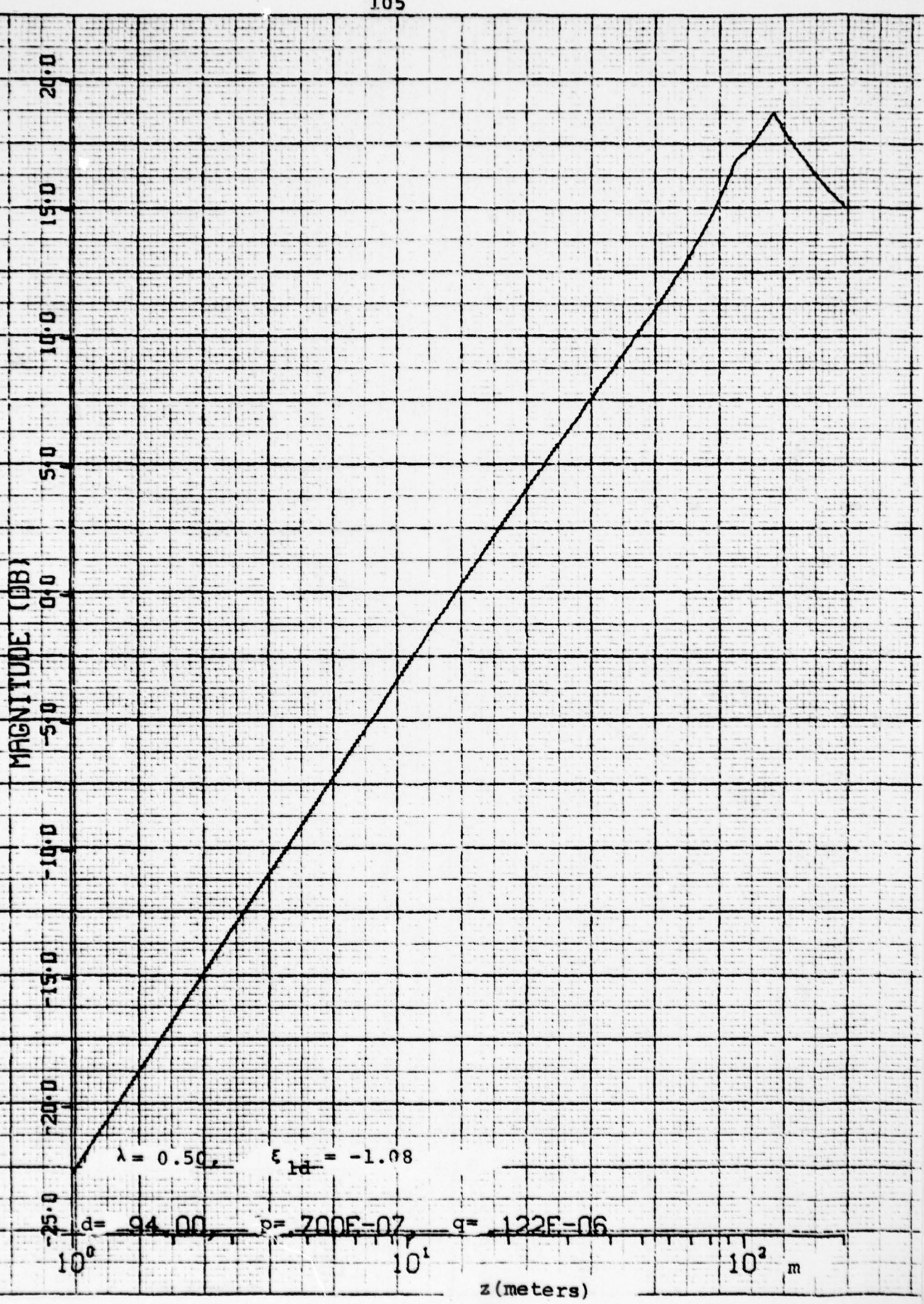


Fig. (4-45) Height-Gain Functions - September

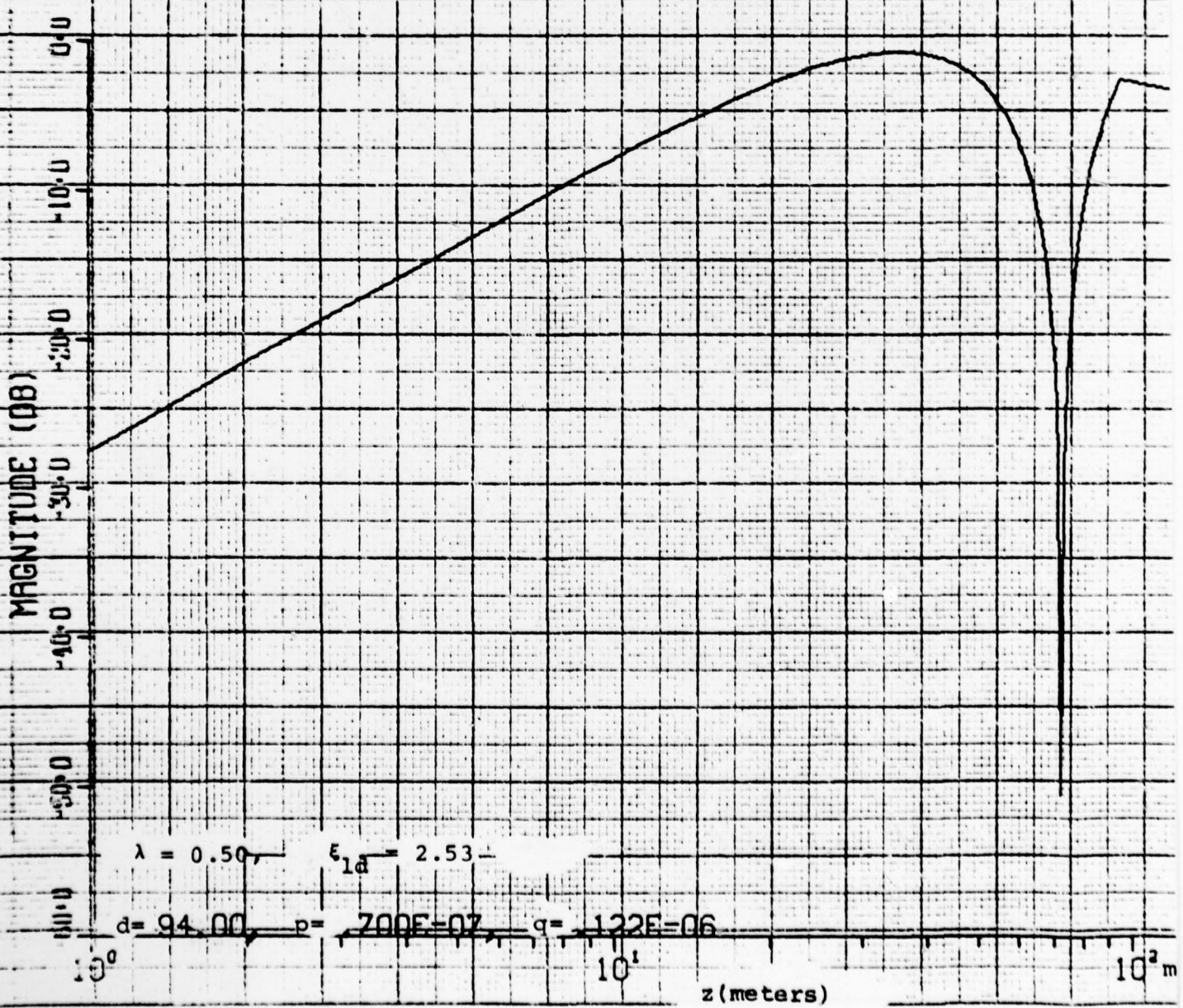


Fig. (4-46) Height-Gain Functions - September

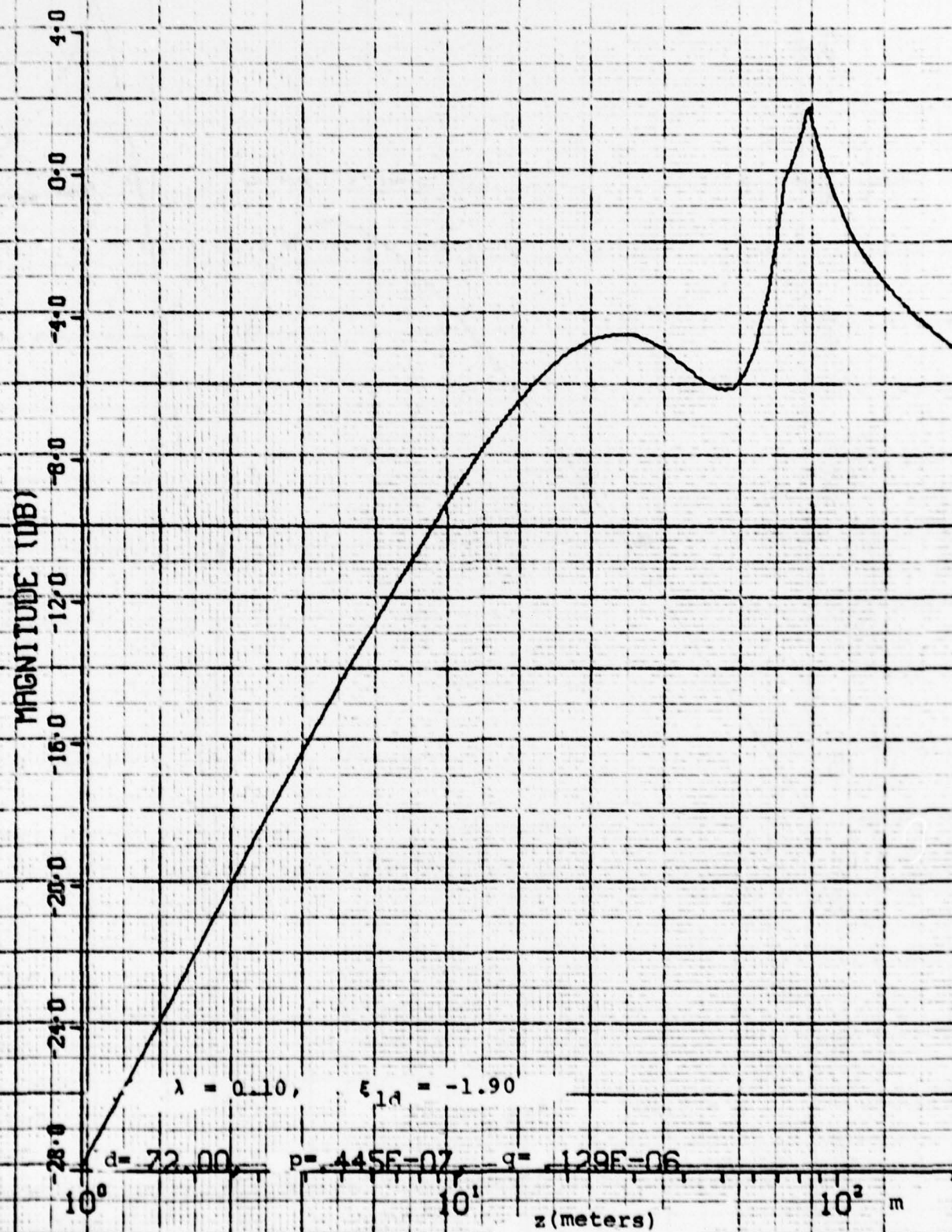


Fig. (4-47) Height-Gain Functions - December

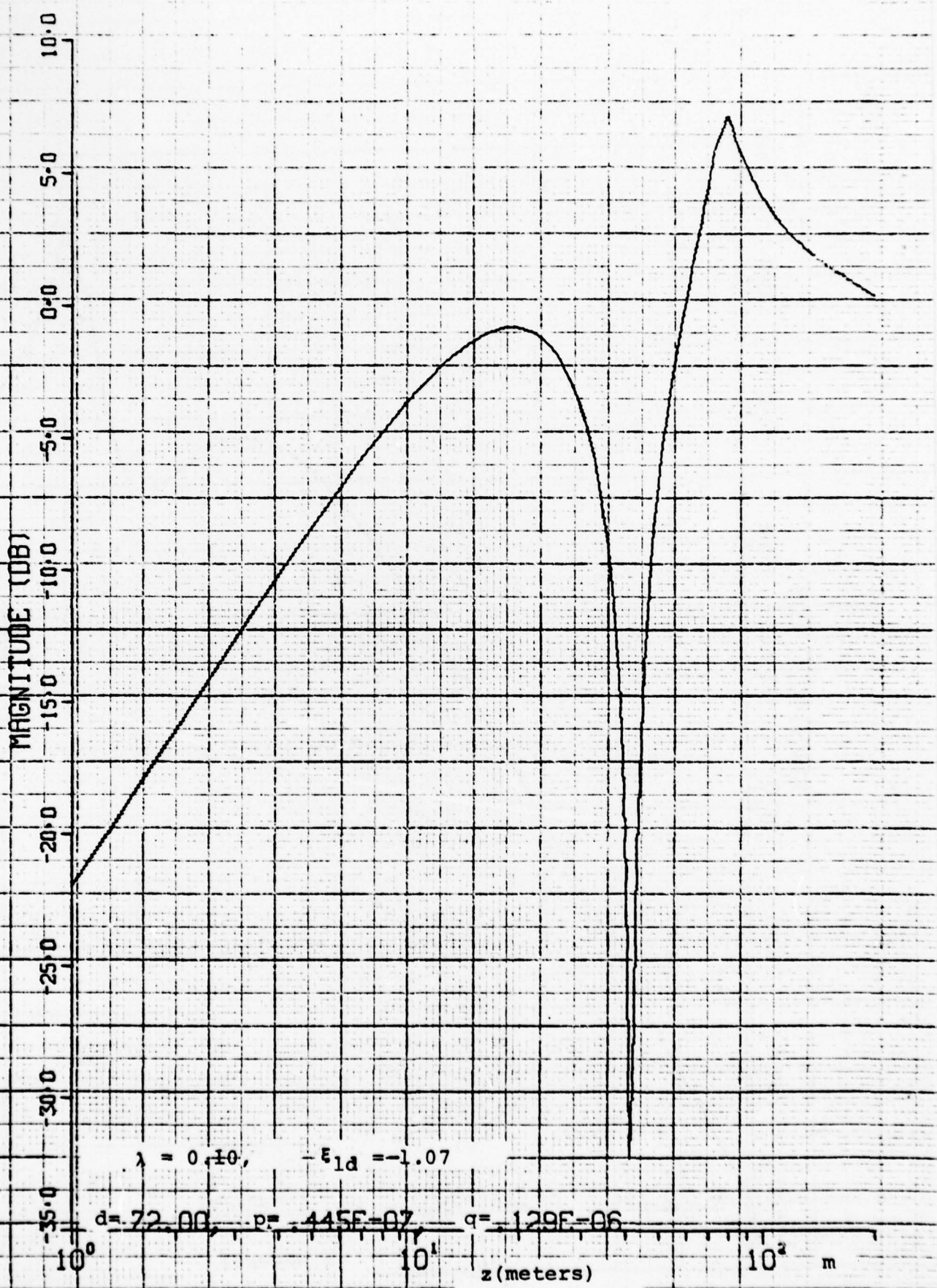


Fig. (4-48) Height-Gain Functions - December

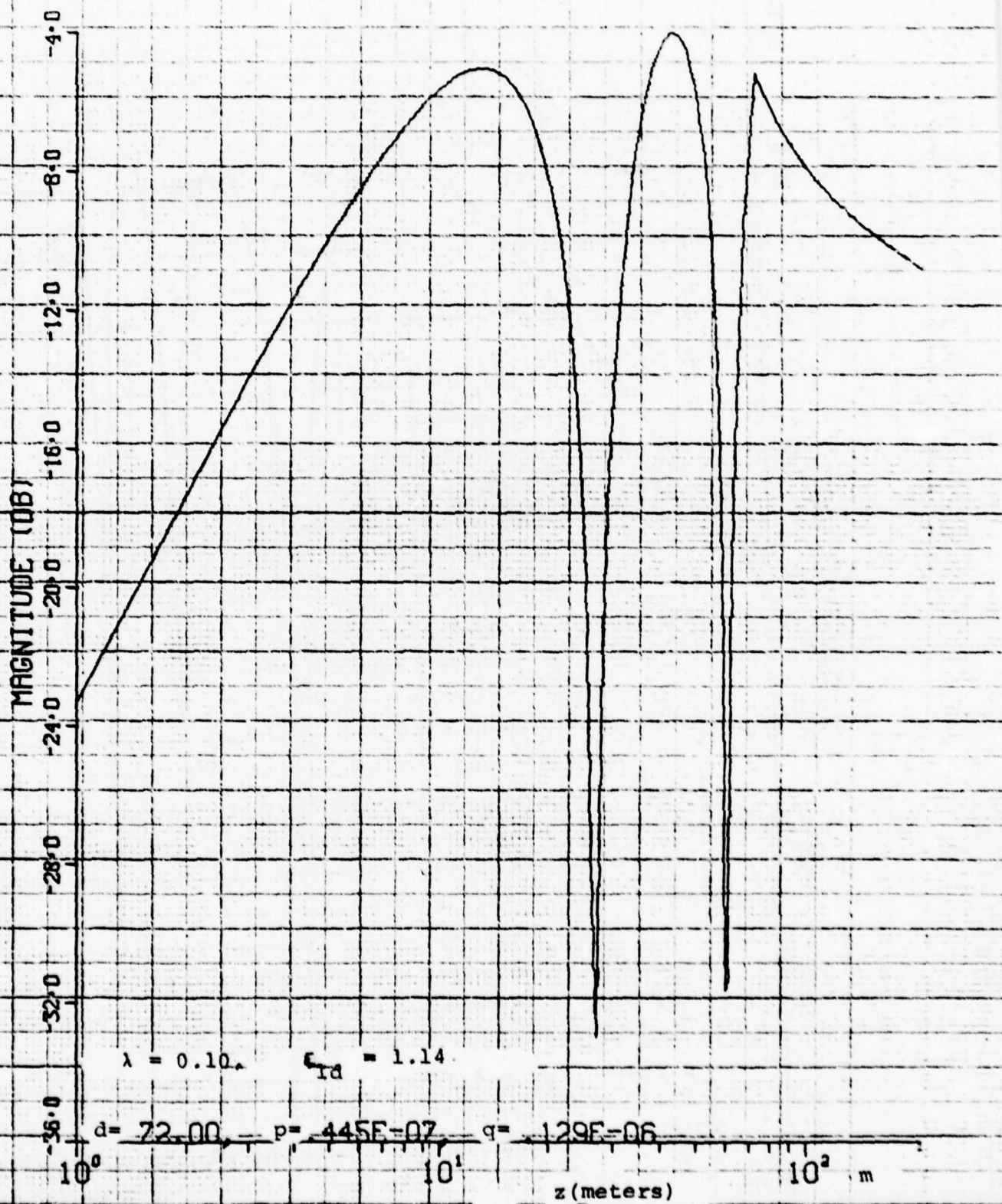


Fig. (4-49) Height-Gain Functions - December

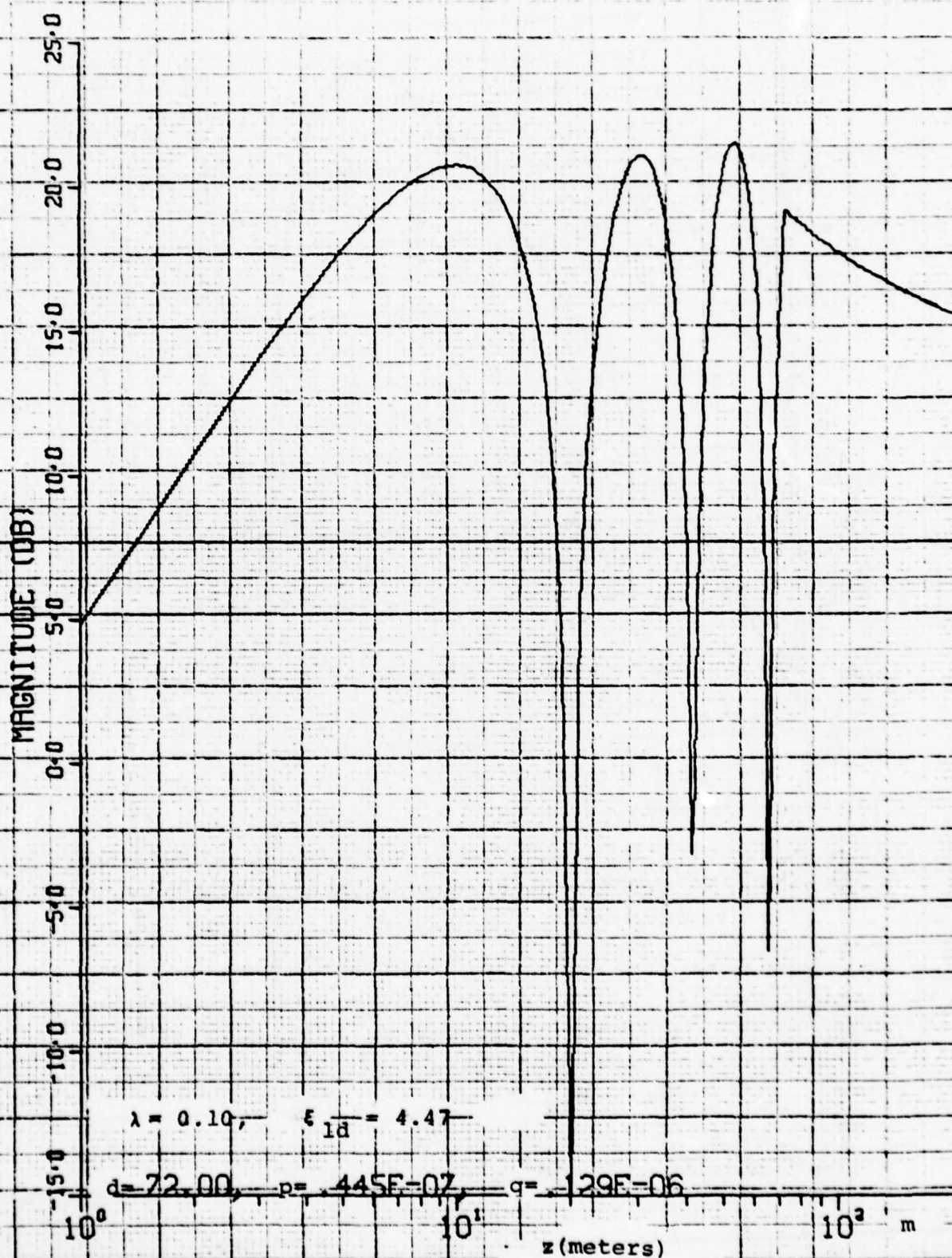


Fig. (4-50) Height-Gain Functions - December

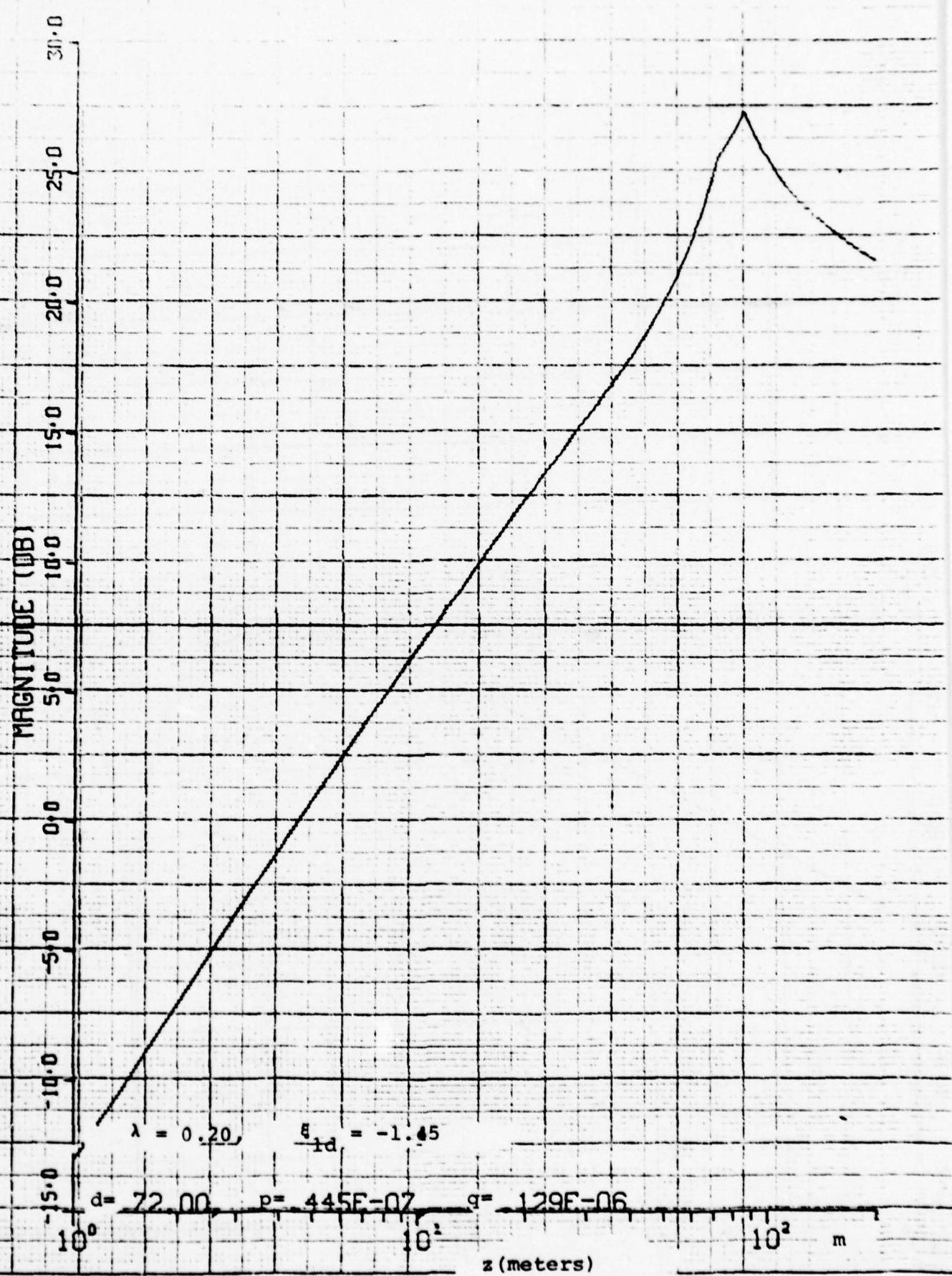


Fig. (4-51) Height-Gain Functions - December

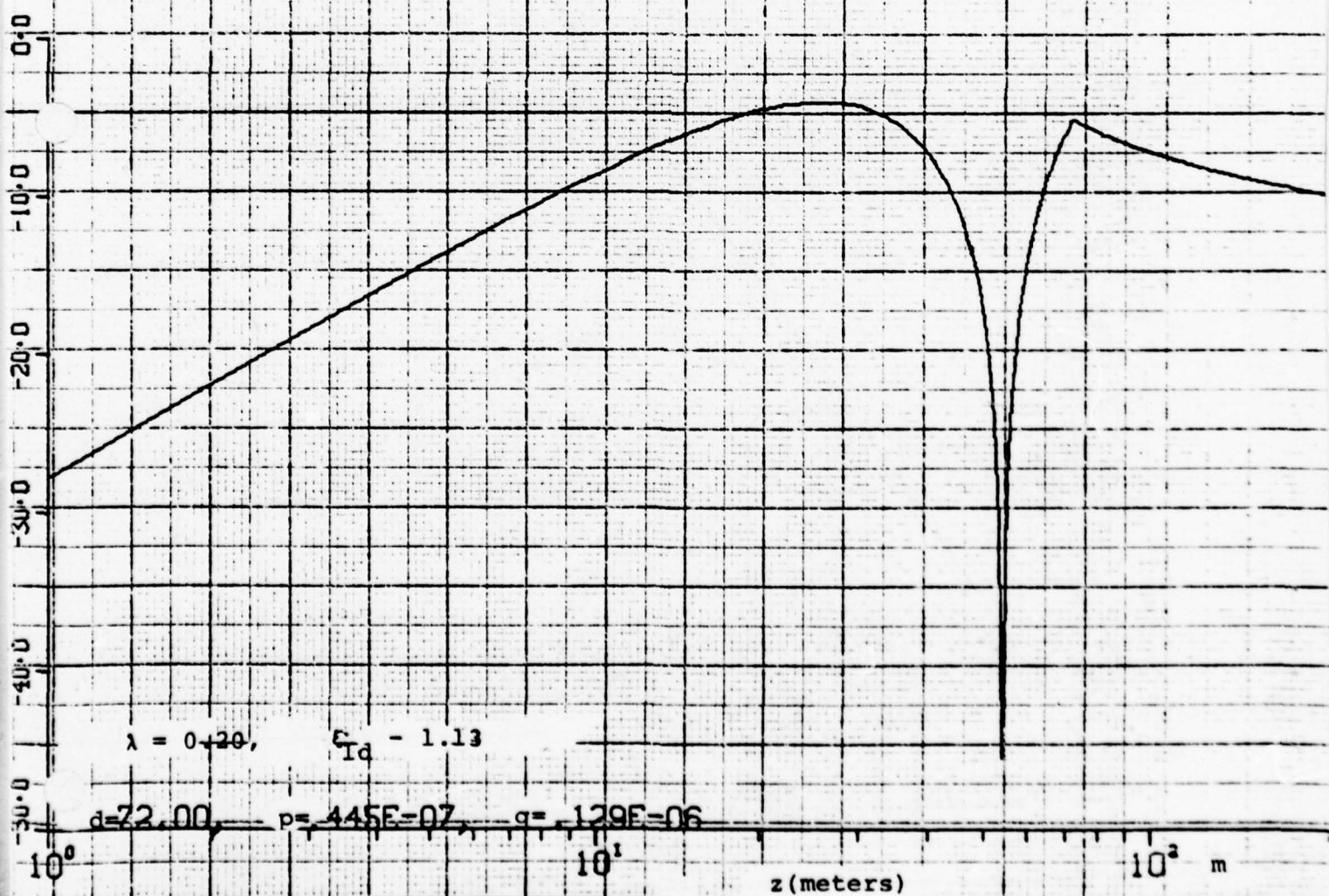


Fig. (4-52) Height-Gain Functions - December

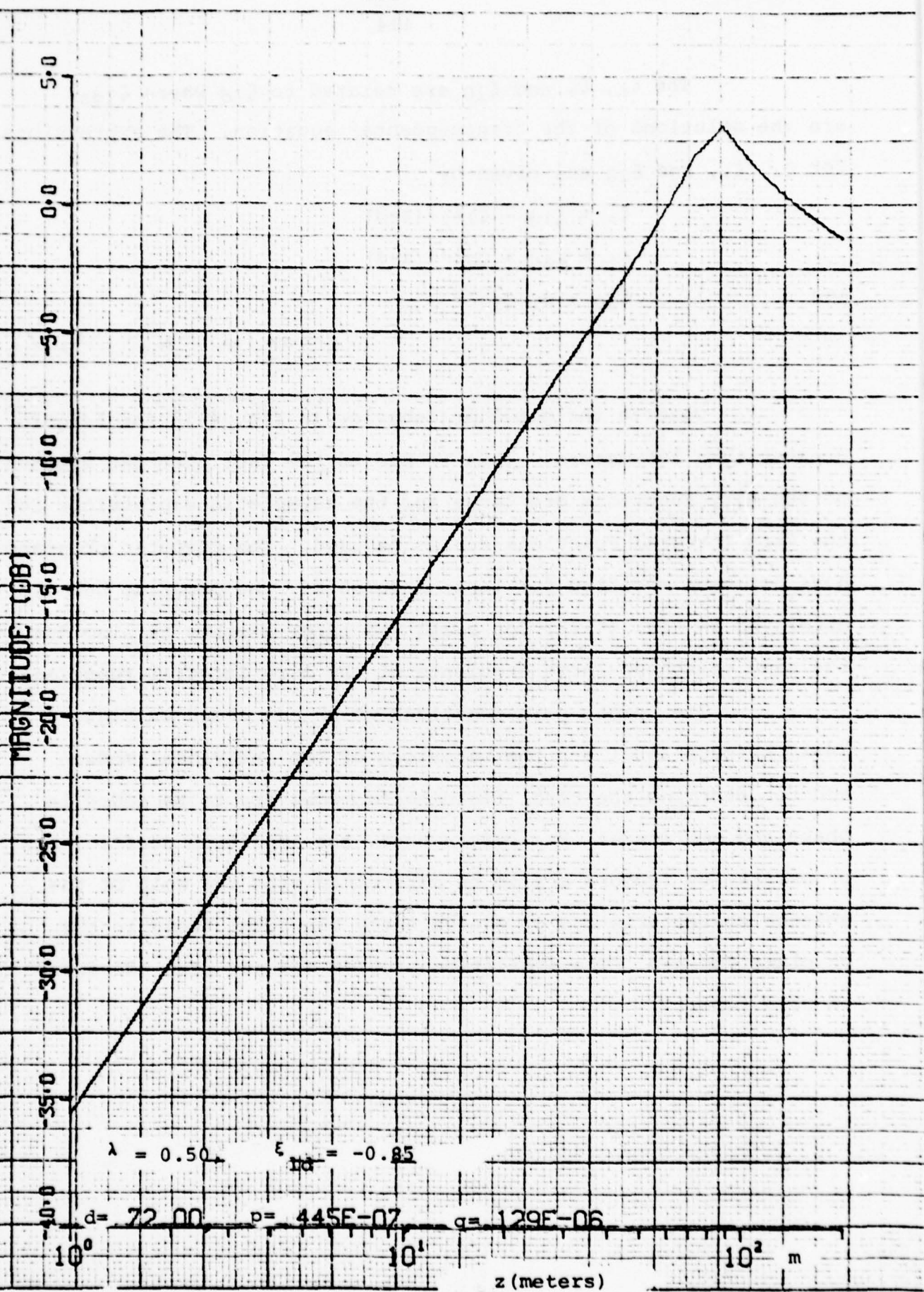


Fig. (4-53) Height-Gain Functions - December

The  $\xi_<$ ,  $\xi_>$  and  $\xi_{10}$  are related to  $\xi_{1d}$  where  $\xi_{1ds}$  are the solutions of the transcendental equation. The expressions for  $\xi_<$ ,  $\xi_>$ , and  $\xi_{10}$  are given by

$$\xi_< = \xi_{1d} - C_1^{1/3}(z-d)$$

$$\xi_> = \xi_{zd} + C_2^{1/3}(z-d)$$

and

$$\xi_{10} = B_1/C_1^{2/3}$$

---

Observe the peculiar behavior in Fig. 4-18 for heights greater than 100 meters. This is due to the fact that the arguments of the Airy Functions are large and the asymptotic expressions for the Airy Integral Functions are to be used. The computer programs have not been modified for large arguments. The peculiar behavior displayed in Fig. (4-28) for small and large heights is also due to the same reason of large arguments of the Airy Integral Functions.

The height gain functions which are shown in Figs. (4-17 through 4-53) are the behaviors of the individual modes and to determine the total field these modes are to be added in phase and amplitude. But before that, the amplitude coefficients or excitation factors are to be determined with the help of the antenna characteristics or equivalently the total field in the  $yz$  plane for  $x=0$ . The excitation problem has not been addressed in this report.

## 5. SUMMARY / RECOMMENDATIONS

### 5.1 Summary

In this phase of the program, the electromagnetic propagation through a medium, which was characteristic of meteorological conditions around Canton Island, was considered in depth. The meteorological conditions around Canton Island were represented by bilinear and trilinear refractive index profiles.

For the propagation analysis, both the geometrical optics or ray trajectory approach and the physical optics or the guided wave approach were considered. The relative merits of these approaches were highlighted. The ray trajectories for four different days of meteorological data were also generated.

The guided mode approach was pursued to determine the propagation behavior for both the bilinear and trilinear refractive index profiles.

The numerical analysis to determine the modal solutions and the corresponding height-gain functions was carried out only for the bilinear profile. The modal solutions were obtained by iterative numerical analysis of the transcendental equation for the trapped modes only.

For the leaky modes, a previously developed approximate expression was used. The validity of the expression for duct heights smaller than the frequency dependent scale height was established.

Although leaky modes are indicative of the field above the duct height, for quantitative assessment of the field intensity in the shadow zone, the excitation problem has to be solved. This has not been addressed in this phase of the program.

### 5.2 Recommendations

The usefulness of the guided wave propagation analysis hinges on the ability to generate radar coverage diagrams. The radar coverage diagrams in the presence of different kinds of meteorological ducts would enable one to evaluate the performance degradation of ESD sponsored surveillance radar systems.

For the generation of radar coverage diagrams, the following tasks need to be completed.

1. An effective analytical technique to determine the complex eigenvalues representing leaky modes.
2. Determining the amplitude coefficients of the trapped and leaky modes by addressing the excitation problems or by specifying the antenna characteristics.
3. Applying these techniques to different meteorological conditions and different radar systems parameters.

These tasks can constitute the second phase of the program.

## 6. REFERENCES

1. B.R. Bean and E.J. Dutton - Radio Meteorology, Dover Publication, 1968
2. D.E. Kerr - Propagation of Short Radio Waves, Radiation Laboratory Series Vol. 13, McGraw-Hill, 1951
3. A. Zancla - (Editor) - Modern Topics in Microwave Propagation and Air-Sea Interaction, Proceedings of the NATO Advanced Study Institute, Sorento, Italy, June 5-14, 1973 - D. Reidel Publishing Company
4. J.R. Wait - Electromagnetic Waves in Stratified Media, Macmillan Company, 1962
5. P. Beckman and A. Spizzichino - The Scattering of Waves from Rough Surfaces, Macmillan Company, 1963
6. D. Barton - Radar Clutter ARTECH House, 1975
7. M. Abramowitz and L.A. Stegun (Edited by) Handbook of Mathematical Functions National Bureau of Standards - Applied Mathematics Series - 55, June 1964
8. K.G. Budden - The Wave Guide Mode Theory of Wave Propagation Prentice Hall, 1961
9. J.H. Richter and H.V. Hitney - The Effect of the Evaporation Duct on Microwave Propagation, NELC Report TR-1949, April 1975
10. H.V. Hitney - Propagation Modeling in the Evaporation Duct, NELC Report - TR-1947, April 1975
11. H. Jeske and K. Brooks - Comparison of Experimental on Duct Propagation above the Sea with the Mode Theory of Booker and Walkinshaw, Radio Science Vol. 1, August 1966
12. H.W. Fruchtenicht - Notes on Duct Influences on Line-of-Sight Propagation, IEEE Transactions on Antennas and Propagation Vol. AP-22, No. 2 - March 1974
13. J.K. DeRosa - Refractive Multipath in Low Angle Radar Tracking, IEEE International Radar Conference, 1975
14. G.H. Joshi - Propagation Modeling in the Presence of Meteorological Ducts, Raytheon Technical Memo No. GHJ:76:09, August 1976
15. L.M. Brekhovshikh - Waves in Layered Media, Academic Press, 1960

## REFERENCES (CONT)

16. Tables of the Modified Hankel Functions of Order One-Third and of Their Derivatives, The Annals of the Computation Laboratory of Harvard University, Vol. II, Harvard University Press, 1945
17. J.C.P. Miller - The Airy Integral - Mathematical Tables, University Press Cambridge, 1946
18. G.N. Watson - The Diffraction of Electric Waves by the Earth, Proc. Roy. Soc. A, 95, 83, 1919
19. G.N. Watson - The Transmission of Electric Waves Round the Earth, Proc. Roy. Soc. A, 95, 546, 1919

APPENDIX I

Computer program to determine the roots  
of the transcendental equation.









PROGRAM JOBT

73/74 OPTICAL TAPE

RIN 0.69433

11/00/20, 12.59.31

PAGE

82128

STATISTICS  
PROGRAM LENGTH  
BUFFER LENGTH  
IN LINES/OUT COMMON LENGTH  
920000 CH USED

7343 676  
33618 1777  
17343 993

124  
Appendix I  
I-5

THIS PAGE IS BEST QUALITY PRACTICABLE  
FROM COPY FURNISHED TO DDC



END

## SYNTHETIC REFERENCE MAP (PAGE)

ENTRY POINTS DEF LINE REFERENCES  
#1 #2

VARIABLES ON TYPE

RELLOCATION

REFS

126  
Appendix I  
I-7THIS PAGE IS BEST QUALITY PRACTICABLE  
FROM COPY FURNISHED TO DDCFILE NAMES MODE  
OUTPUT FMT  
FILE NAMES MODE  
INTRIN 01 66  
FILE NAMES MODE  
INTRIN 26 27  
FILE NAMES MODE  
INTRIN 26 27  
FILE NAMES MODE  
INTRIN 26 27SYNTHETIC FUNCTIONS TYPE ANG DEF LINE REFERENCES  
abs REAL 1 INTRIN 26 27  
abs DOUBLE 1 INTRIN 26 27



```

      C SUBROUTINE CFACT
      C COMMON /XFACT/XFACT(1100),P1(99),GT(99),GP(99),GTP(99),
      C      * FMULT,GMULT,JHOL(120),AP1(120),VP1(120),JHOL(1100)
      C DOUBLE PRECISION FMULT,P1,GMULT,GT,GTP,XFACT
      C
      C XFACT(1100)
      C      DO 100 100,102,100
      C      XFACT(11)XFACT(11+1)91
      C
      C 9999 RETURN
      CEND

```

## SYMBOLIC REFERENCE MAP (Page)

ENTRY POINTS	DEF LINE	REFERENCES
CFACT	2	13

VARIABLES	ON	TYPE	RELOCATION	REFERS
I200	FMULT	DOUBLE	XFACT	REFS
G90	P1	DOUBLE	XFACT	REFS
T10	GTP	DOUBLE	ARRAY	REFS
I200	GMULT	DOUBLE	ARRAY	REFS
G92	GT	DOUBLE	XFACT	REFS
I050	GTP	DOUBLE	XFACT	REFS
J22	J	INTEGER	XFACT	REFS
I212	JHOL	INTEGER	ARRAY	REFS
I210	JHOL	INTEGER	ARRAY	REFS
0	XFACT	DOUBLE	ARRAY	REFS
I212	XP1	REAL	ARRAY	REFS
I062	VP1	REAL	ARRAY	REFS

STATEMENT LABELS	DEF LINE	REFERENCES
0 100	11	10
0 999	INACTIVE	13

LOOPS	LABEL	INDEX	FROM-TO	LENGTH	PROPERTIES
13 109	1	10 11	98	INITACK	

COMMON BLOCKS	LENGTH	MEMBERS - BIAS NAME (LENGTH)	REFS
XFACT	999	0 XFACT (300)	300 P1 (601)

COMMON BLOCKS	LENGTH	MEMBERS - BIAS NAME (LENGTH)	REFS
XFACT	999	472 GTP (605)	958 GTP (605)
		646 GMULT (2)	646 JHOL (2)
		770 VP1 (120)	890 JHOL (120)

STATISTICS	PROGRAM LENGTH	17360 960
	COMMON LENGTH	920000 CH USED

Appendix  
I-9

THIS PAGE IS BEST QUALITY PRACTICABLE  
FROM COPY FURNISHED TO DDC

821238

11/10/01 11pm10m 11/13/01 11pm10m 11pm10m 11pm10m

177/00/22, 11:54:33

JUNCIUM 1M2HZP(MG,M2,M3P)

COMMON /FACT1/IFACT1(150),IF1(43),IF1P(43),  
PRM1,GMOL1,GMOL(12),XP1(120),VP1(120),INAT(12)

9 JOURNAL OF LAW AND MEDICINE

សំណើលាម និងសំណើលាម

**DOUBLE PRECISION** **DOUBLE PRECISION** **DOUBLE PRECISION**

PRINT & ADVERTISING

RETHAKING

100 on 2000

卷之三

卷之三

卷之三

JF CANS (HFT) 1

卷之三

卷之三

HAIKU (CONT'D)

卷之三

卷之三

FORMAT (13, 1X, 1)

00 203 101 95

1000 CANADA

202 CONCLUDING

卷之三

602 JOURNAL OF CLIMATE

卷之三





THIS PAGE IS BEST QUALITY PRACTICABLE  
FROM COPY FURNISHED TO DDC

```

      C COMPLEX #2D
      C DOUBLE PRECISION H2,H2P,EYP,EYH,800,800,P1,P2,DIL0OP,C1,XNUM,XDEN
      C DOUBLE PRECISION A00P,B00P,A000,B000,A000P,B000P
      C DOUBLE PRECISION XNUM,XDEN,C1,PAS

      C
      C 18U110
      C 82D=SQRTCEXP(CMPLX(0.+2.*PI/3.))#PA3002
      C IF (I8U112#H2P#B2D#H2P) .NE. 1#GO TO 970
      C EYP#H2/H2P
      C 840008004001000C1#0(.1.)
      C IF (I8U112#B2D#A00P#B00P#A000P#B000P#A000P#B000P)
      C IF (I8U112#B2D#A00#B00#A000#B000#A000P#B000P#A000P#B000P)
      C EYN=(A00-/A000/B000#B001#B0000)/(A00P#B000#B000#B000#B000P)
      C XNUM=EYH#PA3002
      C XDEN=1.+#B2D#B2D#EYH#B2D#PA3002#EYH#B2D#PA3002#EYH#B2D#PA3002#EYH#B2D#PA3002
      C GO TO 999

      10   C 970 18U11-1
      C 999 RETURN
      C END

      20   C 970 18U11-1
      C 999 RETURN
      C END

      C
      C 18U11
      C
      C SYMBOLIC REFERENCE MAP (Re11)
      C ENTRY POINTS DEF LINE REFERENCES
      C 18U11 1 21
      C
      C VARIABLE $ $N TYPE RELOCATION
      C 212 A00 DOUBLE REF#
      C 216 A00P DOUBLE REF#
      C 222 A000 DOUBLE REF#
      C 226 A000P DOUBLE REF#
      C 214 B00 DOUBLE REF#
      C 220 B00P DOUBLE REF#
      C 224 B000 DOUBLE REF#
      C 230 B000P DOUBLE REF#
      C 21 C1 DOUBLE REF#
      C 0 DIL0OP REAL REF#
      C 210 EYN DOUBLE REF#
      C 206 EYP DOUBLE REF#
      C 202 H2 DOUBLE REF#
      C 204 H2P DOUBLE REF#
      C 201 I8U11 INTEGER DEFINED
      C 201 PAS DOUBLE REF#
      C 201 P1 REAL REF#
      C 201 P2 DOUBLE REF#
      C 800 DOUBLE DEFINED
      C 820 COMPLEX DEFINED
      C 800 DOUBLE DEFINED
      C XDEN DOUBLE DEFINED
  
```

132  
Appendix I  
I-13

FUNCTION 18100

PTN 4.66998

PAGE 2

VARIABLES ON TYPE  
0 INUM DOUBLE

13/10 OPTICAL TRACE

RELOCATION

V.P.

EXTERNALS  
C1XP  
I1BJ  
IN242P  
INTERNAL  
COMPLEX  
INTEGER  
INTEGER

TYPE

AREA

REFERENCE

COMPLEX

1 LIBRARY

9

INTEGER

2

10

INTEGER

3

10

IN-LINE FUNCTION TYPE

COMPLEX

AREA

REF LINE

REFERENCE

COMPLEX

3 INT16

REF LINE

REFERENCE

STATEMENT LABEL

REF LINE

REFERENCE

15

10

10

10

10

10

10

10

10

10

10

10

10

10

10

10

10

10

10

10

10

10

10

10

10

10

10

10

10

10

10

10

10

10

10

10

10

10

10

10

10

10

10

10

10

10

Appendix I  
I-14THIS PAGE IS BEST QUALITY PRACTICABLE  
FROM COPY FURNISHED TO DDG

821232

HIS PAGE IS BEST QUALITY PRACTICABLE  
FROM COPY FURNISHED TO DDC

```

C SUBROUTINE IPLOT(JCNT,XLINK,01P,00P,PALLOOP)
C
COMMON /XFACT/XFACT(150),FT(43),BT(43),FT(45),BT(45)
      * FMULT,5MLT,JJHOL(2),XPL(120),YPL(120),IMUL(100)
      *
      * DINHLE PRECISION XFACT,01P,00P,01P,00P,01P,00P
      * CALL TITLE(mn,100P,00P,100P,
      *           n,100,100,12,00,0)
      *
      * XMSGC9.
      * XMSGC9,25
      * ENCODE(100,111,1H0L)XL1L
      * FORMAT(9I6,1,000)
      * CALL MESSAG(1H0L,100,XMSGC,YMSGC)
      *
      * XMSGC9,25
      * ENCODE(100,121,1H0L)DIL00P
      * CALL MESSAG(1H0L,100,XMSGC,YMSGC)
      *
      * 121 FORMAT(9D,1,000)
      * 122 ENCODE(100,131,1H0L)PAL00P
      * 123 FORMAT(9P/A 0,0P,1,000)
      * 124 CALL MESSAG(1H0L,100,XMSGC,YMSGC)
      * 125 CALL GRAPH(*0,*1,*0,*2,*)
      * 126 CALL CURVE(XP1,YP1,TENT,0)
      * 127 CALL ENDPL(0)
      *
      C 999 RETURN
      END.

```

Appendix I  
I-15

## SYMBOLIC REFERENCE MAP (R00)

ENTRY POINTS	DEF LINE	REFERENCES
I IPLOT	28	

VARIABLES	BN	TYPE	RELOCATION	REFS	DEFNED
0	DIL00P	REAL	P_P	REFS	1
1204	FMUL,T	DOUBLE	XFACT	REFS	1
454	FT	DOUBLE	ARRAY	REFS	1
730	BT	DOUBLE	ARRAY	REFS	1
1206	5MLT	DOUBLE	XPACT	REFS	1
602	C1	DOUBLE	XPACT	REFS	1
1050	6TP	DOUBLE	ARRAY	REFS	1
0	JCNT	INTEGER	P_P	REFS	1
1972	1H0L	INTEGER	XPACT	REFS	1
1210	PALLOOP	REAL	21	REFS	1
0	XFACT	DOUBLE	ARRAY	REFS	1
0	XLINK	REAL	XFACT	REFS	1
0	XMSG	REAL	P_P	REFS	1
102	XP1	REAL	REAL	REFS	1
1212	YP1	REAL	ARRAY	REFS	1
141	YMSG	REAL	REAL	REFS	1

VARIABLES	ON	TYPE	REFLOC/1100	REFNAME	REFLINE	REFPAGE	REFSEG	REFTYPE	REFVAL	REFX	REFY	REFZ
1001 - YP1		REAL										
1002 - YP2		REAL										
1003 - YP3		REAL										
1004 - YP4		REAL										
1005 - YP5		REAL										
1006 - YP6		REAL										
1007 - YP7		REAL										
1008 - YP8		REAL										
1009 - YP9		REAL										
1010 - YP10		REAL										
1011 - YP11		REAL										
1012 - YP12		REAL										
1013 - YP13		REAL										
1014 - YP14		REAL										
1015 - YP15		REAL										
1016 - YP16		REAL										
1017 - YP17		REAL										
1018 - YP18		REAL										
1019 - YP19		REAL										
1020 - YP20		REAL										
1021 - YP21		REAL										
1022 - YP22		REAL										
1023 - YP23		REAL										
1024 - YP24		REAL										
1025 - YP25		REAL										
1026 - YP26		REAL										
1027 - YP27		REAL										
1028 - YP28		REAL										
1029 - YP29		REAL										
1030 - YP30		REAL										
1031 - YP31		REAL										
1032 - YP32		REAL										
1033 - YP33		REAL										
1034 - YP34		REAL										
1035 - YP35		REAL										
1036 - YP36		REAL										
1037 - YP37		REAL										
1038 - YP38		REAL										
1039 - YP39		REAL										
1040 - YP40		REAL										
1041 - YP41		REAL										
1042 - YP42		REAL										
1043 - YP43		REAL										
1044 - YP44		REAL										
1045 - YP45		REAL										
1046 - YP46		REAL										
1047 - YP47		REAL										
1048 - YP48		REAL										
1049 - YP49		REAL										
1050 - YP50		REAL										
1051 - YP51		REAL										
1052 - YP52		REAL										
1053 - YP53		REAL										
1054 - YP54		REAL										
1055 - YP55		REAL										
1056 - YP56		REAL										
1057 - YP57		REAL										
1058 - YP58		REAL										
1059 - YP59		REAL										
1060 - YP60		REAL										
1061 - YP61		REAL										
1062 - YP62		REAL										
1063 - YP63		REAL										
1064 - YP64		REAL										
1065 - YP65		REAL										
1066 - YP66		REAL										
1067 - YP67		REAL										
1068 - YP68		REAL										
1069 - YP69		REAL										
1070 - YP70		REAL										
1071 - YP71		REAL										
1072 - YP72		REAL										
1073 - YP73		REAL										
1074 - YP74		REAL										
1075 - YP75		REAL										
1076 - YP76		REAL										
1077 - YP77		REAL										
1078 - YP78		REAL										
1079 - YP79		REAL										
1080 - YP80		REAL										
1081 - YP81		REAL										
1082 - YP82		REAL										
1083 - YP83		REAL										
1084 - YP84		REAL										
1085 - YP85		REAL										
1086 - YP86		REAL										
1087 - YP87		REAL										
1088 - YP88		REAL										
1089 - YP89		REAL										
1090 - YP90		REAL										
1091 - YP91		REAL										
1092 - YP92		REAL										
1093 - YP93		REAL										
1094 - YP94		REAL										
1095 - YP95		REAL										
1096 - YP96		REAL										
1097 - YP97		REAL										
1098 - YP98		REAL										
1099 - YP99		REAL										
1100 - YP100		REAL										
1101 - YP101		REAL										
1102 - YP102		REAL										
1103 - YP103		REAL										
1104 - YP104		REAL										
1105 - YP105		REAL										
1106 - YP106		REAL										
1107 - YP107		REAL										
1108 - YP108		REAL										
1109 - YP109		REAL										
1110 - YP110		REAL										
1111 - YP111		REAL										
1112 - YP112		REAL										
1113 - YP113		REAL										
1114 - YP114		REAL										
1115 - YP115		REAL										
1116 - YP116		REAL										
1117 - YP117		REAL										
1118 - YP118		REAL										
1119 - YP119		REAL										
1120 - YP120		REAL										
1121 - YP121		REAL										
1122 - YP122		REAL										
1123 - YP123		REAL										
1124 - YP124		REAL										
1125 - YP125		REAL										
1126 - YP126		REAL										
1127 - YP127		REAL										
1128 - YP128		REAL										
1129 - YP129		REAL										
1130 - YP130		REAL										
1131 - YP131		REAL										
1132 - YP132		REAL										
1133 - YP133		REAL										
1134 - YP134		REAL										
1135 - YP135		REAL										
1136 - YP136		REAL										
1137 - YP137		REAL										
1138 - YP138		REAL										
1139 - YP139		REAL										
1140 - YP140		REAL										
1141 - YP141		REAL										
1142 - YP142		REAL										
1143 - YP143		REAL										
1144 - YP144		REAL										
1145 - YP145		REAL										
1146 - YP146		REAL										
1147 - YP147		REAL										
1148 - YP148		REAL										
1149 - YP149		REAL										
1150 - YP150		REAL										
1151 - YP151		REAL										
1152 - YP152		REAL										
1153 - YP153		REAL										
1154 - YP154		REAL										
1155 - YP155		REAL										
1156 - YP156		REAL										
1157 - YP157		REAL										
1158 - YP158		REAL										
1159 - YP159		REAL										
1160 - YP160		REAL										
1161 - YP161		REAL										
1162 - YP162		REAL										
1163 - YP163		REAL</										

NAME OF THE LOAD 111  
LNA+ OF THE LOAD 57415  
TRANSFER ADDRESS -- J007 3437

## PROGRAM AND BLOCK ASSIGNMENTS.

BLOCK	ADDRESS	LENGTH	FILE	DATE	PROCESSOR	VIA LEVEL	HARDWARE	COMMENTS
/XFFACT/								
J007	111	1736	L60	77/09/22	FTN	0-52	666X	PROGRAM OPT1 OPT2 TRACE
IABIJ	2007	4317	L60	77/09/22	FTN	0-52	666X	FUNCTION OPT1 TRACE
CFACT	6164	472	L60	77/09/22	FTN	0-52	666X	SUBROUTINE OPT1 TRACE
IM2W2P	7069	23	L60	77/09/22	FTN	0-52	666X	FUNCTION OPT1 TRACE
IABIM1	7103	1286	L60	77/09/22	FTN	0-52	666X	FUNCTION OPT1 TRACE
IPL01	10351	232	L60	77/09/22	FTN	0-52	666X	SUBROUTINE OPT1 TRACE
MGARMA	10663	154	L60	77/09/22	FTN	0-52	666X	OPT1
UGRTAT	10757	573	UL-0188PLA	77/09/22	FTN	0-24	666X	OPT1
NOMIT	11552	76	UL-0188PLA	77/09/26	FTN	0-20	666X	OPT1
ALFNET	11650	41	UL-0188PLA	77/09/26	FTN	0-20	666X	OPT1
	11711	3	UL-0188PLA	76/03/20	FTN	0-10	666X	
/QUPPL01/								
/BU191/	12010	50						
/BU177/								
/BU1712/	12069	72						
/QMLK1/	12142	43						
/QMLCD/								
/QMLFD/	12222	13						
/QMLFP/	12235	4						
/QMLPP/	12241	4						
/QMLB18/	12245	2						
/QMLB2/	12247	79						
/QMLC1/	12337	11						
/QMLC2/	12350	24						
/QMLP/	12374	1154	UL-0188PLA	76/03/29	FTN	0-5	666X	OPT1
CMPR8	13550	11	UL-0188PLA	76/03/29	FTN	0-5	666X	OPT1
CR038	13561	4	UL-0188PLA	76/03/29	FTN	0-5	666X	OPT1
DOMEPL	13565	22	UL-0188PLA	76/03/29	FTN	0-5	666X	OPT1
/QMLC2/								
/ENDPL	13607	24	UL-0188PLA	76/03/29	FTN	0-5	666X	OPT1
GRAPH	13613	2						
INTAX	13615	624	UL-0188PLA	76/03/29	FTN	0-5	666X	OPT1
ISOASC	14641	162	UL-0188PLA	76/03/29	FTN	0-5	666X	OPT1
14647	14643	24	UL-0188PLA	76/03/29	FTN	0-5	666X	OPT1
14656	14647	43	UL-0188PLA	76/03/29	FTN	0-5	666X	OPT1
/QMLHTP/	14757	17	UL-0188PLA	76/03/29	COMPASS	3,-2-410	666X	
14950F	14776	52	UL-0188PLA	76/03/29	FTN	0-5	666X	OPT1
1495HT	15050	710	UL-0188PLA	76/03/29	FTN	0-5	666X	OPT1
149PRG	15760	14	UL-0188PLA	76/03/29	FTN	0-5	666X	OPT1
/QMDAT/	15774	67						
160J08	16063	767	UL-0188PLA	76/03/29	FTN	0-5	666X	OPT1
160J18	17092	133	UL-0188PLA	76/03/29	FTN	0-5	666X	OPT1
160LCA	17205	16	UL-0188PLA	76/03/29	FTN	0-5	666X	OPT1
160MOL	17223	101	UL-0188PLA	76/03/29	FTN	0-5	666X	OPT1
/QMLU87/	17129	7						
160BLU	17335	117	UL-0188PLA	76/03/29	FTN	0-5 010	666X	OPT1

Appendix  
I-17THIS PAGE IS BEST QUALITY PRACTICABLE  
FROM COPY FURNISHED TO DDC

APPENDIX II

Computer program for the Hankel (16) Function  
of second kind and one third order.

PROOFMAN JOSH 73/74 OPTICAL TRACE

PML 6064498 11/09/2010 09:00:39 PAGE

```

6 100 00 200 10111
   DO 120 J011100
   8000-5.0E-110.0
   1F(800.0E0.0)C0 70 120
   IF(IWSU1(800,0,20,0,000,PI,PIA3,001100P),C1,NUM,X02M)
   *ME.0160 TO 300
   PRINT 121,800,NUM
   FORMAT(800M,0,815,0,0M
   130 CONTINUE
   1F(100E-5.0E-2)C0 10 150
   IF(IWSU1(800.0E0.0)C0 100001PI,PIA3,001100P),C1,NUM,X02M)
   *ME.0160 TO 300
   IF(IWSU1(800.0E0.0)C0 100002,PI,PIA3,001100P),C1,NUM,X02M)
   *ME.0160 TO 300
   IF(IWSU1(800.0E0.0)C0 100003,PI,PIA3,001100P),C1,NUM,X02M)
   *ME.0160 TO 300
   IF(IWSU1(800.0E0.0)C0 100004,PI,PIA3,001100P),C1,NUM,X02M)
   *ME.0160 TO 300
   IF(IWSU1(800.0E0.0)C0 100005,PI,PIA3,001100P),C1,NUM,X02M)
   *ME.0160 TO 300
   PRINT 111,1,020,000,011
   111 FORMAT
   14,1H(1,2015.0,1M),3019.0)
   200 80001
   60
      PRINT (11,250)X1 (1M),001100P),C1,NUM,X02M)
      JMDL (10EN)
      FORMAT(9G12.0,1M),001100P),C1,NUM,X02M)
   250 CONTINUE
   100 PRINT(11,251)
   111 FORMAT(1M)
   004 ENDFILE II
   END

```

139  
Appendix  
II-2

THIS PAGE IS BEST QUALITY PRACTICABLE  
FROM COPY FURNISHED TO DDC

PAGE NO. SECURITY DETAILS - DIAGNOSTIC OR PROBLEM

00 1 Lower Limit .00. Upper Limit .00. Trip Limit .00.  
00 1 Lower Limit .00. Upper Limit .00. Trip Limit .00.

STRUCTURE REFERENCE MAP (RMS)

ENTER POINTS	DEF LINE	REFERENCES
3212-J007	2	
VARIABLES	00	RELATION
3770 C1	DOUBLE	
0040 0	REAL	ARRAY
0204 PI01	DOUBLE	IFACT
054 PI	DOUBLE	FACT
710 PI02	DOUBLE	FACT
1206 0001	DOUBLE	IFACT
		DEFINE

VARIABLES	ON	TYPE	RELATION		REFS
			XFACT	XFACT	
602 67		DOUBLE	ARRAY		56
1030 0TP		DOUBLE	ARRAY		74
0035 1		INTEGER			75
4634 1DIN		INTEGER			61
4630 1ERI	0	INTEGER			53
4631 1ER2	0	INTEGER			69
4635 1LOOP	0	INTEGER			54
4633 1XL		INTEGER			21
4637 J		INTEGER			22
1210 JHQL		INTEGER	ARRAY		49
4644 P		REAL	ARRAY		51
4650 PA		REAL	ARRAY		64
3770 PAS		DOUBLE			70
4632 PI		REAL			71
4600 800		DOUBLE			72
4632 800		DOUBLE			73
4614 8001		DOUBLE			53
4601 8002		DOUBLE			52
4604 811		DOUBLE			66
3766 820		COMPLEX			79
3770 82071		COMPLEX			72
3772 82012		COMPLEX			64
4600 XDEN		DOUBLE			75
4624 XDEN1		DOUBLE			70
4624 XDEN2		DOUBLE			72
4624 XFACT	0	XFACT	ARRAY		10
4610 XKO		DOUBLE	ARRAY		51
4654 XL		REAL	ARRAY		62
4612 XNUM		DOUBLE			64
4620 XNUM1		DOUBLE			70
4622 XNUM2		DOUBLE			74
FILE NAMES					
0	INPUT				
1030 OUTPUT		PTMT			56
2130 TAPE11		PTMT			61
EXTERNALS					
	ATAN	REAL	ARGC	REFERENCES	
	CABS	REAL	1	LIBRARY	26
	CEXP	COMPLEX	1	LIBRARY	52
	CFACT	CFACT	0	LIBRARY	41
18001	INTEGER	9	64	DEF LINE	REFERENCES
		3	21	30	29
			22	41	42
INLINE FUNCTIONS					
	TYPE	ARGC	ARGC	DEF LINE	REFERENCES
	COMPLEX	2	INTRIN	41	
STATEMENT LABELS					
3570 0	PTMT	PTMT			
3630 05	PTMT	PTMT			

Appendix II  
II-3THIS PAGE IS BEST QUALITY PRACTICABLE  
FROM COPY FURNISHED TO DDG



## FUNCTION TABIJ(ARG,AI,BI,AIP,BIP)

```

1      C   COMMON /FACT/XFACT(150),FT(43),G(43),GTP(43),GTPC(43)
2      C   FMULT,GMUL,T,JHOL(2)
3      C   DOUBLE PRECISION FP,FT,PTP,0.6MUL,CP,0.6TP,XFACT
4      C   DATA CI/C2/80073Y,353020330E-23301037,1.7320300000/
5      C
6      C   PRINT 90 ARG,ARG
7      IABI,JAI
8      A1,
9      B1,
10     F1,
11     G1,
12     G2,
13     G3,
14     FP=0.,
15     GTP=0.,
16     FTMAX=CTMAX=0
17
18      E 100  DN 200 KNL,03
19      ANA(30)=2
20      BAN(30)=1
21      FT(K)=XFACT(30K)/XFACT(30K-1)
22      CT(K)=XFACT(30K+1)/XFACT(30K)
23      G1(K)=XFACT(30K+1)*XFACT(30K+1)
24      IF(DANB(FT(K)),.61,ANA(FTMAX))FTMAX=ANA(FT(K))
25      IF(DANB(G1(K)),.61,ANA(31MAX))G1MAX=G1(K)
26      FAF+F1(1)
27      GAK+GT(1)
28      FTP(K)=FT(3+CK)*ANA(ARGS(30K-1))/XFACT(30K)
29      GTP(K)=CT(3+CK)*XFACT(30K)/XFACT(30K+1)
30      FP=FP+FTP(K)
31      GTPC=CTP(K)
32      PRINT 190,K,A,B,FT(K),CT(K),F,G,TTP(K),GTP(K),FP,BP
33
34      E 191  FORMAT(130IX,10D11.3)
35      CONTINUE
36      DO 202 1NL,5
37      IF(1000,0,DABA(FT(30+1)),LT,ABS(FTMAX)),AND,
38      + 1000,0,DABA(CT(30+1)),LT,ABS(CTMAX))GO TO 203
39      GO TO 204
40      CONTINUE
41      GO TO 220
42
43      PRINT 205,ARG,F1
44      FORMAT(MORE ACT, REQUIRED IN ANY CALC, A, B, C, D, E, F, G, H, I, J, K, L, M, N, O, P, Q, R, S, T, U, V, W, X, Y, Z, /)
45      +  " F1 = 0.015,4,5/10 0.015,6"
46      PRINT 206,(1,FT(1),G1(1),01E-13)
47      FORMAT(15.2015,6)
48      IABI,JAI=-1
49      GO TO 999
50
51      E 220  A1,C1,B1,C2,B2
52      G1BABA(130(C10FP+C20GP)
53      A1P+10P-C2GP
54      B1P+G0130(C10FP+C20GP)
55
56      C210  PRINT -21,L,K,A,B,F,G,H,I,J,K,L,M,N,O,P,Q,R,S,T,U,V,W,X,Y,Z
57      C211  FORMAT(K,A,B,F,G,H,I,J,K,L,M,N,O,P,Q,R,S,T,U,V,W,X,Y,Z)
58      RETURN
59

```



## FUNCTION TABLE

PTN 4.66452

77/09/160.09.40.59

PAGE 3

## STATEMENT LABELS

	DEF LINE	REFERENCES
260 202	41	37
265 206	43	49
376 205	44	43
420 206	47	46
423 211	47 NO REPS	55
310 220	50	52
352 999	57	49

## LOOP

INDEX	FROM-TO	PROPERTIES
1	21-36	ENT REFS
1	37-41	OPT
1	42-46	EXITS
1	47-51	EXT-REFS

## COMMON BLOCKS

NAME - DIAS NAME (LENTH)	LENGTH	MEMBERS
XFACT	650	0 XFACT (300)
FTP	0	472 FTP (66)
CHU	1	646 CHU (2)

## STATISTICS

PROGRAM LENGTH	316
ON-LABELED-COMMON LENGTH	14120
52000 CH USED	500

144

Appendix II  
II-7THIS PAGE IS BEST QUALITY PRACTICABLE  
FROM COPY FURNISHED TO DDC

ROUTINE CFACI

PTN 466492

77/00/10 00:00:10

ROUTINE CFACI

COMMON /XFACT/XFACT(150),P7(45),S7(45),P8(45),P9(45),P10(45),P11(45),P12(45)

PML,TRNL,JNL(12)

DOUBLE PRECISION PML,P7,P8,P9,P10,P11,P12

REAL

IFACT(150)

DO 100 I=1,150

XFACT(I)=XCR(1-I)

100 CONTINUE

END

RETURN

SYMBOLIC REFERENCE MAP (MOS)

ENTRY POINTS DEP LINE REFERENCES  
 CFACI 2

VARIABLES BN TYPE RELOCATION

120	PML	DOUBLE	XFACT
050	P7	DOUBLE	XFACT
730	P8	DOUBLE	XFACT
120	P9	DOUBLE	XFACT
603	P10	DOUBLE	XFACT
103	P11	DOUBLE	XFACT
120	P12	DOUBLE	XFACT
22	JML	INTEGER	XFACT
0	CFACI	DOUBLE	XFACT

STATEMENT LABELS  
 0 100  
 0 000  
 0

COMMON BLOCKS LENGTH

XFACT 650

PML 100

P7 100

P8 100

P9 100

P10 100

P11 100

P12 100

JNL(12) 100

TRNL 100

PML 100

P7 100

P8 100

P9 100

P10 100

P11 100

P12 100

JNL(12) 100

145  
Appendix II  
II-8

THIS PAGE IS BEST QUALITY PRACTICABLE  
FROM COPY FURNISHED TO DDC

STATISTICS  
PROGRAM LENGTH 1226 10  
IN LABLED COMMON LENGTH 12120 650  
520000 CR-DDED.

```

1      FUNCTION IM2H2P(ARC,H2,H2P)
2
3      COMMON /XFACT/XFACT(150),P1(43),S1(43),P7P(43),S7P(43),
4      * PMUL1,GMUL1,JHOL(2)
5
6      DIMENSION HFT(43),HGT(43),HFTP(43),HGTP(43)
7
8      COMPLEX ARG,HFT,HGT,HFTP,P,HFTP,P,HFTP,HP,
9      * PT,SP,FTP,SP,HC,HPC
10
11      DOUBLE PRECISION A,B,PMUL,T,GHULY
12      DOUBLE PRECISION H2,H2P,XFACT
13
14      DATA BORT3/1.73205000000E-00/
15
16      PRINT 999 ARG,ARC
17      PRINT 999 ARG,ARC
18      PRINT 999 ARG,ARC
19      PRINT 999 ARG,ARC
20
21      DO 300 J8=1,13
22      DN 300 18=1,13
23      X8=7.+J8
24      Y8=7.+J8
25      IF (X8.EQ.0.0,AND,Y8.EQ.0.0) GO TO 300
26      ARGCmplX(X8)
27      IM2H2P1
28
29      A81=
30
31      B81=
32      F81=
33      G8ARC
34      F88=
35      G8P1=
36
37      HFTMAX80=
38      HGTMAX80=
39
40      100  DN 200 K8=1,43
41      AGAS(30K-2)
42      B88(30K-1)
43      HFTK8((-1.)**K8))8/XFACT(30K)
44      HFT(K8)**HFTK8*AG8(30K)
45      HGTK8((-1.)**K8))8/XFACT(30K+1)
46      HG1(K8)**HGCK8*AG8(30K+1)
47      IF (CAG8(HFT(K8)).GT.ABS(HFTMAX)) HFTMAX=CA88(HFT(K8))
48      IF (CAG8(HGT(K8)).GT.ABS(HGTMAX)) HGTMAX=CA88(HGT(K8))
49      FB8**HFT(K8)
50      GAG+HG1(K8)
51      HFTK8((-1.)**K8))8/XFACT(30K)
52      HFTP(K8)**HFTP*AG8(30K-1)
53      HGTPK8((-1.)**K8))8/XFACT(30K+1)
54      HGTP(K8)**HGTP*AG8(30K)
55      FP8P**HFTP(K8)
56      GAGP+HGTP(K8)
57
58      PRINT 191,K8,A,B,HFT(K8),HGTP(K8),P,G,HFTP(K8),HGTP(K8),PP,SP
59      FORMAT(15,15,10011,3)
60      CONTINUE
61
62      DO 202 10015
63      IP(1000,SCAB8(HFT(30+1))),LT,AG8(HFTMAX),AND,
64      IP(1000,SCAB8(HGT(30+1))),LT,AG8(HGTMAX),AND,
65      200  CONTINUE
66
67      99

```

## Appendix II

146  
II-9THIS PAGE IS BEST QUALITY PRACTICABLE  
FROM COPY FURNISHED TO DDC

141120V20

FUNCTION INSPECTOR 7.3/74 INPUT TRACE

卷之三

四

REFERENCE-NAS (sh-3)

UNIVERSITY PUBLICATIONS OF LINGUISTICS • MERRIMACK COLLEGE

## FUNCTION INTRINSIC

11/17/10 09:44:19

PAGE

PIN 4.00000 11/09/10, 09:44:19

NAME	TYPE	LOCATION	OPTIONAL TRACE
934 HPI	COMPLEX	ARRAY	
947 HPIX	REAL		
544 HPIX	REAL		
1030 HPIP	COMPLEX	ARRAY	
951 HPIPS	REAL		
702 HPI	COMPLEX	ARRAY	
550 HPIK	REAL		
545 HPIKX	REAL		
1156 HPIP	COMPLEX	ARRAY	
552 HPIPK	REAL		
532 HPIC	COMPLEX		
0 H2	DOUBLE		
0 H2P	DOUBLE		
953 1	INTEGER		
917 1H202P	INTEGER		
541 18	INTEGER		
1210 JHQA	INTEGER	IMPACT	
540 JQ	INTEGER		
546 K	INTEGER		
926 SCRT3	REAL		
942 X	REAL		
9 IMPACT	DOUBLE		
943 Y	REAL		

## FILE NAMES

WRITING

148 Appendix II-11

REFERENCES

148 Appendix II-11

## EXTERNALS

REFERENCES

148 Appendix II-11

## INLINE FUNCTIONS

REFERENCES

148 Appendix II-11

## STATEMENT LABELS

REFERENCES

148 Appendix II-11

## FILE

REFERENCES

148 Appendix II-11

## LOOPS

REFERENCES

148 Appendix II-11

## LABEL

REFERENCES

148 Appendix II-11

## PROPERTIES

REFERENCES

148 Appendix II-11

## EXT-REFS

REFERENCES

148 Appendix II-11

THIS PAGE IS BEST QUALITY PRACTICABLE  
FROM COPY FURNISHED TO DDC

FUNCTION NUMBER 75/70 OPTICAL TRACE

LABEL NUMBER 4007-10 LEECHIN, PROTEUS CRY REPS

BLOCK LENGTH 5000 - DATA NAME (LEECHIN)  
FACT 650

030

PRINTED ON 01/01/70

PRINTED ON 01/01/70  
CPI PRINTING SYSTEMS INC.

DATA ON CRYSTAL 701

001

000 01 000 000

000 01 000 000

000 01 000 000

000 01 000 000

000 01 000 000

000 01 000 000

000 01 000 000

000 01 000 000

000 01 000 000

000 01 000 000

000 01 000 000

000 01 000 000

000 01 000 000

000 01 000 000

000 01 000 000

000 01 000 000

000 01 000 000

000 01 000 000

000 01 000 000

000 01 000 000

000 01 000 000

000 01 000 000

000 01 000 000

000 01 000 000

000 01 000 000

000 01 000 000

000 01 000 000

000 01 000 000

000 01 000 000

000 01 000 000

000 01 000 000

000 01 000 000

000 01 000 000

17/09/69 00:00:00 FILE NUMBER

17/09/69 00:00:00 PAGE NUMBER

17/09/69 00:00:00

17/09/69 00:00:00

17/09/69 00:00:00

17/09/69 00:00:00

17/09/69 00:00:00

17/09/69 00:00:00

17/09/69 00:00:00

17/09/69 00:00:00

17/09/69 00:00:00

17/09/69 00:00:00

17/09/69 00:00:00

17/09/69 00:00:00

17/09/69 00:00:00

17/09/69 00:00:00

17/09/69 00:00:00

17/09/69 00:00:00

17/09/69 00:00:00

17/09/69 00:00:00

17/09/69 00:00:00

17/09/69 00:00:00

17/09/69 00:00:00

17/09/69 00:00:00

17/09/69 00:00:00

17/09/69 00:00:00

17/09/69 00:00:00

17/09/69 00:00:00

17/09/69 00:00:00

17/09/69 00:00:00

17/09/69 00:00:00

17/09/69 00:00:00

17/09/69 00:00:00

17/09/69 00:00:00

17/09/69 00:00:00

17/09/69 00:00:00

17/09/69 00:00:00

17/09/69 00:00:00

17/09/69 00:00:00

THIS PAGE IS BEST QUALITY PRACTICABLE  
FROM COPY FURNISHED TO ADG

149  
Appendix II  
II-12

13/74 Input trace

PAG 2

77/00/116. 00.00.039

卷之三

FUNCTIONAL ANALYSIS

**COMPLEX 820** DOUBLE PRECISION H2=H2P\*EXP(EYN+IYNN+IYNN+IYNN+IYNN)  
DOUBLE PRECISION A00P=A00P\*EXP(A00P+A00P+A00P+A00P)

AYHAN İŞTE DİLEĞİMİZ

ENTRY POINTS	PER LINE	REFERENCES
1	23	1
<b>BZLOCATION</b>		
VARIABLES	BN	TYPE
212 A00	DOUBLE	
216 A00P	DOUBLE	
220 A009	DOUBLE	
222 A00P	DOUBLE	
261 H00H	DOUBLE	
264 H00N	DOUBLE	
268 H00P	DOUBLE	
270 H000	DOUBLE	
276 H000P	DOUBLE	
280 C1	DOUBLE	
284 0	DOUBLE	REAL
288 0	DOUBLE	DOUBLE
292 E7H	DOUBLE	DOUBLE
296 E7P	DOUBLE	DOUBLE
302 H2	DOUBLE	DOUBLE
306 H2P	DOUBLE	INTEGER
308 1	DOUBLE	DOUBLE
312 1	DOUBLE	REAL
316 P1	DOUBLE	REAL
320 0	DOUBLE	DOUBLE
324 0	DOUBLE	COMPLEX
328 0	DOUBLE	DOUBLE
332 KDN	DOUBLE	

**Appendix II**

THIS PAGE IS BEST-QUALITY PRACTICABLE  
FROM COPY FURNISHED TO DDC

150

151

**Appendix II**

THIS PAGE IS BEST QUALITY PRACTICABLE  
FROM COPY FURNISHED TO DDC

11/09/1991, 00,00,00 piece

FUNCTION 18001 73/74 OPTICAL TRACE

**MISSION**  
*of*  
**Rome Air Development Center**

RADC plans and conducts research, exploratory and advanced development programs in command, control, and communications (C<sup>3</sup>) activities, and in the C<sup>3</sup> areas of information sciences and intelligence. The principal technical mission areas are communications, electromagnetic guidance and control, surveillance of ground and aerospace objects, intelligence data collection and handling, information system technology, ionospheric propagation, solid state sciences, microwave physics and electronic reliability, maintainability and compatibility.